

LITHUANIAN UNIVERSITY OF HEALTH SCIENCES  
MEDICAL ACADEMY

**Monika Pankevičiūtė-Bukauskienė**

**HALLMARKS OF AMINO ACID  
METABOLISM IN BREAST CANCER  
CELLS**

Doctoral Dissertation  
Natural Sciences,  
Biophysics (N 011)

Kaunas, 2024

Dissertation has been prepared at the Laboratory of Cell Culture, Institute of Cardiology, Lithuanian University of Health Sciences during the period of 2020–2024.

### **Scientific Supervisor**

Dr. Sergio Bordel Velasco (Lithuanian University of Health Sciences, Natural Sciences, Biophysics – N 011).

### **Consultant**

Prof. Dr. Vytenis Arvydas Skeberdis (Lithuanian University of Health Sciences, Natural Sciences, Biophysics – N 011).

**Dissertation is defended at the Biophysics Research Council of the Lithuanian University of Health Sciences:**

### **Chairperson**

Prof. Dr. Ramunė Morkūnienė (Lithuanian University of Health Sciences, Natural Sciences, Biochemistry – N 004).

### **Members:**

Prof. Dr. Rasa Ugenskienė (Lithuanian University of Health Sciences, Natural Sciences, Biology – N 010);

Prof. Dr. Saulius Šatkauskas (Vytautas Magnus University, Natural Sciences, Biophysics – N 011);

Prof. Dr. Aidias Alaburda (Vilnius University, Natural Sciences, Biophysics – N 011);

Dr. Fernando Santos-Beneit (University of Valladolid, Natural Sciences, Biology – N 010).

Dissertation will be defended at the open session of the Biophysics Research Council of the Lithuanian University of Health Sciences on the 11<sup>th</sup> of October 2024 at 11 a.m. at the Conference Hall of the Institute of Cardiology, Lithuanian University of Health Sciences.

Address: Sukilėlių pr. 15, LT-50162 Kaunas, Lithuania.

LIETUVOS SVEIKATOS MOKSLŲ UNIVERSITETAS  
MEDICINOS AKADEMIJA

**Monika Pankevičiūtė-Bukauskienė**

**KRŪTIES NAVIKO LĄSTELIŲ  
AMINORŪGŠČIŲ METABOLIZMO  
YPATUMAI**

Daktaro disertacija  
Gamtos mokslai,  
biofizika (N 011)

Kaunas, 2024

Disertacija rengta 2020–2024 metais Lietuvos sveikatos mokslų universiteto Kardiologijos instituto Ląstelių kultūrų laboratorijoje.

### **Mokslinis vadovas**

dr. Sergio Bordel Velasco (Lietuvos sveikatos mokslų universitetas, gamtos mokslai, biofizika – N 011).

### **Konsultantas**

prof. dr. Vytenis Arvydas Skeberdis (Lietuvos sveikatos mokslų universitetas, gamtos mokslai, biofizika – N 011).

**Disertacija ginama Lietuvos sveikatos mokslų universiteto Biofizikos mokslo krypties taryboje:**

### **Pirmininkas**

prof. dr. Ramunė Morkūnienė (Lietuvos sveikatos mokslų universitetas, gamtos mokslai, biochemija – N 004).

### **Nariai:**

prof. dr. Rasa Ugenskienė (Lietuvos sveikatos mokslų universitetas, gamtos mokslai, biologija – N 010);

prof. dr. Saulius Šatkauskas (Vytauto Didžiojo universitetas, gamtos mokslai, biofizika – N 011);

prof. dr. Aidis Alaburda (Vilniaus universitetas, gamtos mokslai, biofizika – N 011);

dr. Fernando Santos-Beneit (Valjadolido universitetas, gamtos mokslai, biologija – N 010).

Disertacija bus ginama viešajame Biofizikos mokslo krypties tarybos posėdyje 2024 m. spalio 11 d. 11 val. Lietuvos sveikatos mokslų universiteto Kardiologijos instituto posėdžių salėje.

Disertacijos gynimo vietos adresas: Sukilėlių pr. 15, LT-50162 Kaunas, Lietuva.

# CONTENTS

ABBREVIATIONS .....	7
LIST OF GENES.....	9
INTRODUCTION.....	10
Aim and objectives .....	11
Objectives.....	11
Scientific novelty of the work .....	11
Other important aspects.....	12
1. LITERATURE REVIEW.....	13
1.1. Pathophysiology and treatment strategies of breast cancer.....	13
1.2. Perturbations in tumour metabolism .....	16
1.3. Amino acid metabolism as a target for chemotherapy .....	18
1.4. Branched-chain amino acid metabolism in cancer.....	20
1.5. The mevalonate pathway in cancer .....	22
1.6. Bioinformatics in cancer research .....	24
2. MATERIALS AND METHODS.....	25
2.1. Materials.....	25
2.1.1. Cell culture reagents and materials.....	25
2.1.2. Cell lines .....	25
2.1.3. Chemicals and reagents .....	25
2.1.4. Databases .....	26
2.1.5. Instruments .....	26
2.1.6. Kits.....	27
2.1.7. Other materials .....	27
2.1.8. Software and tools .....	27
2.2. Methods .....	27
2.2.1. Cell cultures and their growing conditions .....	27
2.2.2. Transfection .....	28
2.2.3. Wound healing assay .....	28
2.2.4. Experiments with <sup>13</sup> C isotope-labelled amino acids .....	29
2.2.5. Metabolite extraction from cells.....	29
2.2.6. Plasma preparation for mass spectrometry analysis.....	30
2.2.7. UPLC-ESI-MS/MS.....	30
2.2.8. Analysis of metabolomics data .....	30
2.2.9. <sup>13</sup> C-based flux patterns.....	31
2.2.10. RNA sequencing.....	31
2.2.11. Analysis of RNA-seq data .....	31
2.2.12. Integrated data analysis using pyTARG .....	32
2.2.13. Statistical analysis.....	32
3. RESULTS AND DISCUSSION.....	34
3.1. Quantification of cellular energy derived from the degradation of BCAAs .....	34
3.2. Contribution of BCAAs to mevalonate metabolism .....	38

3.3. The role of BCAAs in cell invasiveness.....	43
3.4. Determination of intermediate metabolites of the BCAA degradation pathway in blood plasma.....	47
3.5. Metabolomic analysis of amino acids associated with malignancy in breast- derived cells.....	50
3.6. Differential gene expression of the three breast-derived cell lines .....	54
3.7. The search for potential drug targets for breast cancer by combining metabolic and genomic data .....	56
CONCLUSIONS .....	62
SANTRAUKA.....	63
BIBLIOGRAPHY .....	80
PUBLICATIONS .....	94
SUPPLEMENTS .....	96
CURRICULUM VITAE .....	108
ACKNOWLEDGEMENTS.....	109

## ABBREVIATIONS

<b>7-AAD</b>	– 7-aminoactinomycin D
<b>Acetoacetyl-CoA</b>	– Acetoacetyl coenzyme A
<b>Acetyl-CoA</b>	– Acetyl coenzyme A
<b>AJCC</b>	– American Joint Committee on Cancer
<b>Akt</b>	– Protein kinase B
<b>ATP</b>	– Adenosine triphosphate
<b>BCAA</b>	– Branched-chain amino acid
<b>BCAT</b>	– Branched-chain amino acid transferase
<b>BCC</b>	– Breast cancer cells (cell line)
<b>CCCP</b>	– Carbonyl cyanide m-chlorophenyl hydrazone
<b>DMEM</b>	– Dulbecco's modified Eagle medium
<b>DMSO</b>	– Dimethyl sulfoxide
<b>DNA</b>	– Deoxyribonucleic acid
<b>EDTA</b>	– Ethylenediaminetetraacetic acid
<b>EGF</b>	– Epidermal growth factor
<b>EMU</b>	– Elementary metabolic units
<b>ER</b>	– Estrogen receptor
<b>ESI</b>	– Electrospray ionization
<b>F-12</b>	– Ham's F-12 nutrient mix
<b>FBS</b>	– Fetal bovine serum
<b>GEO</b>	– Gene Expression Omnibus (database)
<b>GSMM</b>	– Genome-scale metabolic model
<b>HER2</b>	– Human epidermal growth factor receptor
<b>HMG-CoA</b>	– 3-hydroxy-3-methylglutaryl coenzyme A
<b>HS</b>	– Horse serum
<b>JC-1</b>	– 5,5',6,6'-tetrachloro-1,1',3,3'-tetraethylbenzimidazolyl carbocyanine iodide
<b>KEGG</b>	– Kyoto Encyclopedia of Genes and Genomes
<b>MCF-10A</b>	– Michigan Cancer Foundartion-10A (cell line)
<b>MCF-7</b>	– Michigan Cancer Foundation-7 (cell line)
<b>MS/MS</b>	– Tandem mass spectrometer
<b>mTOR</b>	– Mammalian target of rapamycin
<b>NADPH</b>	– Nicotinamide adenine dinucleotide phosphate

<b>NCBI</b>	– National Center for Biotechnology Information
<b>OXPHOS</b>	– Oxidative phosphorylation
<b>PBS</b>	– Phosphate-buffered saline
<b>PC</b>	– Principal component
<b>PCA</b>	– Principal component analysis
<b>pen-strep</b>	– Penicillin-streptomycin
<b>PI3K</b>	– Phosphoinositide 3-kinase
<b>PR</b>	– Progesterone receptor
<b>rHu</b>	– Recombinant human
<b>RNA</b>	– Ribonucleic acid
<b>RNA-seq</b>	– RNA sequencing
<b>ROS</b>	– Reactive oxygen species
<b>RPKM</b>	– Reads per kilobase per million reads
<b>SAM</b>	– S-adenosyl methionine
<b>SE</b>	– Standard error
<b>siRNA</b>	– Small interfering RNA
<b>TNM</b>	– Tumour, node, and metastasis (classification)
<b>UPLC</b>	– Ultra-performance liquid chromatography
<b>WHO</b>	– World Health Organization



## LIST OF GENES

<i>Gene name</i>	<i>Product</i>
<b>AACS</b>	– Acetoacetyl coenzyme A synthetase
<b>AHCY</b>	– Adenosylhomocysteinase
<b>ATP1B3</b>	– ATPase Na <sup>+</sup> /K <sup>+</sup> transporting subunit beta 3
<b>ATP6V1H</b>	– ATPase H <sup>+</sup> transporting V1 subunit H
<b>CA2</b>	– Carbonic anhydrase 2
<b>CA6</b>	– Carbonic anhydrase 6
<b>CHAC1</b>	– Glutathione-specific $\gamma$ -glutamylcyclotransferase 1
<b>HMGCL</b>	– 3-hydroxy-3-methylglutaryl coenzyme A lyase
<b>HMGCR</b>	– 3-hydroxy-3-methylglutaryl coenzyme A reductase
<b>HMGCS1</b>	– 3-hydroxy-3-methylglutaryl coenzyme A synthase 1
<b>HMGCS2</b>	– 3-hydroxy-3-methylglutaryl coenzyme A synthase 2
<b>NDUFB8</b>	– NADH:ubiquinone oxidoreductase subunit B8
<b>PHGDH</b>	– Phosphoglycerate dehydrogenase
<b>PSPH</b>	– Phosphoserine phosphatase
<b>SLC25A44</b>	– Solute carrier family 25 member 44
<b>SLC26A6</b>	– Solute carrier family 26 member 6
<b>SLC36A4</b>	– Solute carrier family 36 member 4
<b>SLC44A5</b>	– Solute carrier family 44 member 5
<b>SLC6A15</b>	– Solute carrier family 6 member 15
<b>UQCR1</b>	– Ubiquinol-cytochrome C reductase core protein 1
<b>UQCRH</b>	– Ubiquinol-cytochrome C reductase hinge protein

## INTRODUCTION

Breast cancer remains the predominant form of cancer worldwide according to the World Health Organization (WHO) [1], which leads to it also being the primary cause of death resulting from malignant tumours. Given its higher incidence in women compared to men (about 0.5–1 % of breast cancers occur in men as reported by WHO), it becomes a daunting aspect in the broader context of women's health. According to the American Cancer Society, it is estimated that one in eight women will develop breast cancer at some point in their lifetime [2]. Despite advancements in breast cancer survival rates through interventions like mastectomies and chemotherapy, early detection and personalised treatments are still a matter of high importance to reduce the psychological burden for patients and to increase their overall survival.

After Warburg's discovery of cancer cells being able to carry out aerobic glycolysis to meet their increased metabolic demands [3], the scientific interest in alterations of cancer metabolism increased amongst scientists. Metabolic reprogramming emerged as a hallmark of cancer [4]. It became clear that exploring these subtle differences in metabolism between malignant and healthy tissues could lead to finding metabolic vulnerabilities of cancer for new targeted therapies. Finding these weak spots poses a challenge, as alterations in metabolic pathways differ even among the same type of cancer.

Besides glucose, amino acids have proven their importance in tumour progression. In addition to being building blocks for proteins, they can also be broken down into intermediates for the Krebs cycle or other biosynthetic pathways. They are not only fuel for rapidly dividing cancer cells but play an important role in controlling immune response, regulating signalling pathways, maintaining redox balance and resistance to various chemotherapeutic agents. Some cancer cells are dependent on non-essential amino acids due to loss-of-function mutations in biosynthetic enzyme-coding genes. In other cases, cancer cells have a higher demand for particular amino acids, that are used as biosynthetic building blocks, making their uptake and synthesis pathways upregulated compared to normal cells. These differences are crucial in the search for therapeutic agents with fewer side effects.

Branched-chain amino acids (BCAAs) – leucine, isoleucine, and valine, have been shown to be involved in different metabolic diseases such as obesity, diabetes, cardiovascular and neurodegenerative diseases [5]. The importance of BCAA catabolism in cancer was noticed in 2013 when Tönjes *et al.* noticed that the first cytosolic enzyme in the breakdown cascade of BCAAs – branched-chain amino acid transferase 1 (BCAT1) was overexpressed in glioblastoma cells and demonstrated that suppression of BCAT1 significantly

reduced proliferation of these cells [6]. Our group also showed that the enzyme branched-chain amino acid transferase 2 (BCAT2), the mitochondrial counterpart of BCAT1, is overexpressed in some breast cancer cell lines and that BCAA degradation accounts for a significant part of the cellular energy metabolism [7]. As a result of the mentioned observations, perturbed BCAA metabolism is considered to be a potential therapeutic target for different cancer types [8], however, the exact reasons for the mentioned metabolic disturbances are not entirely known.

Understanding the intricate landscape of cancer metabolism by unravelling key pathways and molecular players offers promising targets for new targeted therapies and unlocking the full potential of personalised medicine. Advancements in molecular and systems biology as well as genomic sciences are providing deeper insight into cancer metabolism for the development of new, more efficient diagnostic and treatment approaches in the near future.

### **Aim and objectives**

This work aims to determine the role of amino acids in breast cancer cell metabolism by using different omics- techniques and bioinformatic pipelines in search of chemotherapeutic drug targets.

### **Objectives**

1. Identify the role of branched-chain amino acids in cellular energetics and biosynthesis of mevalonate by using isotopically labelled amino acids in breast cancer cells.
2. Perform a comparative analysis of branched-chain amino acid metabolism from the blood plasma of breast cancer patients and healthy controls.
3. Determine alterations of amino acid metabolism in breast cancer cells by combining metabolomic and transcriptomic data to identify possible drug targets.

### **Scientific novelty of the work**

Even though the association between cancer and the overexpression of BCAA-degrading enzymes has been a topic of discussion for about a decade, a clear picture of the links between BCAA metabolism and cancer has yet to emerge. In this work, we shed light on some previously unknown mechanisms by which BCAAs promote the progression of breast cancer by tracing their breakdown and transformation into cellular energy and building blocks. This, in turn, contributes to the search for new therapeutic approaches

and biomarkers for early diagnostics. Novel discoveries of this work include measures of the influence BCAA catabolism has on acetyl coenzyme A and mevalonate production in breast cancer cells, as well as the determination of possible biomarkers for breast cancer, following increased BCAA catabolism in the plasma of women with newly diagnosed invasive ductal carcinoma. Furthermore, by combining metabolomic and transcriptomic data from breast cancer cells using a bioinformatic pipeline, we identify perturbations in one-carbon metabolism, which could be a topic for further investigation on the role of amino acids in cancer progression.

### **Other important aspects**

The results of this dissertation were part of a project called “The effect of branched-chain amino acid degradation on cancer cell metabolism and proliferation” (S-SEN-20-6), funded by the Lithuanian Research Council. The results are divided into seven parts for better discrimination of the different aspects studied, however, the conclusions were written taking into consideration several of these aspects. The results of sections 3.1 and 3.2 were published in one peer-reviewed article. The aforementioned together with the unpublished results of section 3.3 constitute the first conclusion. Due to a different objective for the work in section 3.4, the unpublished results make up the second conclusion, while the results from sections 3.5–3.7 are published in a second peer-reviewed article and constitute the third conclusion of this dissertation.

# 1. LITERATURE REVIEW

## 1.1. Pathophysiology and treatment strategies of breast cancer

The term “breast cancer” covers a range of malignancies that occur in the mammary glands [9]. The classification of breast cancer depends on the specific cells that are affected. Based on cell origin, breast cancers can be broadly categorised into carcinomas and sarcomas. Carcinomas originate from the epithelial cells in the breast, which line the lobules and ducts responsible for milk production [10, 11]. They make up the majority of breast cancers. Sarcomas, on the other hand, are much rarer (<1 % of primary breast cancer), and arise from the stromal components of the breast, like myofibroblasts and blood vessel cells [10]. Based on the pathology and invasiveness of the disease, common breast cancers can be divided into three basic categories: non-invasive (*in-situ*), invasive, and metastatic [11]. Ductal carcinoma *in situ* is a pre-invasive form of breast cancer that develops inside existing milk ducts, while lobular carcinoma *in situ* develops in milk glands or lobules. Although not in itself invasive, breast carcinoma *in situ* has the potential to become invasive, thus early diagnosis and subsequent treatment are essential [12]. Invasive or infiltrating breast cancer invades the surrounding tissues outside of the ducts and lobules. Invasive carcinomas have the potential to spread to other sites of the body, such as lymph nodes or other organs, making their way to the metastatic classification. Based on what tissues and cells are involved, invasive breast cancers can be divided into two main groups: invasive ductal carcinoma (accounting for 80 % of all breast cancers) and invasive lobular carcinoma (10–15 % of all breast cancers) [13]. These can be further divided into subgroups. Distinguishing between subtypes of cancer is crucial as they may have different prognoses and treatment options [9]. Late-stage breast cancers or stage IV metastatic cancers spread to other areas of the body making it very difficult to treat. Unfortunately, about 30 % of women diagnosed with early-stage breast cancer will eventually develop metastases [11].

From a molecular point of view, breast cancer can be divided into subtypes based on the expression of hormone receptors. Breast cancers are typically classified into four categories based on the immunohistochemical expression of these receptors: estrogen receptor (ER), progesterone receptor (PR), and human epidermal growth factor receptor (HER2) positive (+), as well as triple negative, which lacks expression of any of the mentioned receptors. ER plays a crucial role in diagnosis, as around 70–75 % of invasive breast carcinomas exhibit significantly high ER expression [14]. PR is found in over 50 % of ER+ patients and is rarely seen in those with ER negative (–) breast cancer

[15]. Another prominent trait used in cancer classification is the expression of protein Ki-67. It is a proliferation rate marker used in pathology and is absent or low in resting cells [16]. Based on the measurements of these proteins, breast cancers are divided into five subtypes: luminal A, luminal B, HER2 related, triple negative, and normal like. A more detailed explanation of each subtype can be seen in Table 1.1.1 [11, 17].

**Table 1.1.1. Molecular subtypes of breast cancer [11]**

Subtypes	Molecular signatures	Characteristics	Treatment options*
Luminal A	ER+, PR±, HER2-, Low Ki-67	~70 %, most common, best prognosis	Hormonal therapy, targeted therapy
Luminal B	ER+, PR±, HER2±, High Ki-67	10 %-20 %, lower survival than Luminal A	Hormonal therapy, targeted therapy
HER2 related	ER-, PR-, HER2+	5 %-15 %	Targeted therapy
Triple negative	ER-, PR-, HER2-	15 %-20 %, more common in black women, diagnosed at a younger age, worst prognosis	Limited targeted therapy
Normal like	ER+, PR±, HER2-, Low Ki-67	Rare, low proliferation gene cluster expression	Hormonal therapy, targeted therapy

\* Besides conventional surgical and non-surgical treatment.

After the initial diagnosis, tests are performed to determine the stage of the disease, which also determines the possible treatment outcomes. This is done using a classification system based on the American Joint Committee on Cancer (AJCC) and the International Union for Cancer Control. It is called the tumour, node, and metastasis (TNM) breast cancer staging system and it consists of stages 0 to IV based on the anatomical features of a tumour (see Table 1.1.2) [11].

If no metastases are observed, the main goal of the treatment is to eradicate the tumour from the breast and regional lymph nodes. This consists of surgical removal of the mentioned tissues with the consideration of postoperative radiation [18]. There are two major types of surgeries for removing cancerous tissue: breast-conserving surgery or lumpectomy and the complete removal of the breast – mastectomy. Even though a breast-conserving surgery is much more appealing for the patients, the majority of women with previous lumpectomies eventually have to be treated with a full mastectomy [19, 20].

**Table 1.1.2.** Anatomical TNM classification of breast cancer stages defined by AJCC [11]

Stages		Definition
Stage 0		Ductal carcinoma <i>in situ</i>
Stage I	IA	Small primary invasive tumour, measuring $\leq 20$ mm, no involvement of nearby lymph nodes
	IB	Nodal micrometastases ( $>0.2$ mm, $<2.0$ mm) with or without $\leq 20$ mm primary tumour
Stage II	IIA	Movable ipsilateral level I, II lymph node metastases and a primary tumour $\leq 20$ mm; or if the tumour is larger (20–50 mm), with no involvement of nearby lymph nodes
	IIB	Movable ipsilateral level I, II lymph node metastases with 20 mm–50 mm tumour; or a larger ( $>50$ mm) tumour with no nodal involvement
Stage III	IIIA	Movable ipsilateral level I, II lymph node metastases with $>50$ mm tumour; or primary tumour of any size with fixed ipsilateral level I, II or internal lymph node metastases
	IIIB	Primary tumour with chest wall and/or skin invasion
	IIIC	Any size primary tumour with supraclavicular or ipsilateral level III lymph node metastases; or with ipsilateral level I, II and internal lymph node metastases
Stage IV		Any case with distant organ metastasis

Other treatment methods include chemotherapy, radiation therapy, endocrinal (hormonal) therapy and targeted (biological) therapy [20]. Systemic treatment can occur before surgery (neoadjuvant), after surgery (adjuvant), or in both instances [5]. Current chemotherapeutic approaches consist of the following drugs: carboplatin, cyclophosphamide, 5-fluorouracil/capecitabine, taxanes (paclitaxel, docetaxel), and anthracyclines (doxorubicin, epirubicin). Choosing an appropriate drug for the type of breast cancer being treated is essential, as different subtypes of the disease react differently to chemotherapy [20, 21]. While chemotherapy is considered to be effective, it usually results in a number of side effects. These include but are not limited to hair loss, nausea, vomiting, diarrhoea, mouth sores, fatigue, heightened vulnerability to infections, bone marrow suppression, leucopenia, anaemia, and increased susceptibility to bruising or bleeding. Less commonly observed side effects encompass cardiomyopathy, neuropathy, hand-foot syndrome, and impaired cognitive functions. In younger women, disturbances in the menstrual cycle and potential fertility issues may arise [20]. Radiotherapy is a local treatment for breast cancer, often performed after surgery and/or chemotherapy. It is used to ensure that all cancerous cells are destroyed, to minimize reoccurrence. Radiation therapy is associated with a significant

improvement in overall survival but is also associated with several side effects, most commonly: irritation and darkening of the exposed skin, fatigue, and lymphoedema [20, 22]. Endocrinal therapy is another type of systemic therapy that aims to reduce estrogen levels or prevent the hormonal stimulation of cancer cells. Medications that inhibit ER include selective ER modulators like tamoxifen and toremifene, as well as selective ER degraders such as fulvestrant. Treatments aimed at reducing estrogen levels include aromatase inhibitors like letrozole, anastrozole, and exemestane [20, 23]. Unfortunately, about half of hormone receptor positive breast cancers develop resistance to hormonal therapy as they undergo this form of treatment [20]. Resistance to endocrine therapies remains a challenge in both clinical and scientific realms. Current efforts to enhance the outcomes of ER+ breast cancer focus on targeting pathways, that are associated with ER function, such as the phosphoinositide 3-kinase/mammalian target of rapamycin (PI3K/mTOR) and cyclin pathways, that often undergo mutations in ER+ cancers [6]. This can be done through targeted therapies that exploit biological entities like interferons, interleukins, or monoclonal antibodies for a more specific approach. These include trastuzumab (targeting HER2), everolimus (targeting mTOR), palbociclib (targeting cyclin-dependent kinase 4/6), etc. Regardless, these therapies still produce off-target adverse effects like thrombocytopenia, fatigue, and anaemia [24].

## **1.2. Perturbations in tumour metabolism**

Cancer is a disease in which cells, due to certain mutations at the genomic level, begin to divide uncontrollably, grow into tumours, and spread to other organs. Increased proliferation requires a lot of inner resources of the cell, which makes it hard to maintain sustained proliferation without additional sources of fuel. Thus, another characteristic trait of cancer cells is the ability to obtain essential nutrients from an often nutrient-deprived environment and utilize these nutrients for both keeping cell viability and synthesizing biomass. Cancer-derived metabolic reprogramming has a significant impact on gene expression, cellular differentiation, and the tumour microenvironment [25]. The first study to spark the interest in cancer metabolism was the work carried out by Otto Warburg in the 1920's [3]. It showed that cultured cancer cells, as compared to normal ones, have a higher uptake of glucose and production of lactic acid, even in the presence of oxygen, suggesting glycolysis – the main form of energy production in anaerobic organisms, might have an impact in tumour metabolism. This added to the usual primary source of energy for aerobic organisms, that is oxidative phosphorylation (OXPHOS), results in a higher production rate of adenosine triphosphate (ATP). Glycolysis might



be a way to generate additional energy without the formation of excess mitochondrial reactive oxygen species (ROS) that come with OXPHOS, but it is not the most efficient way for producing ATP, meaning the main function of aerobic glycolysis in cancer might be different. Even though a century has passed since Warburg's discovery, the reasoning behind this phenomenon is not yet clearly understood. Experimental models show that withdrawal of glucose or inhibition of glycolysis disrupts tumorigenicity and the proliferation of cancer cells [26–28]. Rapid glucose uptake might be there to feed the pathways, leading to non-mitochondrial macromolecular synthesis. These involve the pentose-phosphate pathway (produces ribose for nucleotide synthesis and nicotinamide adenine dinucleotide phosphate (NADPH) for certain biological processes), the hexosamine pathway (necessary for adding sugar molecules to proteins – glycosylation), serine-glycine-one-carbon metabolism (helps in producing glutathione, nucleotides, and supports methylation reactions) and glycerol synthesis (involved in creating complex lipids). These are all pathways often activated in cancer [26]. However, lactic fermentation does not provide the biosynthetic pathways with any carbon, as all the carbon from glucose is secreted as lactic acid, meaning that if the Warburg effect really does supply the biosynthetic pathways, it does so indirectly, by providing pools of glycolytic intermediates, which feed the metabolic pathways involved in biomolecular synthesis [26, 29]. Even though exploiting the Warburg effect was proven to be an effective targeting strategy for cancer, the difficulty in finding the Holy Grail of chemotherapy lies in the flexibility of the metabolic systems involved. It is essential to track the contribution of multiple nutrients at the same time, as when it comes to cancer, reprogramming the preferred bioenergetic pathway can always get in the way.

Another of the key nutrients that tumours rely on is glutamine, a nonessential amino acid and the most abundant in the bloodstream. Experimental evidence underscores the significance of glutamine in tumour cells, ranking it second only to glucose [30]. Glutamine's role is to provide reduced hydrogen atoms for the production of NADPH. The latter is then used by cancer cells for fatty and nucleic acid synthesis. Another way glutaminolysis contributes to biosynthesis is by fueling the Krebs cycle, providing it with  $\alpha$ -ketoglutarate. Glutamine is also involved in the synthesis of an antioxidant tripeptide glutathione (comprised of glutamic acid, cysteine, and glycine), which serves as a protective agent against ROS, repairs DNA damage, activates transcription factors, etc. [31]. Although glutathione is an important part of healthy cell detoxification, which in terms helps reduce carcinogens, increased levels of glutathione in malignant cells are associated with tumour progression and increased resistance to chemotherapeutic agents [32], thus making it an attractive reprogramming strategy for cancer.

As cancer cells are derived from the same organism as healthy ones (as opposed to bacteria or other pathogenic microorganisms, whose treatment can rely on the differences in structural components of the cell) a better understanding of the differences in intracellular metabolism between healthy and malignant cells is crucial for finding a therapeutic window, in which cancer cells have a greater dependence on certain metabolic enzymes, than normal cells. This makes targeting cancer cells more specific than relying only on the rapid proliferation of the cells, which can be also seen in other quickly regenerating tissues like hair follicles, bone marrow, or skin, accounting for most of the side effects of traditional chemotherapy.

### **1.3. Amino acid metabolism as a target for chemotherapy**

A high rate of proliferation requires not only energy but also an array of different “building blocks” for biosynthesis. When faced with an increased demand, cancer cells can either depend on exogenous amino acids or *de novo* synthesis [33]. The latter would be much more effective in a nutrient-low environment, where cancer usually grows. However, due to the mutant nature of cancer, some of the enzymes, responsible for *de novo* synthesis of amino acids can get “lost in translation”, making the cells depend on exogenous sources, thus even the nonessential amino acids come to be essential, as cancer becomes auxotrophic to them [34]. One example would be the non-essential amino acid arginine. Arginine is the precursor of an array of different biomolecules, such as urea, creatine, glutamate, nitric oxide and polyamines. Although it is a nonessential amino acid that could be synthesised in the body under normal conditions, some cancers lack the enzyme argininosuccinate synthetase 1, which converts citrulline to arginine, making them dependent on exogenous arginine [35]. Reduced expression of the mentioned enzyme was also shown to be a biomarker for metastasis in osteosarcoma patients [36], as it plays an important role in cancer cell motility [34, 37, 38]. This makes arginine synthesis a potential target for arginine auxotrophic cancers [39–41]. Another example of amino acid dependency in cancer is the so-called Hoffman effect or methionine dependency. It was first noticed in 1959 when conducting experiments with diets, each lacking an essential amino acid, in tumour-bearing rats [42]. Sugimura *et al.* noticed a reduction in tumour size with a lack of methionine in the diet. Later, experiments proved that some cancer cells cannot proliferate if methionine in their nutritional media is replaced by its precursor L-homocysteine [43] (Fig.1.3.1). Even though cancer cells are able to synthesize methionine, the rate of biosynthesis does not meet the demand for cell proliferation, and malignant cells become auxotrophic to extracellular methionine, while normal cells have no problem

with making their own. The mechanisms involved in methionine dependency are still not fully understood [44].

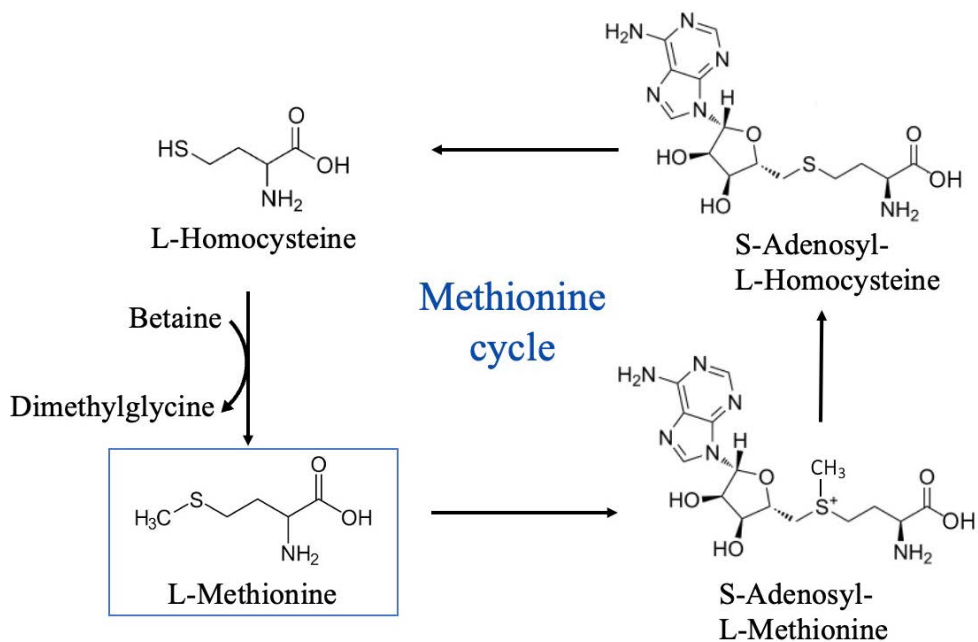


**Fig. 1.3.1.** A simplified diagram of the methionine cycle.

These alterations in amino acid metabolism in cancer are already a subject for drug design with some of the newly found compounds showing great success in clinical trials. One strategy for targeting auxotrophic cancers is enzymatic depletion. For example, the mentioned dependency on arginine in some cancers is exploited with a microbial-derived enzyme – arginine deiminase [33]. It catalyses the transformation of arginine to its precursor citrulline and has proved its effectiveness in clinical trials with metastatic melanoma [45] and hepatocellular carcinoma [46]. Using arginine deiminase together with a chemotherapeutic agent cytarabine also proved to be more effective than using cytarabine alone to treat acute myeloid leukaemia [47]. Another example of enzymatic depletion is recombinant methioninase, which is involved in the degradation of methionine into  $\alpha$ -ketobutyrate, ammonia, and methanethiol. It recently displayed promising results by lowering free methionine levels in the blood plasma of xenografic mice [48] and humans with prostate and ovarian cancer [49]. Other strategies for targeting amino acid metabolism in cancer include dietary restriction of certain amino acids and pharmacological inhibition of their metabolic enzymes [33].

## 1.4. Branched-chain amino acid metabolism in cancer

Leucine, isoleucine, and valine are three essential amino acids called branched-chain amino acids (BCAAs). Alterations in their metabolism are associated with obesity, diabetes, cardiovascular and neurodegenerative diseases as well as immune response [5, 50]. Increasing evidence also suggests BCAAs are important modulators of cancer progression due to their role in cellular energetics, biomolecular synthesis, and activation of various signalling pathways [33], making them an exciting new object for further research.

As essential amino acids, BCAAs cannot be synthesised in human cells, meaning they usually are a product of protein degradation or the outcome of reversible transamination reactions [51]. Animal cells are thus dependent on outside sources of BCAAs – they are transferred through the membrane by L-type amino acid transporters [52, 53] and into mitochondria by SLC25A44 [52, 54]. BCAAs can have several fates after entering the cell – they can either be directly incorporated into protein [55] or come in contact with branched-chain amino acid transaminases (BCATs), that carry out the first and reversible step in BCAA metabolism – their conversion to respective  $\alpha$ -keto acids (Fig. 1.4.1). This step yields glutamate after the amino group is transferred to  $\alpha$ -ketoglutarate [52]. BCAT has two isoforms: cytosolic BCAT1 and mitochondrial BCAT2 [51]. BCAT2 can be found ubiquitously in most tissues, however, BCAT1 can only be found in certain organs, such as the brain, kidney and ovaries [8, 56]. While these two isoforms are similar in substrate specificities, they have different amino acid sequences and play different roles in diseases [8, 56]. For example, BCAT1 is highly expressed in HER2+ and luminal B subtypes of breast cancer, whereas BCAT2 expression mostly correlates with luminal A subtype [57]. Some researchers also report the two having different regulatory mechanisms and physiological functions [8, 58]. The second step of the BCAA catabolism is catalysed by the multienzyme complex called branched-chain  $\alpha$ -ketoacid dehydrogenase, which irreversibly transforms  $\alpha$ -ketoacids to corresponding acyl-coenzyme A esters, releasing CO<sub>2</sub> and NADH as byproducts. Finally, metabolic intermediates of BCAAs enter the Krebs cycle, thus providing energy to the cell [56].

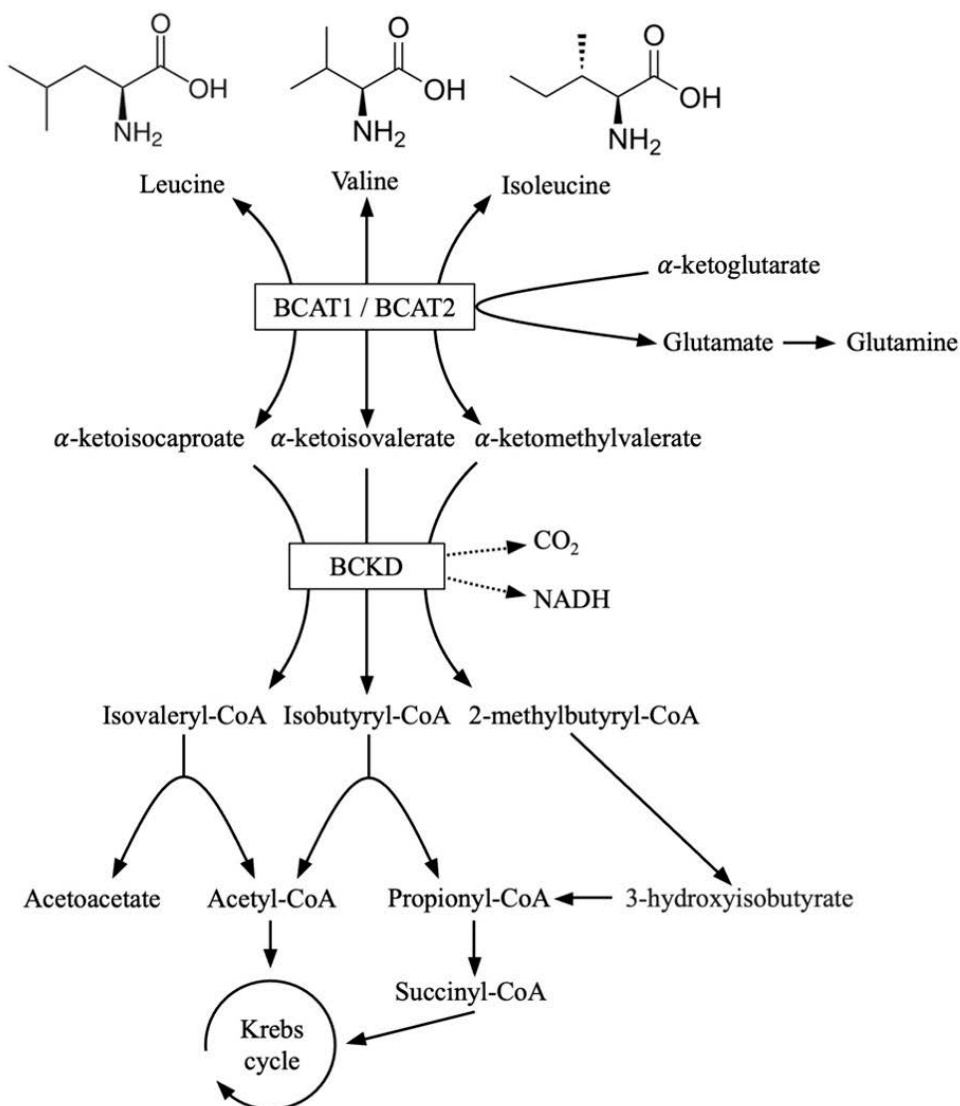


**Fig. 1.4.1.** A simplified diagram of BCAA degradation.

BCKD – branched-chain ketoacid dehydrogenase.

In previous experiments, our group showed BCAT2, as well as other enzymes involved in the pathway, to be overexpressed in most cancer cells by conducting an extensive microarray data analysis from the National Center for Biotechnology Information’s (NCBI’s) Gene Expression Omnibus (GEO) database [7]. Metabolic reprogramming associated with BCAA degradation was observed in different human cancer types by other researchers too. BCAT1 for example was found to be exclusively expressed in glioblastoma

with functioning isocitrate dehydrogenase 1 while also promoting glioma cell proliferation by increasing glutamate production [6]. It was also shown, that hypoxic conditions upregulate BCAT1, but not BCAT2 in glioblastoma cells [59]. Mice models with bearing blast crisis phase of chronic myeloid leukaemia had significant elevations of glutamate, alanine and BCAAs in their plasma, as compared to the chronic phase, suggesting that increased BCAA uptake might contribute to the progression of leukaemia [60]. Accumulation of BCAAs was also seen in clear-cell renal carcinoma [61]. Higher expression of the enzyme BCAT1 is deemed to be responsible for progression of chronic myeloid leukaemia, endometrial, and ovarian cancers [60, 62–65]. BCAT2 on the other hand is elevated in pancreatic ductal adenocarcinoma – knockdown of BCAT2 results in reduced cell proliferation [66, 67]. Osteosarcoma tumour biopsies were found to have higher expression of both BCAT1 and BCAT2, as compared to chondrosarcoma samples, showing that differential expression of these enzymes can be seen in different types of bone cancer [68]. The same discrepancies between the expression of BCAT isoforms can be seen in breast cancer [7, 57, 69]. The inhibition of both enzymes showed damaging effect on non-small cell lung carcinoma tumour formation as well [55].

It is not completely understood, why cancer cells have a higher demand for these amino acids specifically. Like most amino acids, they break down to produce acetyl coenzyme A (acetyl-CoA), propionyl coenzyme A, and succinyl coenzyme A, which could then be used for energy production. However, in almost every step of the BCAA degradation pathways, the resulting metabolites can be used for different purposes, such as fatty acid or cholesterol synthesis. Yang et al. revealed that increased consumption of BCAAs is activated under glutamine-starved conditions in hepatocellular carcinoma cells, suggesting BCATs have another important function – providing the byproduct glutamine to highly proliferating cells [70]. Leucine, the most abundant of the three amino acids, is also responsible for regulating the mTOR signalling pathway, highly associated with malignancy [71].

Contrary to glutamine or methionine, BCAAs are still quite a new field in cancer research [6], meaning there is still a lot to learn about the underlying mechanisms of why and how BCAAs benefit cancer, however, the sheer number of evidence linking BCAA metabolism to cancer suggests it as an attractive drug target for several cancer types.

### **1.5. The mevalonate pathway in cancer**

The product of BCAA breakdown – acetyl-CoA, contributes to more than just energy in the cell. It also provides precursor molecules for the biosynthesis of fatty and amino acids, as well as secondary metabolites, like

flavonoids and isoprenoids [72]. The latter are highly diverse molecules with functions including gene expression regulation, involvement in signalling pathways and membrane integrity, while also being precursor molecules for vitamin and reproductive hormone synthesis [73]. They are also involved in the synthesis of small GTPases such as those of Ras and Rho families, that are essential for invasion and metastasis of different types of cancer, including breast carcinomas [73]. The first and rate-limiting step in the synthesis of isoprenoids, as well as cholesterol and steroid hormones, is the conversion of 3-hydroxy-3-methylglutaryl coenzyme A (HMG-CoA), derived from acetyl-CoA, into mevalonate [74] (Fig. 1.5.1). Enzymes involved in the so-called mevalonate pathway are overexpressed in various types of cancer [76], including melanoma [77], glioblastoma [78, 79], breast [80], lung [81, 82], colorectal [83], prostate [84], and ovarian cancer [85], prompting researchers to investigate them as potential chemotherapeutic targets. However, the relevance of HMG-CoA reductase as a target for cancer treatment seems to be highly tumour type specific, therefore is a controversial topic in the scientific community [76].

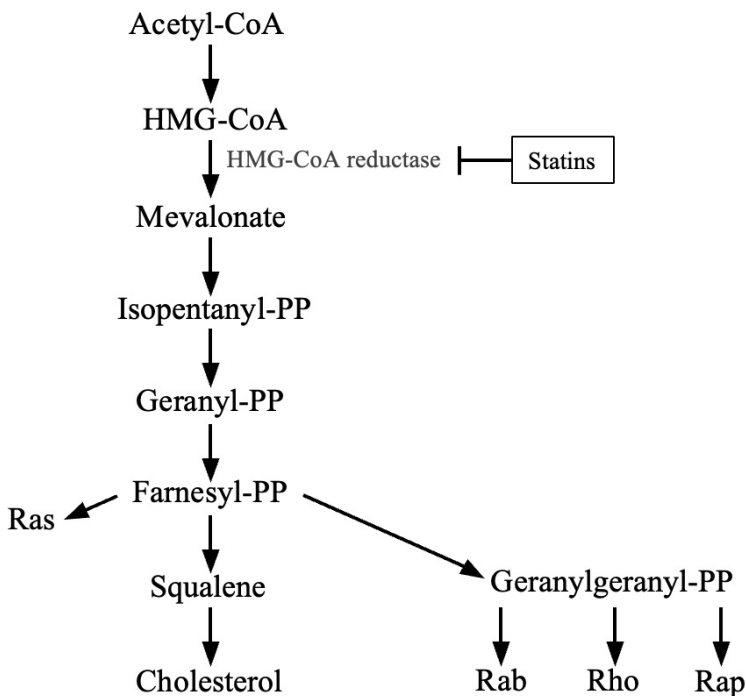


**Fig. 1.5.1.** *The mevalonate pathway.*

The rate-limiting step, catalysed by the enzyme HMG-CoA reductase can be inhibited by antihypercholesterolemic drugs – statins, which are used to control the risk of atherosclerotic events in patients with dyslipidemia. Figure adapted from Rikitake et al. [75].

## 1.6. Bioinformatics in cancer research

Even though medicine progressed a lot in the field of oncology, there is still a considerable amount of work ahead to enhance clinical results. Two main issues still stand in the way: the need for a definitive and early diagnosis and options for effective and long-lasting therapy. Understanding the molecular mechanisms of cancer is needed for both problems to be solved [86]. Following the initial version of the human genome project, the focus shifted from the genes themselves to their products. Functional genomics explores the role of genetic information, examining genes, the proteins they code, and their functions. Proteomics examines all the proteins in the cell, while transcriptomics looks at all the transcripts of the cell's RNA, known as the transcriptome. Due to the large amount of data generated by such techniques, these sciences go hand in hand with information technology [87]. For example, findings from metabolomics undergo multiple rounds of processing. This procedure can be broken down into two primary phases: the first step involves handling the initial mass spectrometry data, including peak detection, alignment, and annotation. This step results in a table containing all identified metabolites in the samples. The second stage of data processing involves computations of metabolite quantities, statistical analysis, and aligning the results with the biological context of the study [88].

Understanding metabolic flux distributions is crucial for figuring out how metabolic reactions interplay in the cell. All bioinformatics methods mentioned can be used to tackle cancer, starting with genetic studies of tumours [89] and ending with mapping out their metabolic pathways on a genome-scale [90].

Modelling of metabolism at the genome scale is rapidly increasing in popularity among scientists as a sufficiently accurate method to predict metabolic phenotype, for example: the rate of growth and nutrient absorption or the importance of certain genes [91]. Briefly, metabolic modelling consists of five steps: 1) selection of an appropriate database, 2) mapping of metabolic pathways, 3) network pruning, 4) search algorithm implementation, and 5) metabolic pathway evaluation to select the best one. Genome-scale metabolic models (GSMMs) are databases of all biochemical reactions, metabolites, and genes of a given organism. GSMMs also describe the biophysical constraints of metabolic systems, such as nutrient uptake, oxygen availability or the stoichiometry and reversibility of reactions [91].

Computational studies like these can help find principal metabolic pathways in cancer and form hypotheses, which can then be used for further research and eventually – drug development. With the help of computer systems, we can now learn more about cancer than we could ever imagine.



## 2. MATERIALS AND METHODS

### 2.1. Materials

#### 2.1.1. Cell culture reagents and materials

Reagent/Material	Distributor
Cholera toxin from <i>Vibrio cholerae</i>	Sigma-Aldrich, St. Louis, MO, USA
Dulbecco's Modified Eagle Medium (DMEM)	Sigma-Aldrich, St. Louis, MO, USA
Fetal bovine serum (FBS)	Sigma-Aldrich, St. Louis, MO, USA
Fibronectin	Sigma-Aldrich, St. Louis, MO, USA
Ham's F-12 Nutrient Mix (F-12)	Life Technologies, Carlsbad, CA, USA
Horse serum (HS)	GE Healthcare Life Sciences, Logan, UT, USA
Hydrocortisone	Sigma-Aldrich, St. Louis, MO, USA
Penicillin-Streptomycin (10,000 units penicillin and 10 mg streptomycin/mL) (pen-strep)	Sigma-Aldrich, St. Louis, MO, USA
Phosphate-buffered saline (PBS)	Life Technologies, Carlsbad, CA, USA
Recombinant human epidermal growth factor (rHu EGF)	Thermo Fisher Scientific, Frederick, MD, USA
Recombinant human insulin (rHu insulin)	Life Technologies, Carlsbad, CA, USA
Trypsin-EDTA	Sigma-Aldrich, St. Louis, MO, USA

#### 2.1.2. Cell lines

Cell line/biomaterial	Distributor
Breast cancer cells (BCC)	[7]
Michigan Cancer Foundation-10A (MCF-10A)	ATCC, Wesel, Germany
Michigan Cancer Foundation-7 (MCF-7)	CLS-Cell Lines Service, Eppelheim, Germany

#### 2.1.3. Chemicals and reagents

Reagent	Distributor
5,5',6,6'-tetrachloro-1,1',3,3'-tetraethylbenzimidazolylcarbocyanine iodide (JC-1)	Merck, Darmstadt, Germany
7-aminoactinomycin D (7-AAD)	Thermo Fisher Scientific, Frederick, MD, USA
Acetonitrile	Scharlau, Barcelona, Spain
Ammonium bicarbonate	Sigma-Aldrich, St. Louis, MO, USA
Dimethyl sulfoxide (DMSO)	Sigma-Aldrich, St. Louis, MO, USA

DNA/RNA Shield™	Zymo Research, Irvine, CA, USA
Ethanol 96 %	Vilnius Degtinè, Vilnius, Lithuania
Formic acid	Merck, Darmstadt, Germany
Hydrochloric acid 12M	Honeywell, Charlotte, NC, USA
L-Glutamine- <sup>13</sup> C <sub>5</sub>	Sigma-Aldrich, Hamburg, Germany
L-Isoleucine- <sup>13</sup> C <sub>6</sub> , <sup>15</sup> N	Sigma-Aldrich, Hamburg, Germany
L-Leucine- <sup>13</sup> C <sub>6</sub> , <sup>15</sup> N	Sigma-Aldrich, Hamburg, Germany
L-Valine- <sup>13</sup> C <sub>5</sub> , <sup>15</sup> N	Sigma-Aldrich, Hamburg, Germany
Methanol	Sigma-Aldrich, St. Louis, MO, USA
Trypan blue	Sigma-Aldrich, St. Louis, MO, USA

## 2.1.4. Databases

Database	Website
Ensembl Biomart	<a href="https://www.ensembl.org/info/data/biomart/">https://www.ensembl.org/info/data/biomart/</a>
Kyoto Encyclopedia of Genes and Genomes (KEGG)	<a href="https://www.genome.jp/kegg/">https://www.genome.jp/kegg/</a>
NCBI's GEO	<a href="https://www.ncbi.nlm.nih.gov/geo/">https://www.ncbi.nlm.nih.gov/geo/</a>

## 2.1.5. Instruments

Instrument	Distributor
Acquity H-Class Ultra-Performance Liquid Chromatography system (UPLC)	Waters, Milford, MA, USA
Binder CB 150 CO <sub>2</sub> incubator	Binder, Tuttlingen, Germany
Concentrator	Merck, Darmstadt, Germany
Holten Safe 2010 laminar	Holten A/S -Thermo, Allerød, Denmark
Illumina NovaSeq system	Illumina, San Diego, CA, USA
Neubauer hemocytometer	BRAND GMBH + CO KG, Warthelm, Germany
Peristaltic pump (for vacuum filtration)	VWR, Radnor, PA, USA
Sigma 1-14 microcentrifuge	Sigma Laborzentrifugen, Hartz, Germany
Sigma 3-18KS centrifuge	Sigma Laborzentrifugen, Hartz, Germany
Triple quadrupole tandem mass spectrometer (MS/MS) Xevo TQD with an electrospray ionization (ESI) ion source	Waters, Milford, MA, USA
Ultra-low temperature freezer	Thermo Electron Corporation, Marietta, OH, USA
Vortex mixer	IKA-Werke, Staufen, Germany
Water deionisation system	Barnstead Thermolyne, Dubuque, IA, USA
YMC-Triart C18 column, 100 × 2.0 mm, 1.9 μm	YMC, Kyoto, Japan

### 2.1.6. Kits

Kit	Distributor
JetPRIME transfection reagent kit	Polyplus-transfection, Illkirch-Graffenstaden, France
Zymo-Seq RiboFree total RNA library prep kit	Zymo Research, Irvine, CA, USA

### 2.1.7. Other materials

Material	Distributor
siRNA against BCAT2 (cat#4392420 s1905)	Ambion, Austin, TX, USA

### 2.1.8. Software and tools

Software	Company
Bowtie2	Johns Hopkins University (open-source) [92]
COBRAPy	The cobrapy core team (open-source) [93]
HTSeq	the HTSeq team (open-source) [94]
MetaboAnalyst	XiaLab Analytics Inc at McGill University (open-source) [95]
Microsoft Excel 16.75	Microsoft, Redmond, WA, USA
WebGestalt	Zhang Lab at the Baylor College of Medicine (open-source) [96]

## 2.2. Methods

### 2.2.1. Cell cultures and their growing conditions

Throughout this dissertation, two commercial cell lines were used: epithelial breast adenocarcinoma (Michigan Cancer Foundation-7; MCF-7) and normal epithelial breast (Michigan Cancer Foundation-10A; MCF-10A) cells. Our model of ductal carcinoma cells BCC (breast cancer cells) is a patient-derived primary cell culture described in an earlier publication [7]. MCF-7 and BCC cell lines reflect Luminal A and B subtypes of breast cancer. MCF-7 and BCC cells were grown in DMEM/F-12 (1:1) cell culture media, supplemented with 10 % FBS and 1 % pen-strep. MCF-10A cells were cultured in DMEM/F-12 (1:1) supplemented with 5 % HS, 1 % pen-strep, rHu insulin (10 µg/mL), cholera toxin (100 ng/mL), rHu EGF (20 ng/mL) and hydrocortisone (500 ng/mL). For experiments where different amounts of nutrients were needed,

custom media was prepared following the composition of DMEM. All media used was sterile-filtered through a 0.2  $\mu\text{M}$  surfactant-free cellulose acetate membrane vacuum filtration system. Cells were cultivated in surface-treated flasks or plates in a humidified incubator at 37 °C with a CO<sub>2</sub> concentration of 5 %. A solution of trypsin-EDTA, diluted to the final concentration of 0.05 % with PBS was used to detach the cells before re-seeding. DMEM media supplemented with 15 % FBS and 10 % DMSO was used for long-term cryopreservation of cells in an ultra-low temperature freezer at –80 °C.

### 2.2.2. Transfection

All necessary transfection procedures were executed following the protocol for jetPRIME® transfection reagent. Cells were seeded in 6-well plates or 35 mm Ø Petri dishes a night before so that 60-80 % confluency would be reached at the time of transfection. A 5 nM concentration of siRNA against the BCAT2 gene and an appropriate amount of transfection reagent jetPRIME® were used to suppress the BCAT2 gene. An appropriate amount of siRNA was added to a sterile tube with jetPRIME® buffer, mixed by a vortex mixer for 10 seconds, and centrifuged, then the transfection reagent was added to the test tube, mixed again for 10 seconds and incubated at room temperature for 10 min. After incubation, the mixture was dispensed into respective wells. Controls were performed the same way, without the addition of siRNA. Cell culture media is changed 24 hours after transfection to eliminate residues of transfection reagents.

### 2.2.3. Wound healing assay

Prior to the experiment, 35 mm Ø Petri dishes were coated with fibronectin dissolved in a minimal volume of PBS (1  $\mu\text{g}/\text{cm}^2$ ) and air-dried in the laminar at room temperature. Cells were seeded so that their confluence at the time of transfection would be 50 %. A 24-hour period after transfection was used as a starting point for wound healing. A monolayer of cells is then scraped with the sharp edge of a disposable 10  $\mu\text{L}$  pipette tip and the track formed is then fixed into position for time-lapse imaging in a temperature-controlled microscope stage with CO<sub>2</sub> control. 8 hours past the start of the experiment, the first and last images are measured for wound closure, using the calculations below:

$$\text{Wound closure (\%)} = (A(t = 0\text{h}) - A(t = \Delta\text{h})) / (A(t = 0\text{h}))$$

A(t = 0h) – area of the wound immediately after scrape (time zero)  
A(t =  $\Delta$ h) – area of the wound h hours after scrape

## 2.2.4. Experiments with $^{13}\text{C}$ isotope-labelled amino acids

For the isotope labelling experiments, cells were cultured for 24 hours in custom media replacing BCAAs or glutamine (depending on the experiment) with their isotope-labelled counterparts. This media was designed following the composition of DMEM, supplemented with 10 % FBS, and 1 % pen-strep. To assess the BCAA labelling pattern, L-Valine $^{13}\text{C}_5,^{15}\text{N}$ , L-Leucine $^{13}\text{C}_6,^{15}\text{N}$ , and L-Isoleucine $^{13}\text{C}_6,^{15}\text{N}$  were each added to the final concentration of 0.8 mM. Only L-Leucine $^{13}\text{C}_6,^{15}\text{N}$  was added to the media in the concentration mentioned above to determine the labelling pattern of mevalonate. The assessment of glutaminolysis was carried out by supplementing the media with L-Glutamine $^{13}\text{C}_5$  in the final concentration of 4 mM.

## 2.2.5. Metabolite extraction from cells

For the metabolomics analysis, the cell extracts were prepared as in the protocol by Sellick and co-workers [97]. Quenching of the cells (to stop cell metabolism) requires a solution comprised of 60 % methanol (diluted with deionised water) and 0.85 % ammonium bicarbonate. The pH of this solution is adjusted with 12 M hydrochloric acid to 7.4. After detaching and centrifuging the cells, one volume of the pellet is resuspended with 5 volumes of quenching solution and transferred to a 50 mL centrifuge tube. The tubes with the quenching solution are cooled beforehand in an ethanol/dry ice bath to the exact temperature of  $-40\text{ }^\circ\text{C}$ . After the addition of the cells, the tubes are shaken gently and immediately transferred to a refrigerated centrifuge at  $-20\text{ }^\circ\text{C}$ ,  $1000\times\text{g}$  for 1 min. The supernatant is removed, and the cells are resuspended in 500  $\mu\text{L}$  of methanol (chilled at  $-80\text{ }^\circ\text{C}$ ) and transferred to a microcentrifuge tube (tube 1). The tube is then submerged in liquid nitrogen for immediate freezing. After the contents of the tube are completely frozen, the tube is thawed and vortexed for 30 seconds. Then the tube is centrifuged at  $800\times\text{g}$  for 1 min. The supernatant is transferred to a new microcentrifuge tube (tube 2) kept on dry ice for later use. The pellet from tube 1 is then resuspended in methanol and submerged in liquid nitrogen again, following the same steps until after centrifugation, when the supernatant is transferred to tube 2. The pellet from tube 1 is resuspended in 250  $\mu\text{L}$  of cold deionised water and frozen again in liquid nitrogen, thawed and vortexed for 30 seconds, and centrifuged at  $15000\times\text{g}$ . The supernatant is then collected and mixed with the methanol fractions in tube 2. All the extraction fractions are then centrifuged at  $15000\times\text{g}$  for 1 min and the remaining supernatant is transferred to a new tube (tube 3). Tube 3 is then dried with a concentrator at  $30\text{ }^\circ\text{C}$ . The dried metabolite extracts can then be stored at  $-80\text{ }^\circ\text{C}$  or rehydrated with deionised water and analysed with UPLC-ESI-MS/MS.

## **2.2.6. Plasma preparation for mass spectrometry analysis**

A permit from the Kaunas Regional Biomedical Research Ethics Committee (2021-03-23, No. BE-2-32, Supplement S1) was obtained for the analysis of blood plasma. All subjects were women and gave written informed consent. 20 blood samples were taken in total: 10 taken from healthy control subjects and 10 from patients with an early diagnosis of invasive ductal carcinoma of the same subtype as BCC cell line (T1 N0 M0 G2, ER+, PR+, HER2(3+)). The samples consisted of 3 mL of freshly drawn blood in EDTA-treated (purple) blood collection tubes. Immediately after collection, the samples were centrifuged at  $1300\times g$  for 20 min at  $10\text{ }^{\circ}\text{C}$ . 1.5 mL of the supernatant (plasma) was then carefully transferred to a new tube and centrifuged at  $15500\times g$  for 10 min at  $10\text{ }^{\circ}\text{C}$ . The supernatant collected was aliquoted into microcentrifuge tubes and kept in the freezer at  $-80\text{ }^{\circ}\text{C}$  for long-term storage. To prepare the plasma for chromatographic analysis, 1.5 mL of ice-cold methanol was added to 250  $\mu\text{L}$  of plasma for protein separation. Samples were then mixed for 10 seconds and kept at  $-20\text{ }^{\circ}\text{C}$  for 20 min. The precipitated samples were centrifuged at  $18000\times g$  for 10 min at  $4\text{ }^{\circ}\text{C}$ . The supernatant was then dried in a vacuum concentrator and kept at  $-80\text{ }^{\circ}\text{C}$  until instrumental analysis. The dried pellet was dissolved in acetonitrile in preparation for chromatography.

## **2.2.7. UPLC-ESI-MS/MS**

After performing the metabolite extraction, samples were analysed with the Acquity H-Class UPLC system. A YMC-Triart C18 ( $100\times 2.0\text{ mm}$ ,  $1.9\text{ }\mu\text{m}$ ) column was used to separate the extracts and a triple quadrupole tandem mass spectrometer Xevo TQD coupled with an electrospray ionization (ESI) ion source was used for obtaining mass spectrometry data in negative mode with the range of  $50\text{ m/z}$  to  $250\text{ m/z}$ . The column's temperature was set to  $40\text{ }^{\circ}\text{C}$ . Elution with a mobile phase of 0.1 % formic acid aqueous solution (solvent A) and acetonitrile (solvent B) was performed at the flow rate of  $0.4\text{ mL/min}$  in a gradient with the proportions of solvent A changed as follows: 0–0.2 min 95 %, 0.2–1.5 min 10 %, 1.5–1.8 min 90 % and 1.8–2 min back to starting conditions. The mass spectrometer's capillary voltage was set to  $-2\text{ kV}$ , source temperature set at  $150\text{ }^{\circ}\text{C}$ , desolvation gas (nitrogen) temperature was set at  $400\text{ }^{\circ}\text{C}$ , gas flow at  $700\text{ L/h}$ , cone gas flow at  $-20\text{ L/h}$ . Cone voltage was set to 25 V.

## **2.2.8. Analysis of metabolomics data**

Three biological replicates of metabolic samples were carried out. Metabolites, that were present in all the samples, were identified based on their

retention times, reported by Virgiliou and co-authors [98]. MetaboAnalyst [95] was used to analyze the data and a different tool – WebGestalt (webgestalt.org) was used for pathway enrichment analysis, as MetaboAnalyst did not identify clear metabolic relationships between the perturbed metabolites (apart from the obvious, such as taurine and hypotaurine).

### **2.2.9. <sup>13</sup>C-based flux patterns**

The ratios of non-labelled (M0) malate and malate with two carbons labelled (M2), were used for the estimation of acetyl-CoA fractions derived from BCAAs. In the experiments with labelled glutamine, the extent of glutaminolysis was assessed using the fraction of malate with four carbons labelled (M4) as a direct estimation of the fraction of  $\alpha$ -ketoglutarate originating from glutamine. The interactions with enzymes such as malic enzyme and pyruvate carboxylase create complex labelling patterns of the Krebs cycle intermediates, that were not modeled in this work. The metabolic fluxes around HMG-CoA resulted in a complex labelling pattern of mevalonate. The elementary metabolic units (EMU) method [99] was used to calculate the fluxes. A customised Python script was written to predict labelling patterns of mevalonate from flux distributions (Supplement S2). Metabolic fluxes were adapted to minimize the relative errors between predicted and observed mass fractions of mevalonate.

### **2.2.10. RNA sequencing**

We prepared three biological replicates for each of the studied cell lines (MCF-7, MCF-10A, and BCC). After trypsinization,  $1 \times 10^6$  cells from each sample were mixed with 500  $\mu$ L of DNA/RNA Shield™ transport and storage medium in preparation for shipment. Samples were sent to Zymo Research facilities for next-generation RNA sequencing (RNA-seq). The company constructed RNA-seq libraries from 500 ng of total RNA using the Zymo-Seq RiboFree Total RNA Library Prep Kit. The analysis was done on an Illumina NovaSeq system to a sequencing depth of at least 30 million read pairs (150 bp paired-end sequencing) per sample.

### **2.2.11. Analysis of RNA-seq data**

Bowtie2 [92] was used to align the pair-ended reads on a reference sequence (the complete list of human transcripts was obtained from Ensembl BioMart). Customised Python scripts (Supplement S3) based on the HTSeq library [94] were used to analyse the sequence alignment map files obtained. The expression of each gene was calculated in reads per kilobase per million

reads (RPKM). When comparing malignant and non-malignant cell lines, Student's t-test was used to determine upregulated and downregulated genes. The values were corrected for multiple testing as described in previous work (Python code used for differential expression analysis is available as Supplement S4) [7]. Raw and processed data was submitted to NCBI's GEO database (accession number GSE223718).

### **2.2.12. Integrated data analysis using pyTARG**

A GSMM [100] was used to obtain meaningful relationships between metabolomics and transcriptomics so that perturbations in metabolite levels and concomitant changes in gene expression could be correlated. pyTARG – a Python library previously developed [100], was used to estimate metabolic fluxes from the gene expression data. The pyTARG library works as follows: each of the modelled reactions, catalysed by metabolic enzymes, is given a maximal rate that is proportional to the expression level of the gene coding the enzyme (obtained from RNA-seq data). After the model is constrained, a metabolic flux distribution is simulated by optimizing the rate of biomass production. As there are three biological replicates for each of the cell lines, three metabolic flux distributions are obtained. This enables the identification of statistical differences in the reaction rate between different cell lines. Metabolic reactions that differ between malignant and non-malignant cell lines were determined by Student's t-test and a false discovery rate of 0.05 after correction for multiple testing. An average difference in flux that was higher than  $0.001 \text{ mmol h}^{-1} \text{ g-DW}^{-1}$  (millimoles per hour per gram of dry weight) was also required. Broad changes in metabolic flux distributions can be influenced by expression levels of a relatively small number of metabolic genes. To find out the flux-controlling genes, significant changes in both the estimated reaction rate and the expression level of at least one of their associated genes were identified.

### **2.2.13. Statistical analysis**

All the experiments with the cells were performed with a minimum of three biological replicates ( $n = 3$ ). Scattered data in plots was represented by standard error. Pairwise comparisons were performed using the Student's t-test. The confidence level was  $p < 0.05$ . Statistical analysis for wound healing and experiments with blood plasma was performed using "Microsoft Excel 16.75". Metabolomics data analysis was conducted using MetaboAnalyst [101], a web-based software tool widely utilised for its comprehensive suite of analysis functionalities. Principal Component Analysis (PCA) was performed for dimensionality reduction and visualization of metabolite



profiles. Data preprocessing, including normalization and scaling, was carried out prior to PCA. Heat maps were generated to visualize the relative abundance of metabolites across samples, with options for data transformation and scaling selected by the user. Box plots were employed to illustrate the distribution of metabolite abundance among different sample groups, aiding in the identification of significant differences. After alignment, counting and normalization of reads, using a Python script based on the HTSeq library, differential expression analysis of RNA-seq data was also conducted using Python. The script employed a t-test to assess statistical significance between different cell lines, yielding p-values for each gene. Gene identifiers along with fold change values were extracted from the analysis results and organised into a tabular format suitable for plotting. Utilizing Python libraries for data visualization, a volcano plot was generated with fold change values on the x-axis and  $-\log_{10}$  transformed p-values on the y-axis. Each point on the volcano plot represented an individual gene, allowing for customization to highlight genes meeting specific significance criteria. This methodology facilitated the visualization and interpretation of significant differential expression patterns between cell lines, thereby identifying genes of interest for further investigation.

### 3. RESULTS AND DISCUSSION

#### 3.1. Quantification of cellular energy derived from the degradation of BCAAs

It is not currently possible to obtain direct measurements of metabolic reaction rates, however, metabolic fluxes can be quantified indirectly, by measuring labelling patterns of intracellular metabolites. This method assumes that molecules, comprised of isotopic atoms (for example  $^{13}\text{C}$  versus  $^{12}\text{C}$ ) do not have a significant effect on metabolic reaction rates. These isotopic atoms can be used to track the metabolic pathways from which the resulting molecules have originated. The number of labelled atoms in a molecule can be obtained by highly sensitive methods, such as nuclear magnetic resonance or tandem mass spectrometry (MS/MS) [102, 103]. So in order to find out how BCAAs contribute to cellular energetics, we cultivated MCF-7, BCC, and MCF-10A cells in custom-made DMEM growth medium with fully  $^{13}\text{C}$  and  $^{15}\text{N}$  labelled leucine, isoleucine, and valine instead of the naturally occurring BCAAs. We measured the fraction of acetyl-CoA, which originated from the breakdown of BCAAs, as a ratio of malate with two carbons labelled (M2) to non-labelled malate (M0) (see Fig. 3.1.1, a). This ratio provides an estimate of how much acetyl-CoA, originating from labelled amino acids, enters the Krebs cycle. However, first we have to rule out several factors, that can influence the amount of malate from other sources. During the breakdown of glutamine,  $\alpha$ -ketoglutarate also enters the Krebs cycle, causing a dilution in the ratio of labelled/unlabelled malate (Fig. 3.1.1, b). Taking this into account, we performed parallel experiments with fully labelled glutamine to calculate the influence of glutaminolysis. Second, even though a custom media containing labelled amino acids was prepared, a fraction of non-labelled BCAAs could still be present due to protein turnover and bovine serum supplementation. In order to properly identify the fraction of labelled BCAAs, compared to the total BCAAs degraded, we measured fractions of BCAA transamination metabolites (4-methyl-2-oxopentanoate, 3-methyl-2-oxopentanoate and 3-methyl-2-oxobutanoate) with and without isotopic labelling. The relative labelled fraction of the degradation intermediates was  $0.7 \pm 0.02$  for MCF-7 and  $0.7 \pm 0.004$  for BCC (error values correspond to standard deviation). The fractions were remarkably equal for all three amino acids in both cell lines, suggesting that the remaining 30 % of the non-labelled BCAAs came from the complex cell culture media. Now we can divide the labelled acetyl-CoA fraction by 0.7 to find out the amount of mitochondrial acetyl-CoA originating from BCAA degradation. In the experiments with labelled glutamine, we considered the fraction of fully

labelled (M4) malate to be equal to the fraction of  $\alpha$ -ketoglutarate derived from glutamine degradation. The other fractions of labelled malate (M1, M2 and M3) derived from labelled glutamine could be a result of an array of reactions involving enzymes like malic enzyme and pyruvate carboxylase, which are not part of this work. It should be acknowledged, however, that the M2 malate fraction made up almost 50 % of all malate in MCF-10A, while little to none of the M1 fraction was observed, suggesting non-malignant cells use alternative malate synthesis pathways. The measured M4 malate fraction was 0.5 for BCC and 0.17 for both MCF-7 and MCF-10A. This indicates that glutaminolysis is more important for BCC cells. In experiments with labelled BCAAs, other fractions of labelled malate not looked at in this work (M1, M3 and M4) made up very small portions of all malate produced in BCC and MCF-7 and were only moderately higher in non-malignant MCF-10A cells. The complete distribution of labelled malate fractions in different cell lines can be seen in Fig. 3.1.2.

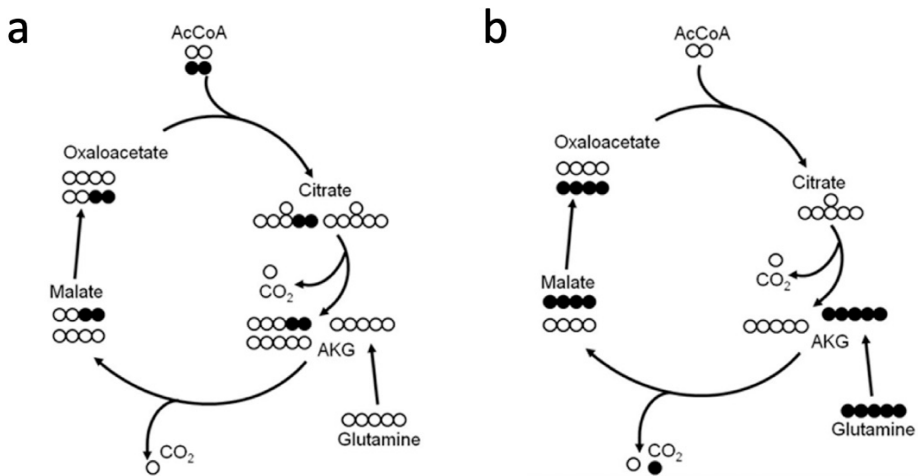


**Fig. 3.1.1.** Malate labelling patterns. Schemes show how the breakdown of labelled acetyl-CoA results in the formation of M2 malate (a) and labelled glutamine results in M4 malate (b).

$^{13}\text{C}$  labelled carbons are shown in black. AcCoA – acetyl-CoA, KG –  $\alpha$ -ketoglutarate.

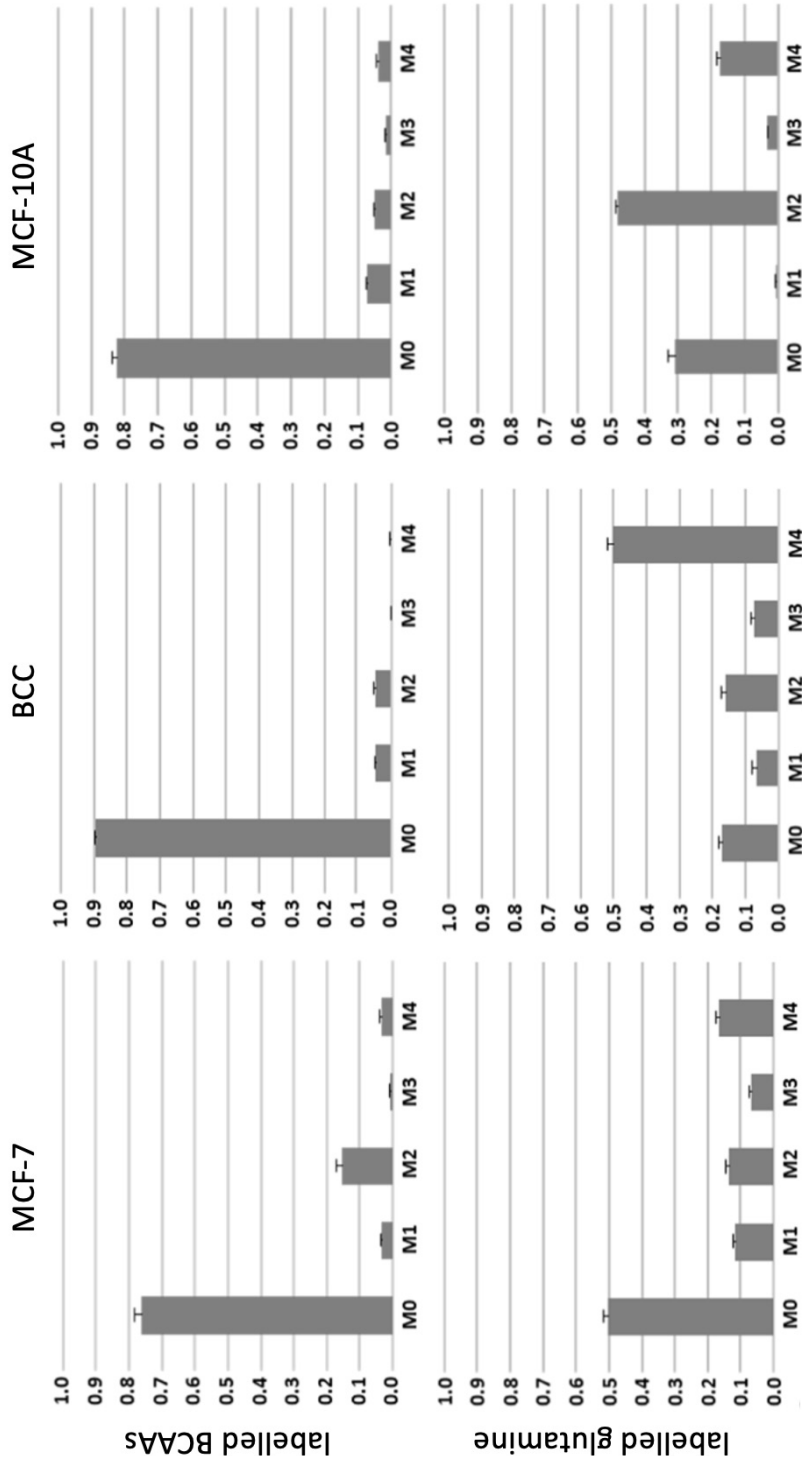


*Fig. 3.1.2. Full experimental labelling patterns of malate fractions.*

Taking into consideration the  $\alpha$ -ketoglutarate fraction calculated earlier and the fact that only 70 % of the BCAAs in the culture media were labelled, we calculated the fraction of acetyl-CoA originated from BCAAs in different cell lines as follows:

$$facetylCoA = \frac{M2/M0 \text{ malate fraction}}{BCAAs \text{ labelled } (1 - \text{glutaminolysis})}$$

$$facetylCoA(BCC) = \frac{M2/M0}{0.7(1 - 0.5)} = \frac{0.05}{0.35} \approx 0.14$$

$$facetylCoA(MCF-7) = \frac{M2/M0}{0.7(1 - 0.17)} = \frac{0.2}{0.58} \approx 0.34$$

$$facetylCoA(MCF-10A) = \frac{M2/M0}{0.7(1 - 0.17)} = \frac{0.06}{0.58} \approx 0.1$$

These results indicate that 34 % of the energy produced by the Krebs cycle in MCF-7 cells is derived from BCAA degradation. As glutaminolysis has a high impact on BCC energy metabolism, BCAA degradation results in only 14 % of acetyl-CoA, which is still higher than in non-malignant MCF-10A cells, where BCAAs account for 10 % of acetyl-CoA.

Our findings suggest, that BCAA degradation accounts for up to a third of the energy produced by the Krebs cycle in MCF-7 breast cancer cells. However, the contribution varies from cell line to cell line, as was estimated in a previous study by our group [7]. During the study, in which all the degraded BCAAs were assumed to feed the Krebs cycle, it was estimated that BCAAs account for up to 47 % of the total energy production in MCF-7. This experiment shows that the actual numbers are lower, suggesting that not all BCAAs are broken down to acetyl-CoA, with some degradation intermediates dedicated to the synthesis of other molecules, such as mevalonate, which is the focus of section 3.2 of this dissertation.

BCAAs playing a role in the energy production of cancer cells by supplying carbon atoms to the Krebs cycle would be the most straightforward explanation for the observed association between BCAA degrading enzymes and cancer progression, however, current research struggles to find a definite answer. In a study focusing on the effect of malic enzyme depletion in pancreatic cancer cells, consequential elevation in BCAA levels was associated with highly aggressive pancreatic ductal adenocarcinoma, but no labelled BCAA intermediates were observed entering the Krebs cycle [104]. The same article also rejected the involvement of mitochondrial respiration, as neither knockdown nor overexpression of BCAT2 had an impact on the consumption rate of oxygen. Nonetheless, they concluded pancreatic cancer cells are

highly dependent on BCAAs and suggested malic enzyme inhibition as a therapy option for a significant amount of patients. Other isotope labelling experiments involving BCAAs conducted by Hattori *et al.* on murine models of chronic myeloid leukaemia found that the BCAAs are more likely to be transformed from corresponding branched-chain keto-acids than to them. That would explain the observations of elevated BCAAs in the plasma of patients and the overexpression of BCAT enzymes in cancer cells, as the first reaction in BCAA breakdown is reversible. However, it still does not explain why and how BCAAs are important for cancer progression. The possibility of BCAAs playing a key role as nitrogen sources via transamination has also been discussed [105], though the experimental uptake rates of BCAAs in cancer cells are in all cases [106] much lower than glutamine uptake, that is the main source of nitrogen by transamination. Taking all this into account we can conclude that even though BCAAs are definitely important for cancer progression, their utilization by different cancer cells can be challenging to understand completely, as it varies quite significantly from cell line to cell line.

Our experiments show that a significant fraction of the cellular energy in MCF-7 is obtained by breaking down BCAAs and incorporating them into the Krebs cycle, which is not the case for other types of cancer. For example, the energy production of our model cell line BCC was less dependent on BCAAs, as their contribution was only 40 % higher than that of the non-malignant MCF-10A cells. These results confirm, that different cancer cells can be very different concerning their metabolism, and suggest the need for a more personalised approach in search of the optimal treatment for each cancer patient. For instance, dietary BCAA reduction or inhibition of BCAA metabolism could be an effective adjuvant therapy for hormone receptor-positive and HER2– luminal breast cancer (as is MCF-7), but might not do much for HER2+ (BCC).

### **3.2. Contribution of BCAAs to mevalonate metabolism**

Acetyl-CoA, besides its main function of energy production, can also be used for lipid synthesis following the mevalonate pathway [72]. Mevalonic acid is a precursor of cholesterol and other sterols essential for the cell. Since mevalonic acid is mostly found in carboxylate anion form in nature, it will be called mevalonate throughout this dissertation. Mevalonate is synthesised from HMG-CoA by an enzyme called HMG-CoA reductase. In humans, this enzyme is coded by a gene named HMGCR. HMG-CoA can be a product of leucine degradation, hence we performed experiments with  $^{13}\text{C}_6^{15}\text{N}$  labelled leucine, to find the extent leucine contributes to the mevalonate pathway. Fig. 3.2.1 illustrates changes in carbon labelling patterns of intermediates in the pathway when leucine is fully  $^{13}\text{C}$  labelled.

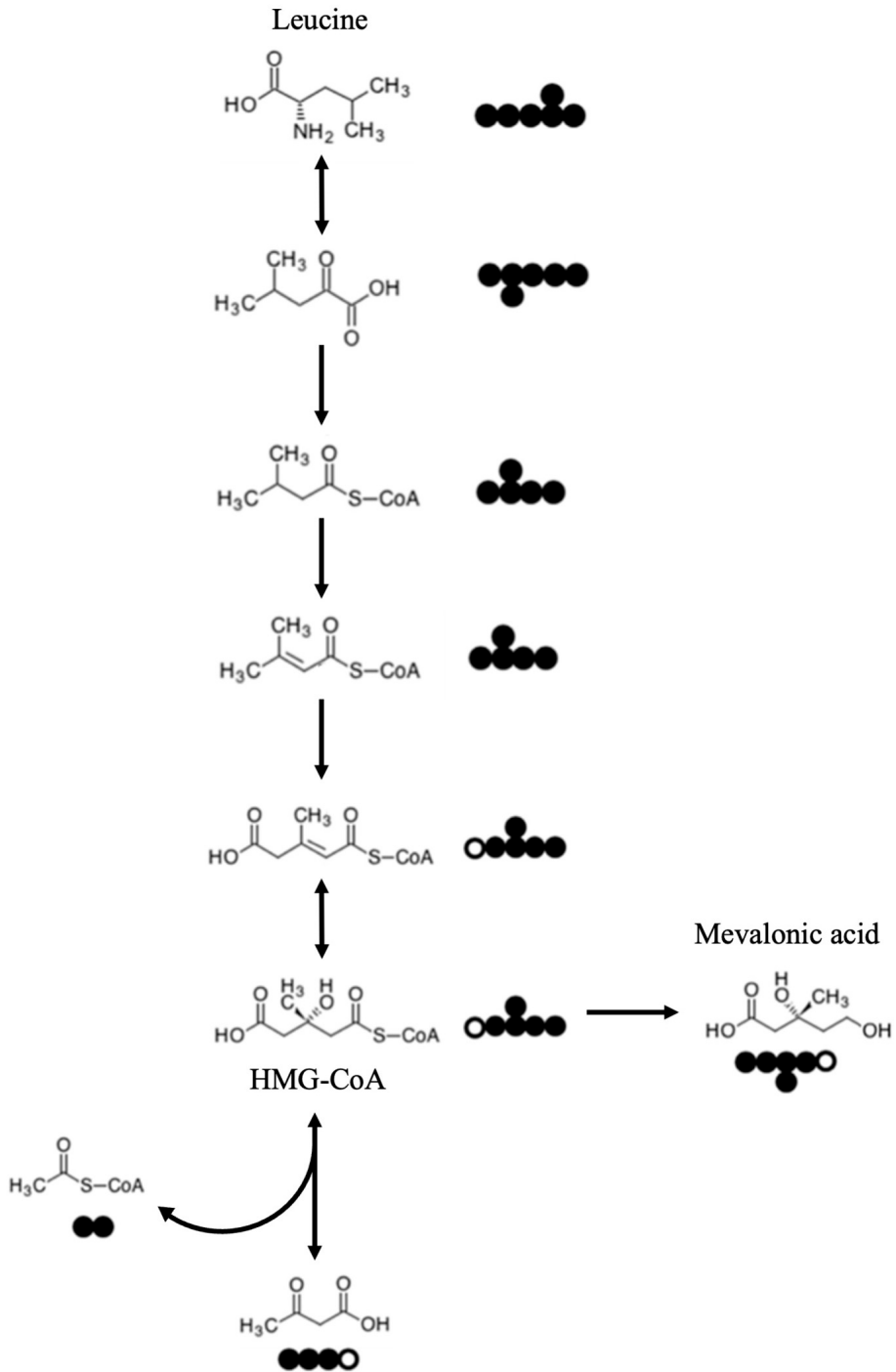


*Fig. 3.2.1. Leucine degradation to HMG-CoA with a carbon labelling pattern of intermediate metabolites.*

HMG-CoA can also be synthesised from acetyl-CoA or acetoacetyl coenzyme A (acetoacetyl-CoA) by the enzyme HMG-CoA synthase, which is coded by two genes in the human genome: HMGCS1 and HMGCS2. Another enzyme in the pathway – HMG-CoA lyase, coded by the gene HMGCL, can break down HMG-CoA back to acetyl-CoA and acetoacetate. Acetoacetate can then be transformed into acetoacetyl-CoA by the enzyme acetoacetyl-CoA synthetase, which is coded by the gene AACS. The resulting acetoacetyl-CoA can be transformed back to HMG-CoA, this would give rise to three-carbon-labelled mevalonate (M3). We could not see this phenomenon in BCC cells, but it appeared to be important in MCF-7 as can be seen in Fig. 3.2.2. It can also be seen in the graph that BCC cells get over 60 % of their mevalonate from other sources (M0), which is not the same in MCF-7, as mevalonate sourced from other substrates contributes to less than half of all mevalonate in the cells. The EMU method predicted the M1 fraction of mevalonate to be higher than it was after our calculations and did not predict the M6 fraction to appear at all, however, we can see it in both of the cell lines, which signifies an array of complex reactions beyond the scope of this work might occur. Both cell lines display the calculated malate fractions M2 and M5 as similar to the ones predicted, as they come quite directly from leucine degradation, while M4 is significantly higher than was predicted and might be a result of a complicated degradation pattern other enzymes might also be involved in.

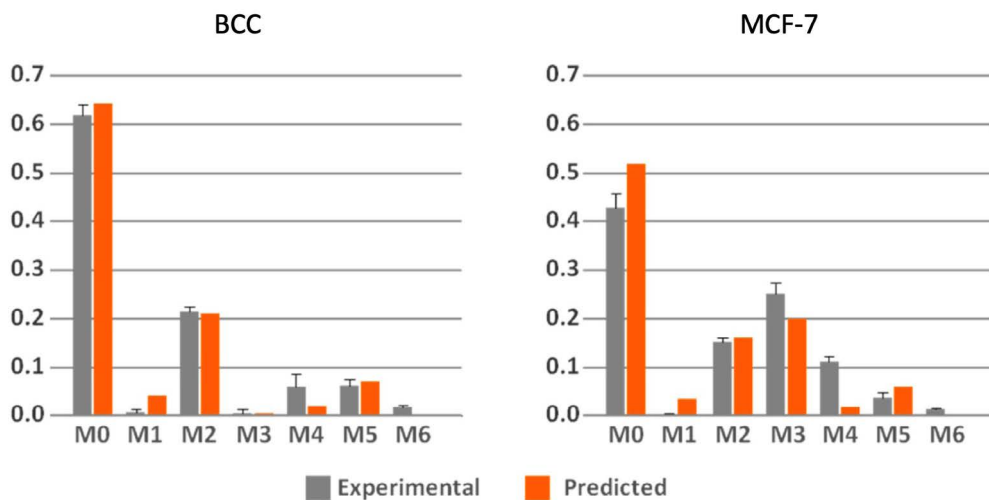


**Fig. 3.2.2.** Relative isotopic distributions for mevalonate in two malignant cell lines after feeding fully labelled BCAAs, experimental versus predicted using the EMU method.



We minimised the sum of the squares of the relative errors to find optimal flux distributions. These distributions, normalised by the amount of mevalonate synthesised, can be seen in Fig. 3.2.3. We also fitted the M2 labelled mitochondrial acetyl-CoA into the calculations and the optimal value of the fraction was 0.1 for both cell lines. We did this assuming that 70 % of HMG-CoA that results from the degradation of leucine is labelled.

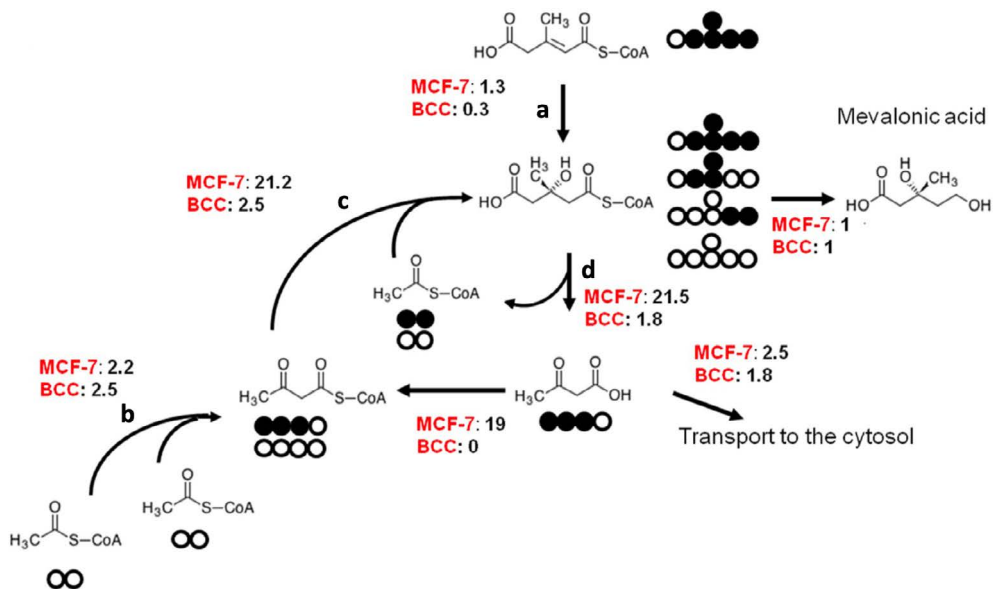


**Fig. 3.2.3.** Scheme showing how different reactions influence changes in labelling patterns of mevalonate. Numbers next to each reaction indicate the estimations of metabolic flux distributions calculated using Metabolic Flux Analysis for each of the studied cell lines.

a – HMG-CoA synthesis from leucine degradation, b – acetoacetyl-CoA synthesis reaction by acetoacetyl-CoA thiolase, c – HMG-CoA synthesis reaction by HMG-CoA synthase, d – break down reaction of HMG-CoA to acetyl-CoA by HMG-CoA lyase.

To quantify how much mevalonate (and acetoacetate) is produced from leucine, we compared the total carbon derived from the leucine degradation pathway with the total carbon that forms acetyl-CoA. The amount of carbon coming from leucine degradation in MCF-7 cells can be calculated like this:

$$C(\text{leucine}) = n \times a$$

$$C(\text{leucine}) = 6 \times 1.3 = 7.8$$

Leucine with 6 carbon atoms (n) in its backbone times the reaction rate of HMG-CoA formed per 1 unit of mevalonate that was produced in MCF-7

(the reaction rates can be seen in Fig. 3.2.3). We need to compare this with the amount of atoms that was consumed as acetyl-CoA. The net consumption of acetyl-CoA can be described as the sum of all reactions that consume it minus the production of acetyl-CoA by HMG-CoA lyase:

$$C(\text{acetyl-CoA}) = n \times (b + c - d)$$

$$C(\text{acetyl-CoA}) = 2 \times (2.2 + 21.2 - 21.5) = 2 \times 1.9 = 3.8$$

Now we can calculate the total carbon atoms that originated from leucine degradation in MCF-7:

$$C(\text{total}) = \frac{C(\text{leucine})}{C(\text{leucine}) + C(\text{acetyl-CoA})}$$

$$C(\text{total}) = \frac{7.8}{7.8 + 3.8} = \frac{7.8}{11.6} = 0.67$$

These calculations indicate that 67 % of the carbon atoms in mevalonate and acetoacetate are derived from the degradation of leucine. Following the same equations, we calculated the contribution of leucine in BCC cells as well:

$$C(\text{leucine}) = 6 \times 0.3 = 1.8$$

$$C(\text{acetyl-CoA}) = 2 \times (2.5 + 2.5 - 1.8) = 2 \times 3.2 = 6.4$$

$$C(\text{total}) = \frac{1.8}{1.8 + 6.4} = \frac{1.8}{8.2} = 0.22$$

Here, only 22 % of the carbon is derived from the degradation of leucine. Contrary to the two cell lines mentioned above, we could not detect any mevalonate in MCF-10A (chromatograms available as Supplement S5).

Interestingly, in BCC cells, the fraction of labelled mitochondrial acetyl-CoA derived from labelled leucine was similar to the one we estimated with all three BCAAs. This could suggest that out of all three BCAAs, leucine is the only one responsible for the supply of mitochondrial acetyl-CoA in this cell line. The fate of isoleucine and valine could be an interesting question to research in future studies of BCAA metabolism in cancer.

The role of cholesterol in cancer progression is still a debated topic. Cholesterol levels are usually higher in cancer cells than they are in normally developing cells [77, 107, 108], however, the explanation for this phenomenon is not yet clear. In a previous work carried out by our group, it was revealed that most of the studied cancer cell lines did not express cholesterol transporters

[100, 109]. As cholesterol is an important structural component of the cell membrane, a key regulator of cellular signal transduction, and a precursor for an array of different signalling molecules [110], cancer cells have to rely on the mevalonate pathway, to synthesize cholesterol. Our findings suggest that leucine plays an important role in the *de novo* synthesis of mevalonate, making it another mechanism by which leucine supports cell proliferation and invasiveness. These results would confirm the findings of other researchers, which concluded that leucine deprivation causes inhibition of proliferation and differentiation of cells by mechanisms, dependent and independent of the mTOR signalling pathway [111, 112]. Cholesterol is a precursor for steroid synthesis, suggesting it might have something to do with hormone-dependent cancer progression. While no clear conclusions regarding its role in breast cancer can be drawn yet, potential mechanisms could include cholesterol's involvement in estrogen's biosynthesis, Ras, Erk1/2, Akt, and p38 signalling pathways as well as being a major component of lipid rafts, crucial for apoptosis, migration, and invasion [113]. While no specific pharmacological inhibitors of BCAA catabolism are yet on the market, the mevalonate pathway already has an array of inhibitors with years and years of clinical use for the prevention of cardiovascular events, that could be used to prove or disprove the hypothesis. Several clinical and pre-clinical trials have shown the antiproliferative effect of statins (inhibitors of HMG-CoA reductase, typically used to treat hypercholesterolemic patients) on cancer [114–116], suggesting them as prospective adjuvant therapy. The conflict emerges, however, following the inconsistencies in the results of epidemiologic studies. While some of them show an association between high serum levels of cholesterol and cancer development or the use of statins minimizing the risk for oncologic diseases and reoccurrences [117–122], almost equally as many studies show there is no association [123–126] or even claim statins can be dose-dependently carcinogenic [127]. Although some criticize these kinds of studies for having many limitations, it should be kept in mind that observational epidemiologic studies use real-world data, as opposed to highly controlled clinical and preclinical trials. While the question of whether cholesterol affects cancer progression is still debated, this additional pathway leucine plays a role in, added to energy production, signalling, and aiding biomolecular synthesis might be enough to have a significant effect on cancer development.

### **3.3. The role of BCAAs in cell invasiveness**

Our previous experiments showed that leucine plays a significant role in the synthesis of cholesterol. As already mentioned in section 1.5 of this

dissertation, the invasiveness of breast cancer cells relies heavily on the mevalonate pathway [128–130]. We were interested in whether a decrease in BCAA levels would affect the invasiveness of our studied cell lines. We used two different methods of BCAA reduction: a knockdown using siRNA against BCAT2 to suppress BCAA catabolism and a reduction of BCAAs in the nutritional media (from the usual 0.8 mM to 0.2 mM). To assess the impact of BCAAs on the invasiveness of breast cancer cells, we used a method called wound healing assay. The *in vitro* wound healing assay is a relatively simple and cost-effective way to assess cell migration under different experimental conditions. It involves opening a “wound” in the cell monolayer with a sharp object, creating a cell-free region for the cells to migrate and close the wound. The two-dimensional (2D) cell monolayer model is most widely used because 2D studies can be performed under normal cell culture conditions available in most cell culture laboratories. We investigated the effect of reduced BCAA content and BCAT2 gene inhibition on BCC, MCF-7, and MCF-10A cell migration. Just after scraping, we changed the cell culture media to either the DMEM/F-12 normally used or the custom 0.2 mM BCAA media to remove the debris that was left after the scratch, and fixed the culture plate into position for time-lapse imaging (Fig. 3.3.1). We chose an interval of 8 hours between the first and the last image taken, to minimise the influence cell division has on the movement of cells in the wound closure area.

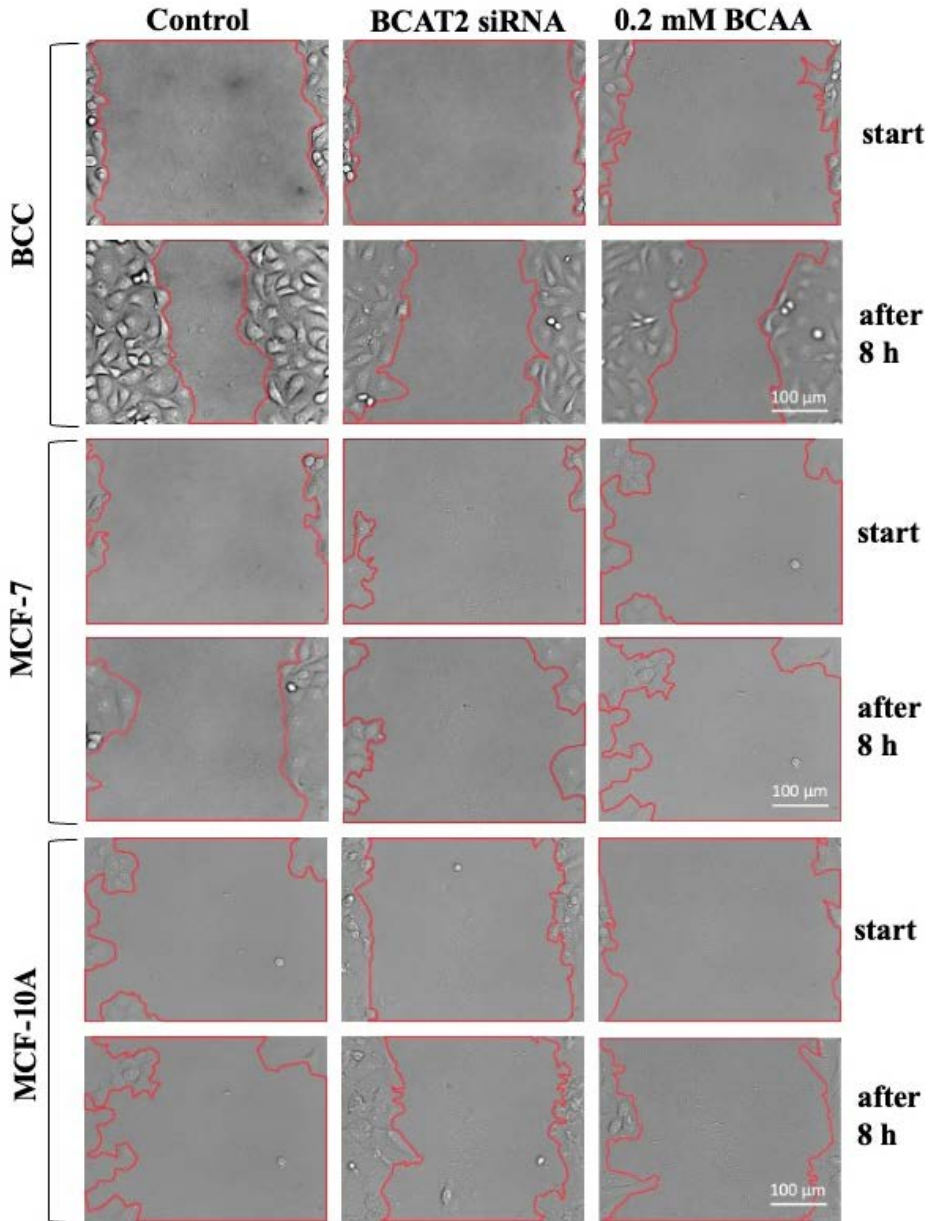


**Fig. 3.3.1.** The depiction of the wound healing assay. The first picture (start) shows the wound area in red at the beginning of the experiment and the second one shows the area 8 hours after the experiment was started.

BCAT2 inhibition had a greater effect on BCC cell invasiveness than the reduction of BCAAs in the media, as compared to the control (Fig. 3.3.2). The wound in the control group contracted 72.05 % ( $\pm$  6.90 % standard

error (SE)) and only 35.96 % ( $\pm 3.88$  % SE) in the BCAT2-inhibited group, meaning BCAT2 inhibition significantly reduced invasiveness. We could also see statistically significant results in the 0.2 mM BCAA group, compared to the control, although it was not as effective as gene silencing (the wound closed 50.54 % ( $\pm 1.21$  % SE) in the group with a reduced amount of BCAAs). Surprisingly, MCF-7 was more affected by the reduced amount of BCAA in the media, while no statistical difference was observed in the BCAT2-inhibited group. This, and the fact, that BCC was more sensitive to changes in BCAA levels, even though they contribute less to mevalonate and mitochondrial acetyl-CoA production, could be a result of MCF-7 cells not being able to form a stable monolayer, thus providing difficulties in evaluating the results of this experiment. Regardless, the 0.2 mM BCAA group had significantly slower wound closure in MCF-7: 7.20 % ( $\pm 1.53$  % SE) after the 8-hour time-lapse, as opposed to the control, in which the closure was 19.35 % ( $\pm 1.12$  % SE). We observed no statistically significant results in the benign MCF-10A cells, which may suggest that BCAAs are involved in cancer invasiveness but not in the migration of healthy epithelial cells or that the contribution is not as significant.

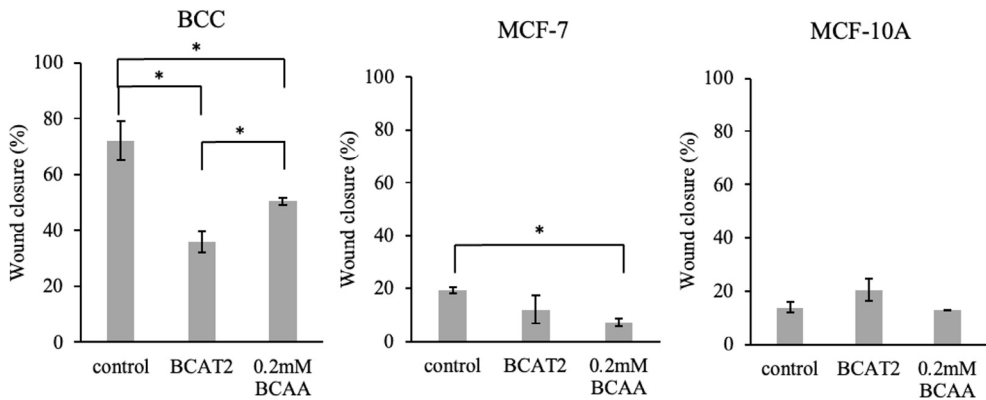


**Fig. 3.3.2.** The effect of reduced BCAA concentration (0.2 mM BCAA) and BCAT2 gene inhibition by siRNA on cell migration, evaluated using the wound healing assay.

The main challenge of this study was the fact that some of the studied cell lines do not form a stable monolayer, meaning that the wound-healing assay might not be the best method to track migration for these cell lines, as they are not as prone to attract one another to try and close the “wound”. Nonetheless, the results still show a significant reduction in wound closure in MCF-7 after BCAA content is reduced, suggesting these cells do need a certain amount of BCAAs to move around and proliferate. Future experiments should involve

another aspect of the migratory properties, such as single-cell migration analysis, also achieved by time-lapse imaging. In this way, the results would not be as influenced by the phenotype of the cell line.

mTOR signalling pathway also plays a huge role in cell migration [131, 132], as does cellular energetics, meaning that the depletion of BCAA catabolism can influence cancer cell migration by a combination of different mechanisms. However, there should be an increase in intracellular BCAAs after BCAT2 inhibition, meaning it is less likely, that the suppression of migration in the BCAT2-inhibited group of BCC cells is caused by mTOR, as the mTOR signalling pathway is activated by intracellular leucine.

Additionally, elevated BCAAs in the media also seem to suppress breast cancer cell migration [133], which may mean that a completely different mechanism takes place. The authors suggest the immune cells, which are also in high demand for BCAAs, might be involved in their unexpected results in animal studies, but less could be said about the wound healing and transwell assays with LM2 breast cancer cells. N-cadherin (but not E-cadherin) was also downregulated in the presence of elevated BCAAs in this cell line, showing that the migration disturbances are not a coincidence. A study by Sciacovelli *et al.* revealed that a part of BCAA-derived nitrogen bypasses the Krebs cycle and channels into the biosynthesis of arginine exclusively in metastatic renal carcinoma cells [38]. Section 1.3. of this dissertation mentioned that the enzyme argininosuccinate synthetase 1, involved in the synthesis of arginine, is also an important factor in cell migration, suggesting yet another mechanism for BCAA-driven migration of cancer cells. Taking all that into account, it is hard to conclude the underlying cause of our results, however, it is clear that BCAAs do have an impact on cancer cell migratory properties, with mechanisms for it still being quite a large knowledge gap, providing interesting questions for further research in the field.

### **3.4. Determination of intermediate metabolites of the BCAA degradation pathway in blood plasma**

In order to determine whether there are any changes in the BCAA degradation pathway of breast cancer patients in a clinical setting, we performed a small-scale experiment using human blood plasma. We performed a targeted chromatographic analysis of blood plasma samples from 10 women with breast adenocarcinoma and 10 healthy individuals for control (more in Materials and Methods). We chose to investigate 5 BCAA metabolites in this study: 3-hydroxyisovalerate and mevalonate, as intermediates of leucine degradation, 3-methyl-2-oxopentanoate as an intermediate of isoleucine degradation and 3-aminoisobutanoate and 3-hydroxyisobutyrate from the degradation pathway of valine.

The differences between the control and study groups are depicted in Fig. 3.4.1. First of all, we found that the amounts of intermediates studied varied widely between different samples. Despite that, we observed a statistically significant increase in the amount of 3-hydroxyisobutyrate (of valine degradation) in the blood plasma of patients as compared to control, while its concentration in MCF-7 and BCC cancer cells was low (results not shown). This could mean, that cancer cells excrete 3-hydroxyisobutyrate, however, the reason for this is still yet to be explained.

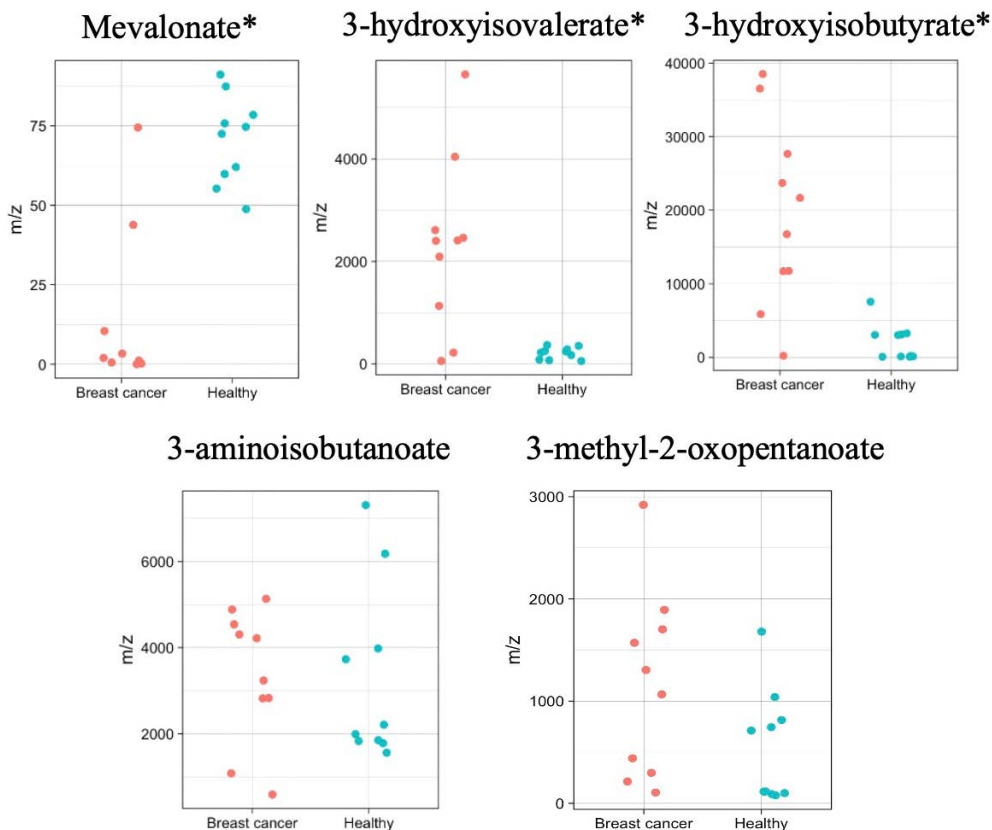


**Fig. 3.4.1.** Metabolic intermediates of BCAA degradation in the blood plasma of healthy individuals and patients with breast cancer.

A star (\*) near the name of the studied metabolite indicates statistically significant differences.

We also observed a statistically significant increase of 3-hydroxyisovalerate in patient plasma samples. 3-hydroxyisovalerate branches out in the degradation pathway of leucine and is not involved in the synthesis of acetyl-CoA or mevalonate for that matter (the scheme for BCAA degradation is



available as Supplement S6). Seeing that mevalonate was significantly downregulated in breast cancer patients, it could be said that there is a higher demand for it in the tumour itself, upregulating the degradation pathway of leucine and the intermediates that do not eventually result in mevalonate are secreted out of the cell, giving rise to 3-hydroxyisovalerate in our plasma samples.

Also, when we tested cell extracts using isotopically labelled BCAAs, malignant cell samples contained relatively high levels of 3-methyl-2-oxopentanoate (results not shown), suggesting upregulated degradation of isoleucine, meanwhile, the amount in blood plasma did not differ significantly between groups of patients and healthy individuals. 3-aminoisobutanoate of valine degradation did not differ between the two groups.

Other metabolomic studies of breast cancer patient plasma samples have also reported a significant increase in BCAA degradation intermediates [134–136]. Having this in mind, a determination of some intermediates of BCAA metabolism, along with other perturbed amino acids and their metabolites, in the blood could be a prognostic marker of early-stage breast cancer and could be applied in clinical practice. As for the BCAAs themselves, higher levels of circulating BCAAs were found to be associated with a lower risk of breast cancer in premenopausal women and a higher risk among postmenopausal women, suggesting hormonal changes have a lot to do with their role in disease progression. As mentioned in the discussion part of section 3.3. of this dissertation, elevated circulating BCAAs could activate the immune response [133], eventually leading to a lower risk of breast cancer in the premenopausal group. In another study with premenopausal women without a known cancer diagnosis, high plasma levels of BCAAs were significantly positively correlated with free testosterone levels [137]. The perturbations in sex hormone levels are established biomarkers for breast cancer risk [138, 139]. The downside of using BCAAs alone as biomarkers is the diversity of metabolic diseases, that could also cause changes in the plasma content of these three amino acids. These are the diseases related to perturbations in BCAA metabolism mentioned earlier. For example, a higher plasma profile of BCAAs and their related metabolites were the most promising biomarkers for cardiometabolic risk and inflammation [140, 141]. Amino acid plasma content can also be influenced by body mass index [142] meaning all of these measures should be taken into account when developing BCAAs and their metabolites into clinically accurate biomarkers.

### 3.5. Metabolomic analysis of amino acids associated with malignancy in breast-derived cells

Next, we were interested in identifying a broader spectrum of amino acid-related changes in the metabolome of the studied cell lines. A metabolomic analysis allowed the quantification of 33 internal metabolites, in all the three studied cell lines. We performed a PCA, which revealed that 97.6 % of the variance in the metabolic data could be assigned to the first two principal components (PCs), with the first one accounting for 61.6 % of variability, and the second for 36 %. The second component clearly separated MCF-10A from the malignant MCF-7 and BCC cell lines, while the first component showed some variation between the three cell lines (Fig. 3.5.1). These results indicate that 36 % of the variation in metabolite concentrations between the three cell lines could be associated with malignancy.

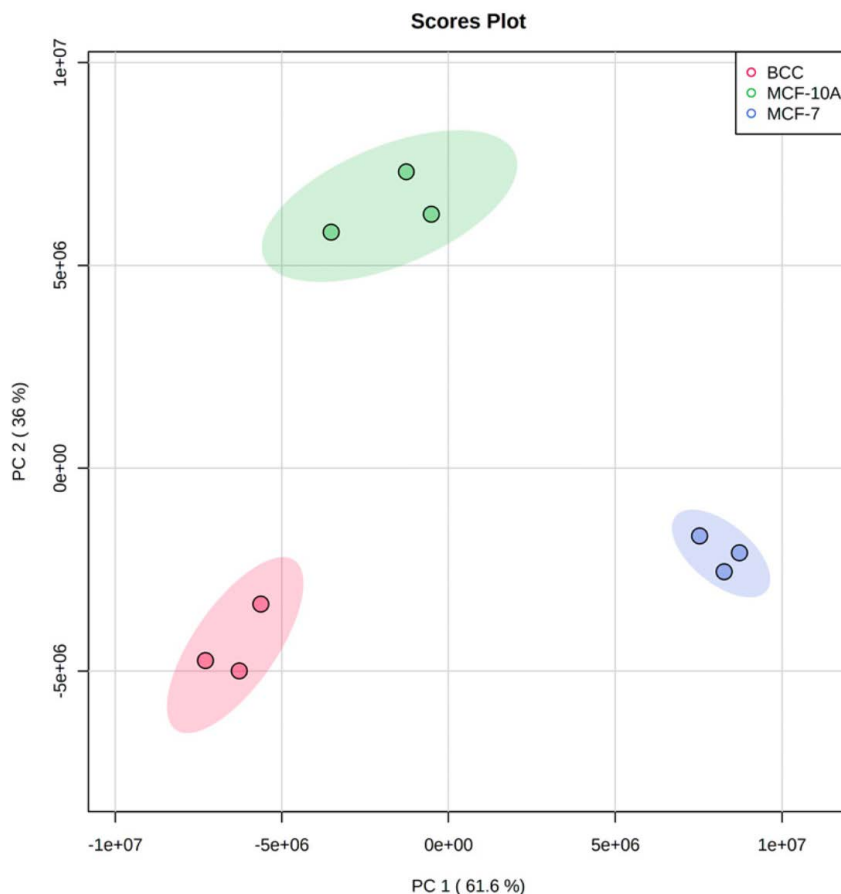


**Fig. 3.5.1.** PCA plot showing the variation in metabolite profiles of the three studied cell lines between the two PCs.

For a better understanding of which metabolites are best for distinguishing malignant cells from non-malignant ones, we represented the concentration data in a heat map (Fig. 3.5.2). Now we can clearly see the diversity of intracellular amino acid profiles. The heat map also shows that the three BCAAs: leucine, isoleucine, and valine have lower relative concentrations in BCC cells. These results could either mean BCAAs are less important for BCC or that the cell line is auxotrophic to them. The latter is more likely regarding our previous experiments where we show that these cells were always in between MCF-7 and MCF-10A regarding BCAA utilisation and that BCAT2 is overexpressed in both cancer cell lines [7].

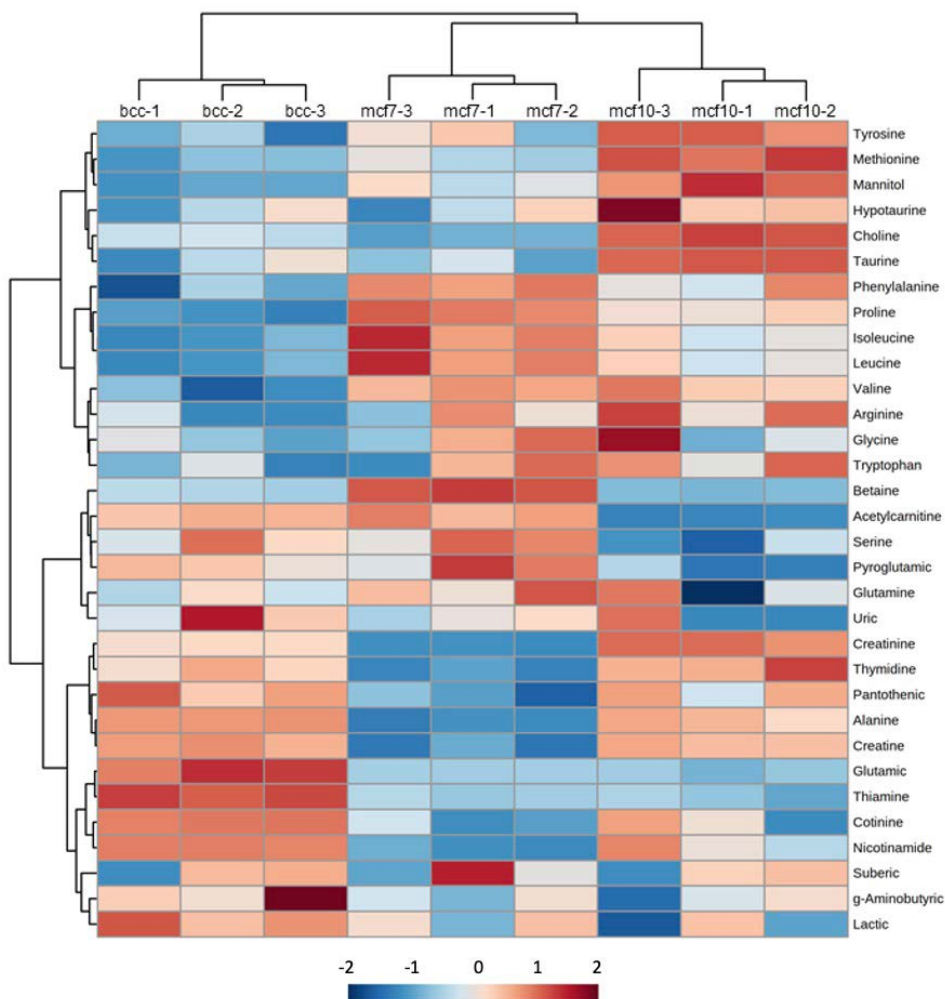


**Fig. 3.5.2.** A heat map showing the relative abundances of the 33 studied metabolites in each sample. Dendrograms identify similarities between groups of metabolites that have similar concentration patterns across different samples, determined by hierarchical clustering.

Broader profiling of metabolomes for the three studied cell lines revealed new amino acid-related perturbations between healthy and malignant cells. Six metabolites at the top of the heat map could be characterised by higher concentrations in MCF-10A than in the malignant cell lines. These metabolites were tyrosine, methionine, mannitol, hypotaurine, choline, and taurine. Another group of metabolites formed a cluster characterised by higher concentrations in MCF-7 and BCC instead. These four metabolites were betaine, acetylcarnitine, serine, and pyroglutamic acid.

Out of all the mentioned perturbed metabolites, six (methionine, taurine, hypotaurine, choline, betaine, and pyroglutamic acid) are related to the methionine cycle to some extent (a more detailed concentration distribution for some of the mentioned compounds is depicted in box plots in Fig. 3.5.3). The downregulation of these metabolites in MCF-7 and BCC cells may mean they are highly consumed due to the importance of the methionine cycle in rapidly dividing cells. Indeed, even though cancer cells have the ability to synthesize methionine, the supply often does not catch up with the demand, making the cells auxotrophic to it [43]. Methionine dependency is a long-known characteristic of cancer but is still a very relevant topic when it comes to personalised treatment strategies [143–146].

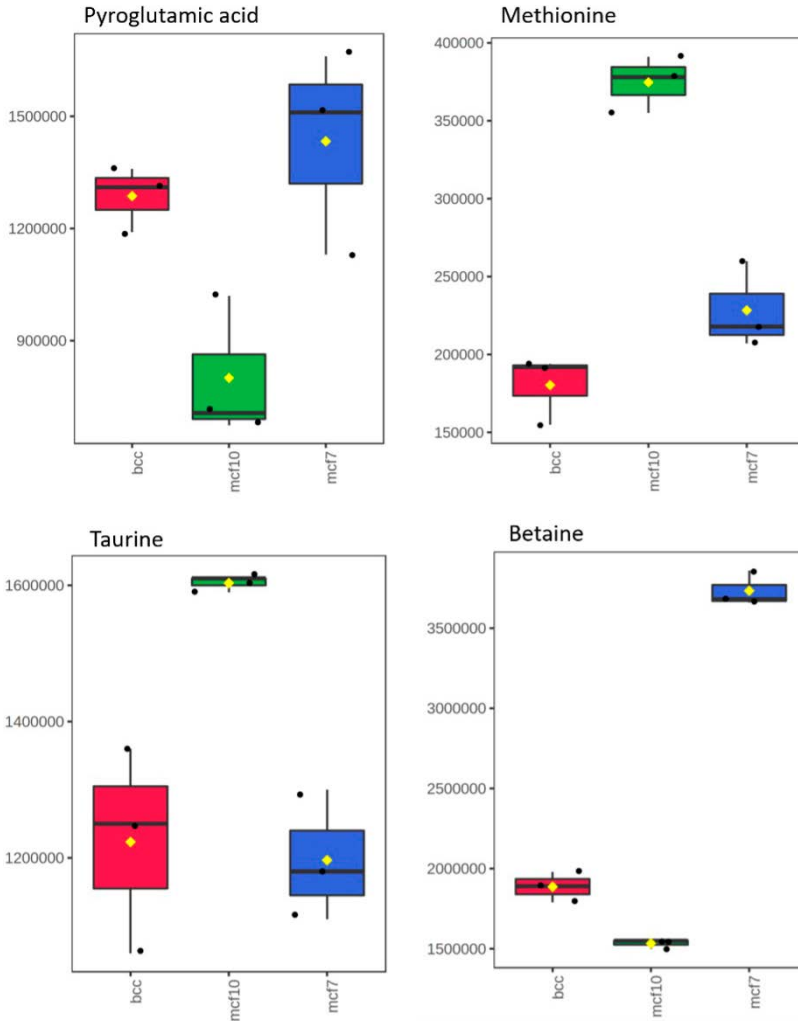


**Fig. 3.5.3.** Box plots showing concentration distributions of the metabolites, related to the methionine cycle.

The concentrations depicted are not absolute and reflect the normalised areas of the corresponding peaks in the chromatograms.

Besides being a building block for proteins, methionine is involved in several crucial metabolic pathways that take part in epigenetics (S-adenosylmethionine), nuclear processes (polyamines), detoxification (glutathione), and the formation of cellular membranes (phospholipids) [144]. The methionine cycle is a part of the so-called one-carbon metabolism [147], which allows cells to generate methyl groups (or one-carbon units) to utilize them in methylation processes crucial for transcription, replication, and DNA

repair. The folate cycle, another part of one-carbon metabolism, has long been a target for treating cancer, followed by the development of antifolates. The best-known drug in this class – methotrexate is being used for the treatment of many cancers to this day, however, it has many side effects caused by the importance of the foliate cycle for healthy proliferating cells [144, 147]. One way to combat this would be to selectively target specific enzymes in the one-carbon metabolism pathways. We will discuss possible drug targets later on in the dissertation.

### **3.6. Differential gene expression of the three breast-derived cell lines**

Extracting conclusions about metabolism, only having the concentrations of metabolites in question, would be unreasonable, as metabolism is a complex net of interactions between different enzymes and their substrates. Keeping that in mind, we paired the metabolomics data with data from next-generation RNA sequencing (RNA-seq) for a bigger picture of the underlying processes involved in cancer progression. Knowing the expression of genes that code different metabolic enzymes gives us valuable information on what could have caused the disturbances in the metabolic profiles of the cells. As we are only interested in the differences between the metabolism of healthy and malignant cells, we performed a differential expression analysis on the RNA-seq data. To find the differentially expressed genes between the three studied cell lines, we used cut-off values of 0.01 for false discovery rate and 2 for fold change. According to the processed RNA-seq data, 1495 genes were significantly upregulated in MCF-7 as compared to MCF-10A, while 1335 genes were significantly downregulated respectively. When comparing BCC to the healthy epithelial cells, 1926 of the genes in common were upregulated, and 1669 were downregulated in BCC cells. 274 of the upregulated genes and 563 of the downregulated genes were common in both cancer cell lines. A broader summary of the differential expression analysis can be seen in Fig. 3.6.1.

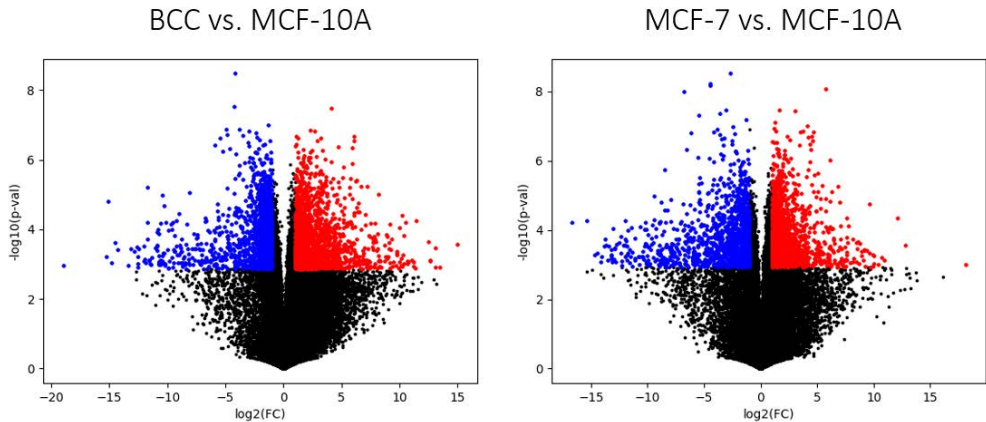


**Fig. 3.6.1.** Volcano plots visualising the genes that are upregulated (red), downregulated (blue), and have no differential expression (black) in both of the studied cancer cells as opposed to the non-malignant MCF-10A cells.

Next, we carried out a Kyoto Encyclopedia of Genes and Genomes (KEGG) pathway enrichment test using the WebGestalt online gene set analysis toolkit [96] and found no significantly enriched pathways among the upregulated genes (the cut-off false discovery rate was 0.05). On the other hand, we identified 10 significantly enriched KEGG-described downregulated pathways, as can be seen in Fig. 3.6.2.

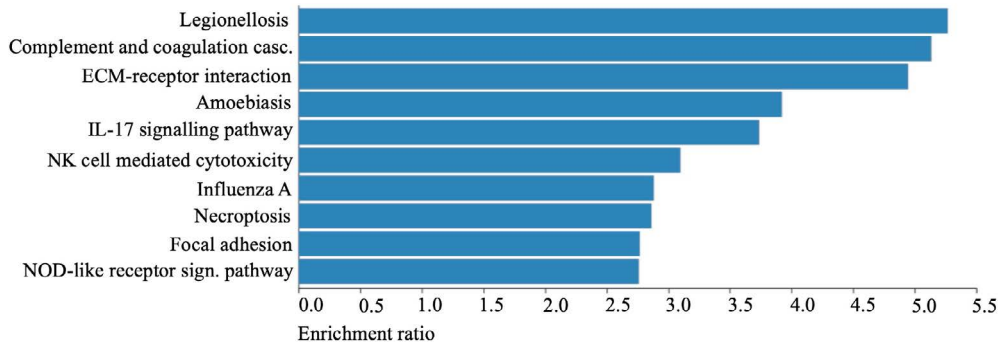


**Fig. 3.6.2.** Enriched pathways among the downregulated genes in BCC and MCF-7.

Names of the pathways correspond to pathologies or other processes the genes are mostly involved in.

Half of the mentioned pathways relate to certain diseases, others are associated with signalling (such as the IL-17 signalling pathway) or cell adhesion. In general, these results indicate that cancer cells are less

sensitive to extracellular signalling and detach from the extracellular matrix easily. However, we could not identify any metabolic processes that were significantly enriched while analysing this gene set, which addressed the need to integrate metabolomic data in the analysis using GSMMs as scaffolds for the interpretation of transcriptomic data. Among the 274 genes that were upregulated in both cancer cell lines, 44 were metabolic genes, involved in 131 metabolic reactions. Among the 563 downregulated genes, 130 were involved in metabolic processes, associated with 832 metabolic reactions. The large number of reactions comes from the fact that downregulated genes are involved in cross-membrane transport. One example would be the solute carrier family 36 member 4 coded by the gene SLC36A4. It is involved in the transport reactions of four amino acids (glycine, alanine, proline, and serine). The solute carrier family 6 member 15 (SLC6A15) is involved in the transport of 11 amino acids. The remaining course of this work will focus on the relationships between the changes at the transcriptomic and metabolomic levels.

### **3.7. The search for potential drug targets for breast cancer by combining metabolic and genomic data**

Three of the perturbed metabolites from the previous analysis (methionine, taurine, and hypotaurine) can be tracked down to a common precursor – homocysteine (Fig. 3.7.1.), an intermediate in the methionine cycle. Another metabolite, pyroglutamic acid, formed by the breakdown of glutathione, can also be traced back to homocysteine, although the carbon atoms in pyroglutamic acid come from glutamine involved in the synthesis of glutathione. We found that the gene AHCY coding the enzyme adenosylhomocysteinase, which is involved in the breakdown of S-adenosylhomocysteine into adenosine and L-homocysteine, is significantly downregulated in MCF-7 and BCC as compared to MCF-10A. AHCY was previously implicated as a tumour suppressor gene involved in p53-induced cell cycle arrest [148]. This function seems to be cell type-specific, as some cancers, for example, neuroblastoma, overexpress AHCY, making it a tumour promoter [149, 150]. In our case, the downregulation of AHCY together with the decreased concentration of methionine in cell extracts, led to the assumption that the malignant cell lines we study have a lower activity of the methionine cycle. Two of the other perturbed metabolites – betaine and choline, also are linked to the methionine cycle. Choline is a vitamin obtained from the diet. It is involved in the synthesis of betaine (Fig. 3.7.1), which provides methyl groups to the methionine cycle. The aforementioned groups are then used in the methylation of DNA and protein with S-adenosyl methionine (SAM) as a methyl donor [151]. The



internal choline pool appeared to be lower in both cancer cell lines. That could be explained by the downregulation of the gene solute carrier family 44 member 5 (SLC44A5), which codes a choline transporter. Betaine, on the other hand, had higher concentrations in malignant cell lines. As mentioned before, betaine is produced from choline, but it can also be a product of glycine metabolism. However, betaine can only be consumed by the enzyme betaine-homocysteine methyl transferase, which is a step in the methionine cycle. Ultimately, due to the reduced activity of the methionine cycle, the consumption of betaine decreases, resulting in its accumulation in the cells.

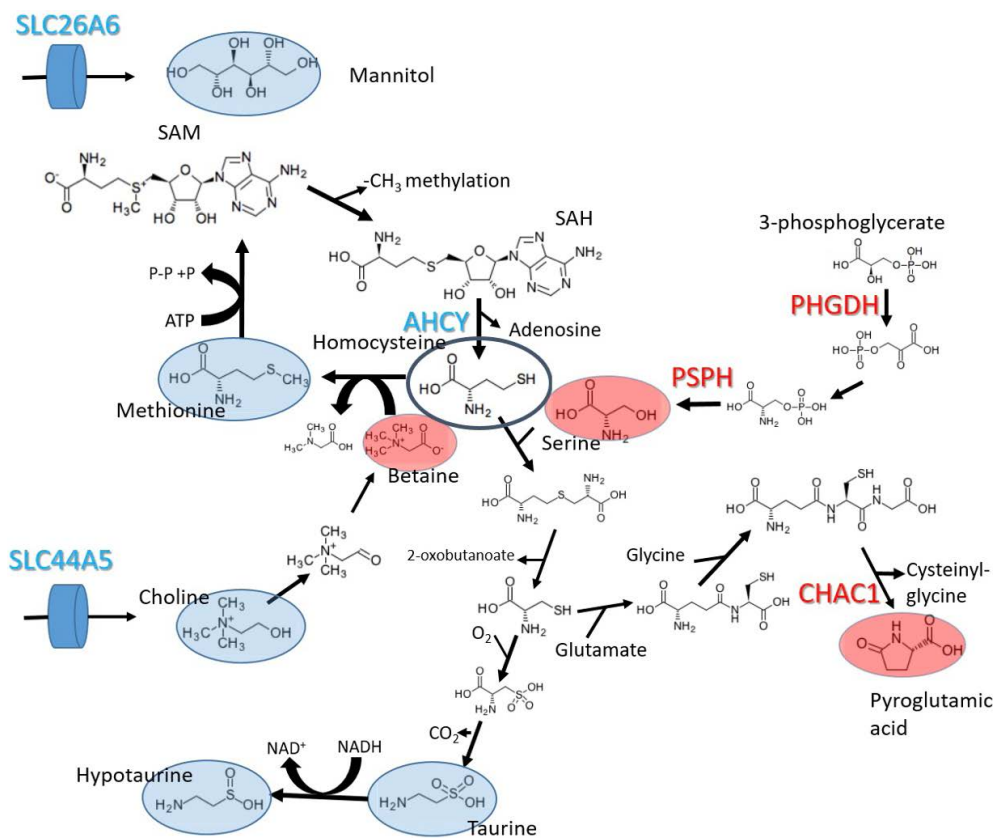


**Fig. 3.7.1.** Altered metabolic pathways in the studied breast cancer cells, identified by an integrated metabolomic and transcriptomic analysis.

Metabolites and genes that are lower in concentration or expression in malignant cells are depicted in blue, while the ones with higher profiles in cancer cells are marked in red.

Methionine is involved in the synthesis of SAM – a donor of methyl groups, used for protein and DNA methylation [152]. High SAM concentrations can have an anti-cancer effect by inducing apoptosis or down-regulating

oncogenes by methylation [153]. Our observations regarding the lower activity of the methionine cycle might mean a lower re-methylation rate of SAM has a protective effect on malignant cells. The possibility of using SAM in cancer therapy was shown by several groups on different breast [154, 155] and liver [156] cancer cells.

Other researchers have shown that methionine sulphoxide reductase A, another enzyme that contributes to the pool of methionine by reducing oxidised methionine, is downregulated in MCF-7 cells, as compared to HEK-293 [157]. The same group also showed that the downregulation of this enzyme is associated with a more aggressive phenotype of breast cancer [158], proposing that this phenomenon is related to the antioxidant nature of the enzyme, as ROS are important mediators of invadopodia formation, necessary for cell invasion [158, 159].

Tumour-suppressor genes are usually neglected when it comes to target-based discovery of anti-cancer agents, mainly because inhibiting the gain-of-function with small molecules looks like an easier approach, than restoring the loss-of-function [160]. However, in terms of nutrition, the methionine cycle in cancer could easily be activated by an increased methionine intake, which would also be a less toxic path in targeting cancer. Several studies have shown that excess methionine stopped the proliferation of MCF-7 and other cells through p53 [161–164], without affecting benign cells. Clinical implications should be addressed with caution though, as some breast and other cancer types are methionine dependent and a higher intake of methionine could benefit the cancer more than the patient. This further stresses the importance of personalised medicine in the field of oncology. In the future, new treatment strategies should consider a thorough metabolic investigation of the tumour beforehand. Other limitations of metabolite supplementation in cancer therapy could include the possibility that using SAM as an adjuvant might trigger the methylation of other tumour-suppressor genes, thus promoting carcinogenesis [156].

Our gene expression data also showed that the two genes involved in the biosynthesis of serine from 3-phosphoglycerate (PHGDH and PSPH) were overexpressed in MCF-7 and BCC as compared to MCF-10A (charts with more detailed gene expression data can be seen in Fig. 3.7.2). The gene PHGDH codes phosphoglycerate dehydrogenase and was shown to be overexpressed in several cancers before [165]. Studies have shown that overexpression of this gene in non-malignant MCF-10A cells can cause phenotypic alterations that predispose cells to malignancy [166]. A higher expression of PHGDH in breast cancer patients was also associated with a shorter time to relapse and decreased overall survival [167]. PSPH codes phosphoserine phosphatase, which is involved in the last step of L-serine synthesis. Overexpression of

PSPH is also a presumed marker for colorectal cancer [168]. The role of these two genes in cancer is still not fully understood. Together with the elevated intracellular serine pool, our results indicate a greater biosynthesis rate of serine. Serine is another important contributor to one-carbon metabolism as it is a major source of methyl groups for methylation reactions [169]. Apart from that, serine is also a precursor for the biosynthesis of many molecules, such as glycine (ultimately resulting in glutathione, purines, and porphyrins), cysteine as well as sphingo- and phospholipids [170]. Because of this, many tumours can develop a dependency on extracellular serine. This was shown on xenografic mice – tumours grew almost twice as fast when on a serine and glycine-rich diet [171]. Other studies show that PSPH can promote cancer invasion and colony formation by pathways, unrelated to synthesis of L-serine [172, 173], suggesting a pharmacologic inhibition of the enzyme would be a better alternative for cancer treatment than dietary restriction in this case.

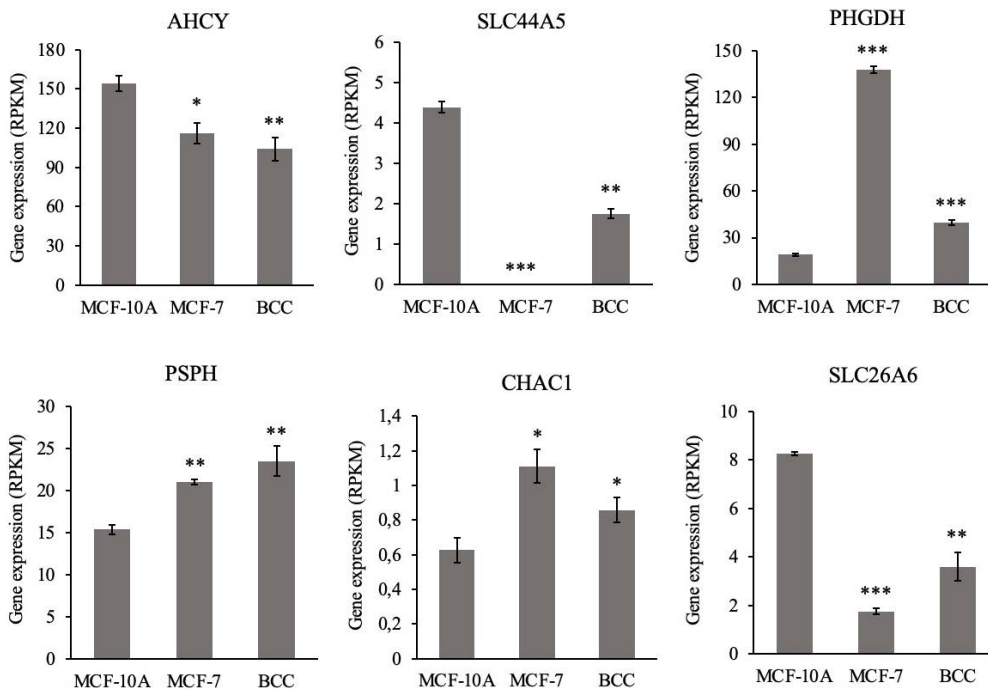


**Fig. 3.7.2.** Expression levels of genes, involved in the observed perturbations in intracellular metabolic pools.

The expression data is presented in RPKM. Error bars represent standard deviations (n=3). Statistical significance determined by t-test as compared to MCF-10A: p<0.05 (\*), p<0.01 (\*\*), p<0.001 (\*\*\*).

Due to increased mitochondrial activity, ROS are usually significantly elevated in cancer. They activate ROS-mediated signalling in cancer, by oxidation of phosphatases in mitogen-activated protein kinase (MAPK) signalling cascades or the PI3K/protein kinase B (Akt) signalling pathway [174]. Glutathione scavenges free radicals and acts as a detoxifying agent in cells [175]. Degradation of glutathione results in a metabolic dead end that is pyroglutamic acid (also depicted in Fig. 3.7.1.), which was upregulated in our malignant cell lines. Our transcriptomic analysis revealed that the gene CHAC1 was also overexpressed in both MCF-7 and BCC. The product of this gene – glutathione-specific  $\gamma$ -glutamylcyclotransferase 1, breaks down glutathione into cysteinyl-glycine and pyroglutamic acid [176]. Knock-down of this gene can reduce cell migration and proliferation, while overexpression of this gene can have the opposite effect. Also, a higher expression of the gene correlates with poorer prognosis in breast and ovarian tumours [177, 178]. Taking this into account, our findings suggest pyroglutamic acid could also be a potential metabolic biomarker of breast cancer and CHAC1 a target for drug design and development.

Our results also showed a higher concentration of acetyl-carnitine in malignant cells, suggesting a higher activity of the carnitine shuttle, responsible for the transportation of fatty acids from cytosol to mitochondria. The association between the carnitine shuttle and cancer is also well-established [179]. Acetyl-carnitine was shown to be a prognostic biomarker for hepatocellular carcinoma [180] and effective in enhancing the antitumoural effects of cisplatin or histone deacetylase inhibitors [181]. Other perturbations, like a lower concentration of mannitol in the malignant cell lines, can only be explained by alterations in transporter activity, as mannitol is a metabolically inert molecule in humans. Indeed, SLC26A6, coding a mannitol transporter, showed a lower expression in BCC and MCF-7 compared to MCF-10A.

Finally, the gene expression data was used to constrain a GSMM and it was analysed using a previously created Python library pyTARG [88]. pyTARG is a set of functions that take GSMMs as input and predicts metabolic fluxes as well as outputs a list of possible drug targets in the form of perturbed reactions from the model. We used flux balance analysis to predict metabolic flux distributions. The analysis revealed a downregulation of the respiratory chain in the malignant cell lines, which is consistent with Warburg's effect and was previously observed in a larger panel of different cancer cells [88]. We found that the reaction rate of ATP-synthase was lower in the two cancer cells and genes ATP1B3 and ATP6V1H were downregulated. Similar results were seen in human colon cancer cells with resistance to 5-fluorouracil [182]. Complex III of the respiratory chain had a lower reaction rate, and two of the genes involved (UQCRH and UQCR1) were downregulated. We also

observed a lower metabolic flux in Complex II of the respiratory chain, due to the downregulation of the gene NDUFB8. The lower reaction rate of ATP-synthase can be explained by a metabolic “switch” that was observed in the work of Sánchez-Cenizo *et al.* The ATPase inhibitory factor 1 controls a shift from OXPHOS to enhanced aerobic glycolysis and is highly overexpressed in all lung, colon, and breast cancers [183]. As we have already discussed throughout the dissertation, aerobic glycolysis supports cancer by providing more than just energy and the shift from OXPHOS protects from reaching lethal levels of ROS. We found extracellular serine uptake was also lower in both studied cancer cells because of the downregulation of the serine/proton symporter, coded by the gene SLC36A4. This further supports our previous findings regarding upregulated serine biosynthesis in the studied cancer cells, making serine biosynthesis even more of a prospective target for drug development. Finally, the model predicted lower CO<sub>2</sub> transformation to bicarbonate in malignant cell lines, as a result of the downregulation of two carbonic anhydrases (CA6 and CA2). Carbonic anhydrases have been recognised as crucial regulators of tumour cell pH, as they adjust bicarbonate and proton levels essential for cell survival and growth. This recognition has driven efforts to inhibit particular carbonic anhydrase isoforms as potential cancer drug targets. Only two of the 12 active isoforms, carbonic anhydrases IX and XII have been identified as anti-cancer targets. Other isoforms have not been explored as potential therapeutic targets for cancer therapy [184]. Low carbonic anhydrase II protein expression often serves as a biomarker associated with tumour aggressiveness and poor prognosis in various cancers, including pancreatic ductal adenocarcinomas, colorectal, gastric, and gastrointestinal stromal cancers [185–188]. Because of that, this isoform can be viewed as both a diagnostic and an independent prognostic factor for favourable outcomes and overall survival in the mentioned cancers. However, in other cancers like astrocytomas, oligodendrogliomas, melanomas, pulmonary endocrine tumours, as well as breast cancer, the upregulation of carbonic anhydrase II is linked to poor prognosis, tumour progression, and metastasis [187, 189–191]. There are no studies to this date linking the other isoform we found downregulated – carbonic anhydrase VI to cancer progression [184], suggesting an interesting research question for the future. A complete list of all the perturbed metabolic reactions and their associated genes we found to be significant for cancer can be found in the supplements section as Supplement S7.

## CONCLUSIONS

1. The extent of BCAA degradation in the production of cellular energy by the Krebs cycle was 34 % in MCF-7 cells, 14 % in BCC cells, and 10 % in MCF-10A cells. Mevalonate production from the breakdown of leucine was exclusive to breast tumour cells; the percentage of carbon from leucine that eventually formed mevalonate was 67 % in MCF-7 cells and 22 % in BCC cells. Consequently, the suppression of BCAA metabolism significantly slowed down breast tumour cell invasiveness.
2. An upregulation of 3-hydroxyisovalerate and 3-hydroxyisobutyrate, along with a downregulation of mevalonate was observed in the blood plasma of patients with breast tumours compared to healthy control. The metabolic pathways of breast cancer patients are regulated in a way that satisfies the high demand for mevalonate and acetyl-CoA. Therefore, the aforementioned metabolites could be used as biomarkers for identifying early-onset breast cancer.
3. Thirty-three internal metabolites were identified as common among BCC, MCF-7 and MCF-10A cells. Ten of them – tyrosine, mannitol, acetylcarnitine, serine, methionine, taurine, hypotaurine, choline, betaine, and pyroglutamic acid – were associated with malignant breast tumours. The last six of the aforementioned are metabolically linked to the methionine cycle. An integrated analysis of the metabolome and transcriptome revealed that the genes AHCY, PHGDH, PSPH and CHAC1 involved in methionine and serine metabolism, could be chemotherapeutic targets for the studied breast tumour cells.

# SANTRAUKA

## Įvadas

Pasaulio sveikatos organizacija pripažino krūties piktybinius navikus vyraujančia navikų forma visame pasaulyje [1]. Apskaičiuota, kad šia liga per gyvenimą susirgs viena iš aštuonių moterų [2]. Nepaisant dėl mokslo ir medicinos pažangos pagerėjusių prognozių, ankstyvas ligos aptikimas ir individualizuotas gydymas išlieka svarbūs uždaviniai, siekiant sumažinti pacientų naštą ir padidinti išgyvenamumo rodiklius. Vienas sunkiausiai įveikiamų onkologinių ligų bruožų – metabolinis perprogramavimas – sulaukė didžiulio mokslininkų susidomėjimo prieš beveik šimtmetį, kai Otto Warburg paskelbė apie navikinėse ląstelėse vykstančią aerobinę glikolizę [3]. Nuo to laiko, skirtumų tarp piktybinių ir sveikų audinių tyrimai yra tikslinės terapijos atradimų pagrindas.

Be gliukozės, naviko progresavimui itin svarbi aminorūgščių medžiagų apykaita. Navikui jos ne tik baltymų statybinė medžiaga, bet ir signalinės molekulės, tarpiniai produktai kitoms biologinės sintezės reakcijoms bei papildomas energijos šaltinis [5]. Šakotos grandinės aminorūgštys (angl. *branched-chain amino acids*, *BCAA*) sulaukė didelio susidomėjimo po to, kai navikinėse ląstelėse buvo pastebėta padidėjusi fermentų, atsakingų už jų metabolizmą raiška [6]. Pirmasis fermentas BCAA skilimo kelyje – šakotosios grandinės aminorūgščių transferazė (angl. *branched-chain amino acid transferase*, *BCAT*) yra vienas iš potencialių chemoterapinių taikinių [8], taigi gilesnis navikų aminorūgščių metabolizmo supratimas yra daug žadantis būdas plėtoti tikslinę onkologinių ligų terapiją. Kartu su molekulinės biologijos ir genomikos mokslų pažanga žengia ir noras sumažinti bauginančios krūties piktybinio naviko diagnozės naštą ateities kartoms.

## Tyrimo tikslas

Šio darbo tikslas išaiškinti sudėtingą aminorūgščių vaidmenį krūties piktybinių navikų medžiagų apykaitoje, taikant įvairius omikos metodus bei bioinformacinę analizę chemoterapinių vaistų taikinių paieškoms.

## Tyrimo uždaviniai

1. Nustatyti šakotos grandinės aminorūgščių vaidmenį krūties naviko ląstelių energetikoje ir biologinėje mevalonato sintezėje, naudojant izotopais žymėtas aminorūgštis.

2. Atlikti palyginamąją krūties piktybiniais navikais sergančių pacienčių ir sveikų moterų kraujo plazmos analizę, ieškant šakotos grandinės aminorūgščių metabolizmo tarpinių produktų.
3. Derinant metabolomikos ir transkriptomikos duomenis nustatyti aminorūgščių metabolizmo pokyčius krūties naviko ląstelėse, siekiant rasti potencialius vaistų taikinius.

### **Darbo mokslinis naujumas**

Nors ryšys tarp navikų ir padidėjusios BCAA skaidančių fermentų raiškos yra diskusijų tema jau apie dešimtmetį, aiškus mechanizmas, kuriuo BCAA metabolizmas veikia navikų vystymąsi dar nėra žinomas. Šiame darbe mes atskleidžiame naujus mechanizmus, kuriais BCAA skatina krūties navikų progresavimą, sekdami jų metabolizmą bei vartimą ląstelėse energija ir ląstelės statybinėmis medžiagomis, o tai savo ruožtu prisideda prie naujų terapinių metodų paieškos ir biožymenų ankstyvai diagnostikai atradimo. Nauji šio darbo atradimai apima BCAA katabolizmo įtakos acetilkofermento A ir mevalonato gamybai įvertinimą navikinėse ląstelėse bei potencialių plazmos krūties navikų biožymenų atradimą, atsižvelgiant į padidėjusį BCAA katabolizmą, aptiktą moterų, kurioms naujai diagnozuota invazinė duktalinė karcinoma, kraujyje. Be to, jungdami krūties navikinių ląstelių metabolominius ir transkriptominius duomenis naudodamiesi bioinformaciniais metodais, nustatome sutrikimus navikinių ląstelių vienos anglies metabolizme, kurie galėtų būti tolimesnių tyrimų apie aminorūgščių vaidmenį navikų progresavime tema.

### **Kiti svarbūs su darbu susiję aspektai**

Šios disertacijos rezultatai buvo Lietuvos mokslo tarybos finansuojamo projekto „Šakotosios grandinės aminorūgščių degradacijos įtaka navikinių ląstelių metabolizmui ir proliferacijai“ (S-SEN-20-6) dalis. Tyrimų rezultatai padalinti į septynias dalis, siekiant geriau atskirti skirtingus tiriamus aspektus, tačiau išvados buvo formuluojamos atsižvelgiant į kelis iš jų. Skyrių „Ląstelių energijos, gautos skaidant BCAA, kiekybinis įvertinimas“ ir „BCAA indėlis į mevalonato metabolizmą“ rezultatai buvo paskelbti viename recenzuojamame straipsnyje. Jie, kartu su neskelbtais skyriaus „BCAA reikšmė ląstelių invazyvumui“ rezultatais sudaro pirmąją išvadą. Antrąją išvadą sudaro neskelbti rezultatai pateikti skyriuje „BCAA katabolizmo tarpinių metabolitų nustatymas kraujo plazmoje“, o kitų skyrių rezultatai publikuojami antrajame recenzuojamame straipsnyje ir sudaro trečiąją šios disertacijos išvadą.



# TYRIMŲ METODAI

## Ląstelių kultūros ir jų kultivavimo sąlygos

Šioje disertacijoje buvo naudojamos dvi komercinės ląstelių linijos: epitelinės krūties adenokarcinomos (MCF-7) ir normalaus krūties epitelio (MCF-10A) ląstelės. Mūsų duktalinės karcinomos ląstelių modelis (BCC) yra iš paciento išskirta pirminė ląstelių kultūra, aprašyta ankstesnėje publikacijoje [7]. MCF-7 ir BCC ląstelių linijos atitinka luminalinius A ir B krūties navikų potipius. MCF-7 ir BCC ląstelės buvo auginamos DMEM/F-12 (1:1) mitybinėje terpėje, papildytoje 10 proc. fetaliniu jaučio serumu (angl. *fetal bovine serum, FBS*) ir 1 proc. penicilino-streptomicino (pen-strep) tirpalu (10,000 TV penicilino ir 10 mg streptomicino mililitre tirpalo). MCF-10A ląstelės buvo kultivuojamos DMEM/F-12 (1:1) terpėje, papildytoje 5 proc. arklio serumu, 1 proc. pen-strep, rekombinantiniu žmogaus insulinu (10 µg/ml), choleros toksinu (100 ng/ml), rekombinantiniu žmogaus epiderminiu augimo faktoriumi (20 ng/ml) ir hidrokortizonu (500 ng/ml). Ląstelės buvo kultivuojamos apdoroto paviršiaus flakonuose arba plokštelėse, drėgname 37 °C temperatūros ir 5 proc. CO<sub>2</sub> koncentracijos inkubatoriuje. Trip-sino-EDTA tirpalas, praskiestas fosfatinu buferiu (angl. *phosphate-buffered saline, PBS*) iki galutinės 0,05 proc. koncentracijos, buvo naudojamas ląstelėms atlipinti nuo flakono kitam sėjimui. DMEM terpė, papildyta 15 proc. FBS ir 10 proc. dimetilsulfoksidu, buvo naudojama ilgalaikiam ląstelių krikonservavimui itin žemos temperatūros šaldiklyje –80 °C temperatūroje.

## Transfekcija

Transfekcija buvo atlikta vadovaujantis jetPRIME® transfekcijos reagento protokolu. Ląstelės sėjamos į 6-į šulinėlių plokšteles arba 35 mm Ø Petri lėkšteles naktį prieš transfekciją, kad būtų pasiektas 60–80 proc. padengimas. Mitochondrinės šakotos grandinės aminorūgščių transferazės (BCAT2) genui slopinti buvo naudota 5 nM siRNR prieš BCAT2 geną koncentracija ir reikiamas transfekcijos reagento jetPRIME® kiekis. Į sterilų mėgintuvėlį su jetPRIME® buferiu buvo įpiltas atitinkamas siRNR kiekis, jis 10 sekundžių maišomas sukuriniu maišytuvu, centrifuguojamas, tada į tą patį mėgintuvėlį įpilamas transfekcijos reagentas, mėgintuvėlis vėl 10 sekundžių maišomas ir inkubuojamas kambario temperatūroje 10 min. Po inkubacijos mišinys išpilstomas į atitinkamus šulinėlius. Kontrolinė transfekcija be siRNR buvo atlikta taip pat.

## „Žaizdos gijimo“ metodas

Prieš eksperimentą 35 mm Ø Petri lėkštelės buvo padengtos fibronektinu, ištirpintu minimaliame PBS tūryje ( $1 \mu\text{g}/\text{cm}^2$ ) ir džiovintos laminare, kambario temperatūroje. Lėkštelės buvo sėjamos taip, kad jų padengimas transfekcijos metu būtų 50 proc. Eksperimentas pradamas praėjus 24 val. po transfekcijos. Siauras lėkštelių sluoksnis nubraukiamas aštriu vienkartinio 10  $\mu\text{l}$  pipetės antgalio kraštu. Suformuotas plyšys tuomet reikiama kryptimi fiksuojamas ant mikroskopo staliuko tvirtinamame inkubatoriuje su temperatūrinu režimu bei  $\text{CO}_2$  tiekimu ir paliekamas vaizdinti 8 val. Praėjus 8 valandoms nuo eksperimento pradžios, pirmasis ir paskutinis vaizdai analizuojami matuojant „žaizdos“ užsivėrimo plotą, pagal toliau nurodytus skaičiavimus:

„Žaizdos“ užsitraukimas (%) =  $(A(t = 0\text{h}) - A(t = \Delta\text{h})) / (A(t = 0\text{h}))$

$A(t = 0\text{h})$  – „žaizdos“ plotas iš karto po nubraukimo (laikas nulis)

$A(t = \Delta\text{h})$  – „žaizdos“ plotas praėjus  $h$  val. po nubraukimo

## Eksperimentai su $^{13}\text{C}$ izotopais žymėtomis aminorūgštimis

Lėkštelės buvo kultivuojamos 24 val. terpėje, kurioje BCAA arba glutaminas (priklausomai nuo eksperimento) pakeisti izotopais žymėtais jų atitikmenimis. Terpė buvo gaminama individualiai pagal įprastos DMEM mitybinės terpės sudėtį ir papildyta 10 proc. FBS bei 1 proc. pen-strep. Norint įvertinti žymėtų BCAA skilimo profilį, terpė buvo papildyta 0,8 mM galutinės koncentracijos L-Valinu  $^{13}\text{C}_5, ^{15}\text{N}$ , L-Leucinu  $^{13}\text{C}_6, ^{15}\text{N}$  ir L-Izoleucinu  $^{13}\text{C}_6, ^{15}\text{N}$ . Mevalonato skilimo profiliui įvertinti į terpę buvo pridėta tik aukščiau nurodytos koncentracijos L-Leucino  $^{13}\text{C}_6, ^{15}\text{N}$ . Glutaminolizės įvertinimui terpė buvo papildyta tik 4 mM galutinės koncentracijos L-Glutaminu  $^{13}\text{C}_5$ .

## Metabolitų išskyrimas iš lėkštelių

Metabolominei analizei lėkštelių ekstraktai buvo paruošti kaip nurodyta Sellick ir bendraautorių protokole [97]. Išdžiovinti metabolitų ekstraktai gali būti laikomi  $-80^\circ\text{C}$  temperatūroje arba rehidratuojami dejonizuotu vandeniui ir analizuojami pasitelkiant itin aukšto našumo skysčių chromatografiją su elektropurkštuvinės jonizacijos šaltiniu ir tandeminiu masių spektrometru (angl. *ultra-performance liquid chromatography system with electrospray ionisation source and tandem mass spectrometer*; UPLC-ESI-MS/MS).

## Plazmos paruošimas masių spektrometrijos analizei

Kraujo plazmos analizei gautas Kauno regiono biomedicininų tyrimų etikos komiteto leidimas (2021-03-23, Nr. BE-2-32). Visi tiriamieji buvo mote-

rys ir davė raštišką informuotą sutikimą. Iš viso buvo paimta 20 kraujo mėginių: 10 kontrolinių mėginių iš sveikų moterų bei 10 iš pacienčių, kurioms anksti diagnozuota to paties potipio, kaip BCC ląstelių linijos (T1 N0 M0 G2, ER+, PR+, HER2(3+)) invazinė duktalinė karcinoma. Mėginius sudarė 3 ml šviežiai paimto kraujo vakuuminuose EDTA apdorotuose (purpuriniu dangteliu) kraujo surinkimo mėgintuvėliuose. Iš karto po paėmimo mėginiai buvo centrifuguojami 1300×g 20 minučių 10 °C temperatūroje. Tada 1,5 ml supernatanto (plazmos) buvo atsargiai perkelta į naują mėgintuvėlį ir centrifuguojama 15500×g 10 minučių 10 °C temperatūroje. Surinktas supernatantas buvo paskirstytas į mikrocentrifuginius mėgintuvėlius ir laikomas šaldiklyje –80 °C temperatūroje ilgalaikiam saugojimui. Norint paruošti plazmą chromatografinėi analizei, į 250 μl plazmos buvo pridėta 1,5 ml ledo šaltumo metanolio baltymų nusodinimui. Tada mėginiai buvo 10 sekundžių purtomi, po to 20 minučių laikomi –20 °C temperatūroje. Tuomet mėginiai 10 minučių centrifuguojami 18000×g 4 °C temperatūroje. Supernatantas džiovinamas vakuuminio koncentratoriaus pagalba ir laikomas –80 °C temperatūroje iki instrumentinės analizės. Ruošiantis chromatografijai, išdžiovintos nuosėdos buvo ištirpintos acetonitrile.

### UPLC-ESI-MS/MS

Atlikus metabolitų ekstrakciją, mėginiai buvo analizuojami naudojant Acquity H klasės UPLC sistemą. Ekstraktams atskirti buvo naudojama YMC-Triart C18 (100 × 2,0 mm, 1,9 μm) kolonėlė, o masių spektrometrijos duomenims gauti buvo naudojamas trigubo kvadrupolio tandeminis masės spektrometras Xevo TQD, sujungtas su elektropurkštuvinės jonizacijos (angl. *electrospray ionisation, ESI*) jonų šaltiniu, neigiamu režimu nuo 50 m/z iki 250 m/z. Kolonėlės temperatūra buvo nustatyta ties 40 °C. Eliucija judančia 0,1 proc. skruzdžių rūgšties vandeninio tirpalo (tirpiklis A) ir acetonitrilo (tirpiklis B) faze buvo atlikta 0,4 ml/min tekėjimo greičiu, keičiant tirpiklio A proporcijas gradientu: 0–0,2 min. 95 proc., 0,2–1,5 min 10 proc., 1,5–1,8 min 90 proc. ir 1,8–2 min atgal į pradines sąlygas. Masių spektrometro kapiliarinė įtampa –2 kV, šaltinio temperatūra 150 °C, desolvacijos dujų (azoto) temperatūra 400 °C, dujų srautas 700 l/val, kūgio dujų srautas –20 l/val., o įtampa 25 V.

### Metabolomikos duomenų analizė

Kiekvienam mėginiui buvo atlikti trys biologiniai pakartojimai. Metabolitai, aptikti visuose mėginiuose, atpažinti pagal jų sulaikymo laiką, kurį nustatė Virgiliou ir bendraautoriai [98]. Duomenims analizuoti buvo naudojamas MetaboAnalyst [95], tačiau kelių praturtinimo analizei buvo naudojamas

kitas įrankis – WebGestalt [96], kadangi MetaboAnalyst nepavyko nustatyti aiškių ryšių tarp sutrikusių metabolitų (išskyrus akivaizdžius, tokius kaip taurinas ir hipotaurinas).

### **Metabolizmo srauto modeliavimas remiantis $^{13}\text{C}$ izotopų sekimu**

Apskaičiuojant acetil-KoA frakcijas, gautas skylant BCAA, buvo naudojamas nežymėto (M0) malato ir malato su dviem žymėtomis anglimis (M2) santykis. Eksperimentuose su žymėtu glutaminu, glutaminolizės mastas buvo įvertintas naudojant malato frakciją su keturiomis žymėtomis anglimis (M4), kaip tiesioginis  $\alpha$ -ketoglutarato frakcijos, gautos iš glutamino atitikmuo. Dėl sąveikos su fermentais, tokiais kaip malato dehidrogenazė ir piruvato karboksilazė, susidaro sudėtingi žymėti Krebso ciklo tarpinių produktų profiliai, kurie šiame darbe nebuvo tiriami. Metaboliniai srautai aplink 3-hidroksi-3-metilglutaril-kofermentą A (HMG-KoA) sudarė sudėtingus mevalonato žymėjimo modelius. Srautams apskaičiuoti naudotas elementariųjų metabolinių vienetų metodas [99]. Python programavimo kalba buvo parašytas kodas, kuriuo galima numatyti mevalonato ženklavimo modelius iš srautų pasiskirstymo. Metaboliniai srautai buvo koreguoti, siekiant sumažinti santykinę paklaidą tarp numatomų ir stebimų mevalonato masės dalių.

### **RNR sekoskaita**

Kiekvienai tirtai ląstelių linijai (MCF-7, MCF-10A ir BCC) paruošėme po tris biologinius mėginio pakartojimus. Po tripsinizacijos  $1 \times 10^6$  ląstelių iš kiekvieno mėginio buvo sumaišyta su 500  $\mu\text{l}$  DNA/RNA Shield™ transportavimo terpės, taip paruošiant mėginius siuntimui. Mėginiai buvo išsiųsti į Zymo tyrimų laboratorijas naujos kartos RNR sekoskaitai. Tyrimų laboratorija sudarė RNR sekoskaitos bibliotekas iš 500 ng RNR, naudodama Zymo-Seq RiboFree Total RNA Library Prep Kit rinkinį. Analizė buvo atlikta naudojant „Illumina NovaSeq“ sistemą. Sekos gylis buvo mažiausiai 30 milijonų bazių porų (150 bp porinių galų sekoskaitai) vienam mėginiui.

### **RNR sekoskaitos duomenų analizė**

Gautų sekoskaitos bazių porų prilyginimui standartinei sekai (žmogaus transkriptomo standartas buvo gautas iš Ensembl BioMart duomenų bazės) buvo naudojamas Bowtie2 [92] įrankis. Gautų suderintos sekos žemėlapio failų analizavimui buvo parašytas Python kodas, pagrįstas HTSeq biblioteka [94]. Kiekvieno geno ekspresija apskaičiuota rodmenimis per kilobazę milijonui skaitymų. Padidėjusios ir sumažėjusios raiškos genams įvertinti tarp piktybinių ir sveikų ląstelių linijų buvo naudojamas Stjudento t-testas. Gautos

reikšmės buvo koreguotos siekiant išvengti daugkartinio testavimo paklaidų, kaip aprašyta ankstesniame darbe [7]. Apdoroti ir neapdoroti duomenys patalpinti į NCBI GEO duomenų bazę (įrašo numeris GSE223718).

### **Integruota duomenų analizė pasitelkiant pyTARG**

Reikšmingų ryšių tarp metabolomikos ir transkriptomikos duomenų paieškai buvo naudojamas genomo masto metabolinis modelis (angl. *genome-scale metabolic model, GSMM*). Tokiu būdu siekta rasti koreliaciją tarp metabolizmo ir genų ekspresijos pokyčių. pyTARG – tai anksčiau mūsų komandos sukurta [100] Python biblioteka metaboliniams srautams numatyti pasitelkiant genų ekspresijos duomenis. Metabolinės reakcijos, kurios skiriasi tarp sveikų ir piktybinių ląstelių linijų, buvo nustatytos naudojant Stjudento t-testą su 0,05 klaidingo aptikimo dažniu po daugkartinio testavimo paklaidų korekcijos. Vidutinis srautų skirtumas, didesnis nei 0,001 mmol h<sup>-1</sup> g-DW<sup>-1</sup> (milimolių per valandą vienam gramui sausos masės) buvo reikalingas reikšmingiems rezultatams nustatyti. Plataus spektro metabolinio srauto pasiskirstymo pokyčiams įtakos gali turėti santykinai nedidelis metabolinių genų skaičius. Norint išsiaiškinti srautą kontroliuojančius genus, buvo nustatyti reikšmingi apskaičiuoto reakcijos greičio ir bent vieno su reakcija susijusio geno ekspresijos lygio pokyčiai.

### **Statistinė analizė**

Visi eksperimentai su ląstelėmis buvo atlikti mažiausiai trimis biologiniais pakartojimais ( $n = 3$ ). Duomenų išsibarstymas diagramose išreiškiamas standartine paklaida. Poriniai palyginimai atlikti naudojant Stjudento t-testą. Reikšmingumo lygmuo  $p < 0,05$ . „Žaizdos gijimo“ bei eksperimentų su kraujo plazma statistinė analizė atlikta naudojant „Microsoft Excel 16.75“. Metabolizmo duomenų analizė atlikta naudojant MetaboAnalyst [101] – internetinį įrankį. Pagrindinių komponentų analizė (angl. *principal component analysis, PCA*) buvo atlikta siekiant sumažinti gautų duomenų matmenis ir vizualizuoti skirtingus metabolitų profilius. Prieš PCA atliktas išankstinis duomenų apdorojimas, įskaitant normalizavimą bei mastelio pritaikymą. Po prilyginimo standartinei sekai, duomenų apskaičiavimo ir normalizavimo, naudojant anksčiau minėtus Python kodus, pagrįstus HTSeq biblioteka, RNR sekvenavimo duomenų diferencinės ekspresijos analizė taip pat buvo atlikta naudojant Python. Siekiant įvertinti statistinį reikšmingumą tarp skirtingų ląstelių linijų panaudotas t-testas ir gautos kiekvieno geno  $p$  reikšmės.

## REZULTATAI IR JŲ APTARIMAS

### Ląstelių energijos, gautos skaidant BCAA, kiekybinis įvertinimas

Kol kas dar nėra įmanoma tiesiogiai išmatuoti metabolinių reakcijų greičio, tačiau kiekybiškai įvertinti medžiagų apykaitos srautus galima netiesiogiai, matuojant tarpląstelių metabolitų ženklinimo profilius. Šis metodas apima izotopiškų atomų (pvz.,  $^{13}\text{C}$  vietoje  $^{12}\text{C}$ ) sekimą molekulėse, kad būtų galima atsekti jų metabolizmo kelius. Šiems matavimams naudojami tokie jautrūs metodai kaip branduolinis magnetinis rezonansas arba tandeminė masių spektrometrija. Norėdami išsiaiškinti, kokią įtaką BCAA turi ląstelių energetikai, ląsteles kultivavome terpėje, papildytoje pilnai izotopais pažymėtomis BCAA. Acetilkofermento A (acetil-KoA) dalis, susidariusi BCAA skilimo metu, buvo įvertinta pagal žymėto ir nežymėto malato santykį. Vertinant rezultatus, buvo atsižvelgta ir į glutaminolizę, turinčią įtakos malato santykiui – atlikti eksperimentai su žymėtu glutaminu. Baltymų skilimo reakcijų metu ar terpę papildžius serumu joje gali atsirasti nežymėtų BCAA, taigi norėdami atmesti jų įtaką ląstelių energetiniam metabolizmui, matavome BCAA transaminacijos produktų (4-metil-2-oksopentanoato, 3-metil-2-oksopentanoato ir 3-metil-2-oksobutanoato) frakcijas, žymėtas ir nežymėtas izotopais. Nuoseklios metabolitų frakcijos, susidariusios tirtose ląstelėse sklyant BCAA, parodė, kad maždaug 30 proc. nežymėtų BCAA atsirado iš ląstelių mitybinės terpės. Skaičiavimus atlikome laikydami, kad pilnai pažymėta malato frakcija atitinka  $\alpha$ -ketoglutaratą, gautą glutamino skaidymo metu, o kitos žymėtos malato frakcijos atsirado įvairių fermentinių reakcijų metu. Gauta 0,5 M4 malato frakcija BCC ląstelėse ir 0,17 M4 malato frakcija MCF-7 bei MCF-10A ląstelių linijose byloja apie didesnę glutaminolizės svarbą BCC ląstelėms. Tolimesniais skaičiavimais buvo vertinama acetil-KoA frakcija, atsižvelgiant į glutaminolizę ir nežymėtų BCAA kiekį terpėje. Rezultatai parodė, kad 34 proc. energijos, susidariusios Krebso ciklo metu MCF-7 ląstelėse, buvo gauta BCAA skaidymo metu. Dėl didesnės glutaminolizės įtakos BCAA ląstelių energetiniam metabolizmui, energijos kiekis, susidaręs BCC ląstelėms skaidant BCAA, buvo 14 proc., o MCF-10A – 10 proc. Ankstesnis mūsų grupės tyrimas [7] numatė, kad energija, susidaranti MCF-7 ląstelėms skaidant BCAA, turėtų siekti 47 proc. visos ląstelinės energijos. Šis eksperimentas parodo, kad realybėje šis skaičius yra mažesnis ir kad dalis BCAA sunaudojama kitoms biosintezės reakcijoms, tokioms kaip mevalonato sintezė. Bendrai šio skyriaus rezultatai parodo, kad skirtingų navikinių ląstelių BCAA apykaita gali būti labai skirtinga, o tai tik dar kartą įrodo individualizuoto gydymo svarbą, pavyzdžiui, BCAA sumažinimas dietoje gali būti efektyvus kaip papildoma priemonė hormonų receptorių turinčių ir HER2 neigiamų luminalinių krūties

navikų gydymui (kaip MCF-7), bet mažiau efektyvus HER2 teigiamų (kaip BCC) navikų gydymui.

### **BCAA indėlis į mevalonato metabolizmą**

Be energijos gamybos, acetil-KoA gali būti panaudotas ir lipidų sintezei per mevalonato metabolinį kelią. Mevalono rūgštis arba mevalonatas yra cholesterolio ir kitų sterolių pirmtakas. Mevalonatą iš HMG-KoA sintetina fermentas, vadinamas HMG-KoA reduktaze. HMG-KoA gali būti leucino skilimo produktas, todėl atlikome eksperimentus su  $^{13}\text{C}_6$   $^{15}\text{N}$  žymėtu leucinu, siekdami išsiaiškinti, kiek leucinas prisideda prie mevalonato kelio. HMG-KoA taip pat gali būti sintetinamas iš acetil-KoA arba acetoacetylkofermento A (acetoacetyl-KoA), naudojant fermentą HMG-KoA sintazę. Kitas fermentas – HMG-KoA liazė, gali HMG-KoA suskaidyti atgal į acetil-KoA ir acetoacetatą. Tada fermento acetoacetyl-KoA sintetazės pagalba acetoacetatas gali būti paverstas acetoacetyl-KoA. Gautas acetoacetyl-KoA gali būti paverstas atgal į HMG-KoA – taip susidaro trimis anglimi pažymėtas mevalonatas (M3). Šis reiškinys nebuvo pastebėtas BCC ląstelėse, tačiau jis pasirodė svarbus MCF-7. Tuomet apskaičiavome optimalius metabolinių srautų pasiskirstymus ir normalizavome skaičius pagal pagaminto mevalonato kiekį. Į skaičiavimus taip pat įtraukėme M2 žymėtą mitochondrinį acetil-KoA. Abiejų navikinių ląstelių linijų optimali frakcijos vertė buvo 0,1. Skaičiavimai atlikti darant prielaidą, kad 70 proc. HMG-KoA, susidarančio leucino skilimo metu, yra žymėtas. Norėdami įvertinti, kiek mevalonato (ir acetoacetato) susidaro iš leucino, palyginome bendrą anglies kiekį, gautą iš leucino skilimo kelio, su visa anglimi, kuri sudaro acetyl-KoA. Anglies kiekį, susidarantį MCF-7 ląstelėms skaidant leuciną, galima apskaičiuoti taip: 6 leucino anglies atomai padauginami iš HMG-KoA reakcijos greičio vienam mevalonato vienetui pagaminti ( $6 \times 1,3 = 7,8$ ). Rezultatas lyginamas su suvartoto acetyl-KoA atomų kiekiu. Grynąjį acetyl-KoA suvartojimą galima apskaičiuoti iš visų jį vartojančių reakcijų greičių sumos atėmus reakcijos, kurios metu HMG-KoA liazė pagamina acetyl-KoA, greitį ( $2 \times (2,2 + 21,2 - 21,5) - 2 \times 1,9 = 3,8$ ). Dabar galime apskaičiuoti bendrą anglies atomų, susidariusių MCF-7 skaidant leuciną, kiekį ( $7,8 / (7,8 + 3,8) = 0,67$ ). Skaičiavimai rodo, kad 67 proc. mevalonato ir acetoacetato anglies atomų susidaro leucino skilimo metu. Remdamiesi tais pačiais skaičiavimais, mes išsiaiškinome leucino įtaką mevalonato sintezei ir BCC ląstelėse ( $1,8 / (1,8 + 6,4) = 0,22$ ). Čia tik 22 proc. anglies gaunama iš leucino degradacijos. Priešingai nei navikinėse, sveikose MCF-10A ląstelėse mevalonato visai neaptikome. Įdomu ir tai, kad BCC ląstelių žymėta mitochondrinio acetyl-KoA frakcija, kilusi iš leucino, buvo labai panaši į tą, kuri apskaičiuota eksperimente su visomis trimis BCAA. Tai gali reikšti,

kad šiose ląstelėse, iš trijų BCAA, vienintelis leucinas yra atsakingas už acetyl-KoA tiekimą. Ankstesnis mūsų grupės tyrimas [100, 109] atskleidė, kad daugumoje tirtų navikinių ląstelių linijų nerasta cholesterolio nešiklių, o tai rodo, kad norėdamos apsirūpinti cholesteroliu šios ląstelės yra priklausomos nuo mevalonato kelio. Leucino dalyvavimas *de novo* mevalonato sintezėje yra dar vienas mechanizmas, kuriuo jis palaiko ląstelių proliferaciją ir invaziškumą. Šios išvados sutampa su tyrimais, rodančiais leucino vaidmenį proliferacijoje ir diferenciacijoje, nepriklausomai nuo mTOR signalizacijos kelio [111, 112]. Statinai, skirti cholesterolio kiekio kraujyje mažinimui, mažina navikų proliferaciją klinikinių ir ikiklinikinių tyrimų metu [114–116], o tai reiškia, kad jie galėtų būti pritaikomi kaip pagalbinė priemonė onkologinių ligų gydymui. Tačiau epidemiologinių tyrimų rezultatai nenuoseklūs: kai kurie rodo ryšį tarp didelio cholesterolio kiekio ir navikų arba rodo, kad statinai mažina navikų riziką [117–122], o kiti neranda jokie ryšio [123–126] arba netgi rodo, kad statinai gali būti kancerogeniški, priklausomai nuo dozės [127]. Nors cholesterolio įtaka navikams vis dar neaiški, papildomas leucino vaidmuo cholesterolio sintezėje, kartu su vaidmenimis energijos gamyboje, biomolekulių sintezėje ir signalizavime gali būti viena BCAA poveikio navikų proliferacijai priežasčių.

### **BCAA reikšmė ląstelių invazyvumui**

Žinodami, kad krūties navikinių ląstelių migracija priklauso nuo mevalonato kelio [128, 129], bandėme patikrinti, ar BCAA trūkumas turės įtakos mūsų tirtų ląstelių invazyvumui. Naudojome du skirtingus BCAA kiekio mažinimo ląstelėse metodus: genų slopinimą naudojant siRNR prieš BCAT2 ir BCAA kiekio sumažinimą mitybinėje terpėje (nuo įprastos 0,8 mM iki 0,2 mM koncentracijos). Norėdami įvertinti BCAA įtaką krūties navikinių ląstelių invazyvumui, taikėme „žaizdos gijimo“ tyrimo metodą. *In vitro* „žaizdos gijimo“ tyrimas yra gana paprastas ir ekonomiškai būdas įvertinti ląstelių migraciją skirtingomis eksperimentinėmis sąlygomis. Tyrimas vykdomas vientisame ląstelių sluoksnyje aštrių daiktu atveriant „žaizdą“, t.y. laisvą plotą, į kurį ląstelės galėtų migruoti, siekdamos išlaikyti sluoksnio vientisumą. Tyrėme sumažinto BCAA kiekio terpėje ir BCAT2 geno slopinimo poveikį BCC, MCF-7 ir MCF-10A ląstelių gebėjimui užverti „žaizdą“. Iškart po „žaizdos“ atvėrimo, pakeitėme ląstelių auginimo terpę į įprastai naudojamą DMEM/F-12 arba terpę, kurioje BCAA koncentracija 0,2 mM, siekdami pašalinti po atvėrimo likusias ląstelių nuolaužas, ir tvirtinome lėkštelę ant mikroskopo staliuko esančiame inkubatoriuje, kad būtų galima atlikti uždelsto veikimo vaizdinimą. BCAT2 slopinimas turėjo didesnę įtaką BCC ląstelių migracijai, nei BCAA kiekio sumažinimas terpėje, lyginant su kontrole.



Kontrolės grupės „žaisda“ susitraukė 72,05 proc. (standartinė paklaida (angl. *standard error, SE*)  $\pm$  6,90 proc.) ir 35,96 proc. ( $\pm$  3,88 proc. SE) BCAT2 slopinimo grupėje. Statistiškai reikšmingi rezultatai matomi ir 0,2 mM BCAA terpės grupėje, lyginant su kontrole (50,54 proc.  $\pm$  1,21 proc. SE). Kita vertus, MCF-7 labiau paveikė sumažintas BCAA kiekis terpėje, o BCAT2 slopinimo grupėje statistiškai reikšmingo skirtumo nepastebėta. Šiuo atveju BCC ląstelės buvo jautresnės BCAA kiekio pokyčiams, nors jos ir mažiau prisideda prie mevalonato ir mitochondrinio acetil-KoA gamybos. Taip gali būti dėl to, kad MCF-7 ląstelės nesudaro stabilaus monosluoksnio, todėl atsiranda sunkumų, vertinant šio eksperimento rezultatus. Nepaisant to, MCF-7 ląstelių „žaisda“ žymiai lėčiau užsivėrė 0,2 mM BCAA terpės grupėje: 7,20 proc. ( $\pm$  1,53 proc. SE) po 8 val. laiko intervalo (kontrolės grupėje „žaisdos“ užsivėrimas po 8 val. buvo 19,35 proc.  $\pm$  1,12 proc. SE). Nepiktybinėse MCF-10A ląstelėse statistiškai reikšmingų rezultatų nepastebėjome, o tai gali reikšti, kad BCAA yra susijusios su navikinių, bet ne sveikų epitelio ląstelių migracija arba jų indėlis sveikų ląstelių atveju nėra toks reikšmingas. Norint tiksliau įvertinti šio tyrimo rezultatus, ateityje būtų tikslinga atlikti vienos ląstelės judėjimo įvertinimą. Tokiu būdu būtų sumažintas netolygaus skirtingų ląstelių linijų monosluoksnio sudarymo sukeltas šališkumas.

Ląstelių migracijai įtakos turi ne tik mevalonato sintezė, bet ir ląstelių energetinis metabolizmas bei mTOR signalinis kelias [131, 132], o tai reiškia, kad BCAA ląstelių migraciją gali veikti daugiau nei vienu mechanizmu. mTOR signalinį kelią aktyvina viduląstelinis leucinas, kurio kiekis gali padidėti dėl sutrikdyto BCAA katabolizmo po BCAT2 slopinimo, taigi mažai tikėtina, kad judėjimo sulėtėjimas slopinant BCAT2 yra sukeltas mTOR. Šį teiginį papildoma ir tyrimai, rodantys, kad didesnė BCAA koncentracija terpėje slopina krūties ląstelių judėjimą [133], kas gali reikšti, jog šiame procese dalyvauja visiškai kitas mechanizmas. Autorių teigimu, tam įtakos gali turėti padidėjęs BCAA poreikis imuninėms ląstelėms. Sciacovelli ir kt. atliktas tyrimas atskleidė, kad būtent metastazavusiose inkstų karcinomos ląstelėse dalis BCAA kilmės azoto apeina Krebso ciklą ir patenka į arginino biosintezę [38]. Fermentas argininosukcinato sintetazė 1, kurio pagalba ir sintetinamas argininas, taip pat yra svarbus ląstelių migracijos veiksnys, o tai rodo dar vieną mechanizmą, kuriuo BCAA gali skatinti navikinių ląstelių migraciją.

### **BCAA katabolizmo tarpinių metabolitų nustatymas kraujo plazmoje**

Siekdami nustatyti, ar klinikinėje aplinkoje yra kokių nors pokyčių krūties navikais sergančių pacienčių BCAA skaidymo kelyje, atlikome nedidelio masto eksperimentą, naudodami žmogaus kraujo plazmą. Atlikome tikslią chromatografinę dešimties sveikų moterų ir dešimties moterų, sergančių

krūties adenokarcinoma, kraujo plazmos mėginių analizę (daugiau skyriuje „Medžiagos ir metodai“). Šiame tyrime pasirinkome tirti penkis BCAA metabolitus: 3-hidroksiizovalerata bei mevalonata, kaip tarpinius leucino skilimo produktus, 3-metil-2-oksopentanoata kaip tarpinį izoleucino skilimo produktą ir 3-aminoizobutanoata bei 3-hidroksiizobutirata iš valino skaidymo kelio.

Kiekvieno tirtų tarpinių produktų kiekiai stipriai varijavo tarp skirtingų mėginių. Nepaisant to, pacientų kraujo plazmoje pastebėjome statistiškai reikšmingą 3-hidroksiizobutirato (valino degradacijos produkto) kiekio padidėjimą, lyginant su kontrolės grupe, nors jo koncentracija MCF-7 ir BCC navikinėse ląstelėse nebuvo didelė. Tai gali reikšti, kad naviko ląstelės išskiria 3-hidroksiizobutirata į išorę, tačiau to priežastis nežinoma.

Stebėjome ir statistiškai reikšmingai didesnę 3-hidroksiizovalerato kiekį pacienčių plazmos mėginiuose. 3-hidroksiizovaleratas išsiskvoja leucino degradacijos kelyje ir nedalyvauja acetil-KoA bei mevalonato sintezėje. Matydami, kad mevalonato kiekis krūties navikais sergančių pacienčių plazmoje buvo gerokai mažesnis, galime teigti, kad padidėjęs jo poreikis pačiame navike, taigi aktyvinamas leucino skilimo kelias, o nereikalingi mevalonato sintezei tarpiniai produktai išskiriami į ląstelės išorę – todėl mūsų plazmos mėginiuose stebimas 3-hidroksiizovalerato kiekio padidėjimas.

Be to, atlikdami eksperimentus su izotopiškai žymėtomis BCAA, navikinių ląstelių ekstraktų mėginiuose pastebėjome palyginti didelį 3-metil-2-oksopentanoato kiekį, kas galėtų reikšti padidėjusį izoleucino skaidymo kelio aktyvumą, tuo tarpu šio tarpinio produkto kiekis kraujo plazmoje reikšmingai nesiskyrė tarp pacienčių ir sveikų moterų. Valino degradacijos tarpinio produkto 3-aminoizobutanoato kiekis nerodė statistiškai reikšmingų skirtumų tarp tiriamųjų.

Reikšmingi pokyčiai BCAA skilimo kelyje buvo stebimi ir kitų mokslininkų atliktuose tyrimuose [134, 136], taigi BCAA skilimo produktai galėtų būti panaudojami kaip biožymenys ankstyvos stadijos krūties navikų aptikimui. Didesni pačių BCAA kiekiai kraujo plazmoje siejami su mažesne krūties navikų rizika moterims, dar neturėjusioms menopauzės, ir didesne rizika moterims po menopauzės. Tai gali reikšti, kad hormonų pokyčiai labai svarbūs šių aminorūgščių vaidmeniui ligos progresavime. Kaip jau minėta vienoje šios disertacijos diskusijos dalyje (žr. skyrių „BCAA reikšmė ląstelių invazyvumui“), padidėjęs cirkuliuojančių BCAA kiekis gali sužadinti imunines reakcijas [133] – tai gali turėti įtakos mažesnei krūties navikų rizikai prieš menopauzę. Kitame tyrime, kuriame buvo tiriamos moterys prieš menopauzę be žinomos onkologinės ligos diagnozės, didelis BCAA kiekis plazmoje reikšmingai teigiamai koreliavo su laisvojo testosterono lygiu [137]. Lytinių hormonų lygio pokyčiai yra gerai žinomi krūties navikų rizikos biožymenys [138, 139].

## Aminorūgščių, susijusių su piktybiškumu krūties kilmės ląstelėse, metabolitų analizė

Toliau buvome suinteresuoti nustatyti platesnį su aminorūgštimis susijusių pokyčių spektrą tirtų ląstelių linijų metabolomuose. Metabolizmo analizė leido kiekybiškai įvertinti 33 vidinius metabolitus visose trijose tirtose ląstelių linijose. PCA atskleidė, kad 97,6 proc. metabolinių duomenų dispersijos gali būti priskirta pirmiesiems dviems pagrindiniams komponentams – pirmasis sudaro 61,6 proc. kintamumo, o antrasis – 36,0 proc. Antrasis komponentas aiškiai atskyrė MCF-10A nuo piktybinių MCF-7 ir BCC ląstelių, o šie rezultatai rodo, kad 36 proc. metabolitų koncentracijų skirtumų tarp trijų ląstelių linijų yra susiję su piktybiniais krūties navikais.

BCC ląstelėse pastebėta mažesnė trijų BCAA: leucino, izoleucino ir valino, koncentracija. Tai gali reikšti, kad BCC ląstelėms šios aminorūgštys mažiau svarbios arba kad ši linija joms auksotrofinė. Pastarasis teiginys labiau tikėtinas, atsižvelgiant į tai, kad kituose mūsų atliktuose eksperimentuose BCC visada buvo tarp MCF-7 ir MCF-10A, kas liečia BCAA panaudojimą, bei tai, kad BCC, kaip ir MCF-7, pastebėta padidėjusi BCAT2 raiška [7].

Šeši metabolitai iš 33-jų minėtų metabolitų pasižymi didesnėmis koncentracijomis MCF-10A, lyginant su piktybinėmis ląstelių linijomis. Tai tirozinas, metioninas, manitolis, hipotaurinas, cholinas ir taurinas. Kita metabolitų grupė sudarė klasterį, kuriam būdinga didesnė koncentracija MCF-7 ir BCC ląstelėse. Šie keturi metabolitai buvo betainas, acetilkarnitinas, serinas ir piroglutamato rūgštis. Iš visų paminėtų pakitusios koncentracijos metabolitų šeši (metioninas, taurinas, hipotaurinas, cholinas, betainas ir piroglutamato rūgštis) tam tikru mastu susiję su metionino ciklu. Sumažėjusį šių metabolitų kiekį MCF-7 ir BCC ląstelėse gali lemti didesnis jų suvartojimas, dėl metionino ciklo svarbos greitai besidalijančioms ląstelėms.

Nors navikinės ląstelės ir turi galimybę sintetinti metioniną, jo pasiūla dažnai nepaveja paklausos, todėl ląstelės tampa auksotrofinėmis [43]. Priklausomybė nuo metionino yra seniai žinoma navikų savybė, tačiau vis dar labai aktuali tema, kai kalbama apie individualizuoto gydymo strategijas [44, 143, 144, 146]. Be to, kad metioninas yra baltymų statybinė medžiaga, jis dalyvauja ir keliuose svarbiuose metaboliniuose keliuose epigenetikoje (S-adenozilmetioninas), branduoliniuose procesuose (poliaminai), detoksikacijoje (glutatonas) bei ląstelių membranų (fosfolipidų) susidaryme. Metionino ciklas yra vadinamojo vienos anglies metabolizmo dalis, leidžianti ląstelėms generuoti metilo grupes (vienos anglies struktūrinius vienetus) bei panaudoti jas metilinimo procesuose, kurie yra labai svarbūs transkripcijai, replikacijai ir DNR pažaidų taisymui. Folio ciklas, kita vienos anglies metabolizmo dalis, ilgą laiką buvo taikinyus navikų gydymui – vadovaujantis tuo buvo atrasti fo-

lio rūgšties antagonistai. Žinomiausias šios klasės vaistas – metotreksatas vis dar naudojamas daugelio navikų gydymui [144], tačiau sukelia daug nepageidaujamų reakcijų. To galima būtų išvengti selektyviai taikantis į fermentus vienos anglies metabolizmo keliuose.

### **Krūties navikinių ir sveikų ląstelių diferencinė genų ekspresija**

Išvadų apie ląstelių metabolizmą formulavimas, žinant tik atitinkamas metabolitų koncentracijas, būtų netikslingas, kadangi medžiagų apykaita yra sudėtingas skirtingų fermentų ir jų substratų sąveikos tinklas. Turėdami omenyje tai, sujungėme metabolomikos duomenis su naujos kartos RNR sekoskaitos duomenimis, kad turėtume platesnį pagrindinių su piktybiniais navikais susijusių procesų vaizdą. Žinodami genų, koduojančių skirtingus metabolinius fermentus, raišką, gauname vertingos informacijos apie galimus ląstelių metabolizmo profilių pokyčius. Atlikome RNR sekoskaitos duomenų diferencinės ekspresijos analizę. Klaidingo aptikimo dažniui pasirinkome ribinę 0,01 vertę, o raiškos pokyčiai vertinti, jeigu raiškos skirtumas tarp tiriama grupių buvo mažiausiai 2 kartai. Apdoroti RNR sekoskaitos duomenys parodė, kad 1495 genai MCF-7 ląstelėse pasižymėjo padidėjusia raiška, lyginant su MCF-10A, o 1335 genai – sumažėjusia raiška. Lyginant BCC su sveikomis krūties epitelio ląstelėmis, 1926 bendri genai pasižymėjo padidėjusia raiška, o 1669 – sumažėjusia raiška BCC ląstelėse. Abiejose piktybinėse ląstelių linijose buvo paplitę 274 genai, pasižymintys padidėjusia raiška, ir 563, pasižymintys sumažėjusia raiška, lyginant su sveikomis ląstelėmis. Tuomet atlikome Kioto genų ir genomų enciklopedijos (angl. *Kyoto Encyclopedia of Genes and Genomes; KEGG*) kelių praturtinimo analizę naudodami WebGestalt internetinį įrankių rinkinį (webgestalt.org), tačiau neradome reikšmingai praturtintų kelių tarp padidėjusia raiška pasižyminčių genų (ribinis klaidingo aptikimo dažnis buvo 0,05). Kita vertus, nustatėme 10 statistiškai reikšmingai praturtintų kelių, kuriuose genai pasižymi sumažėjusia raiška. Pusė minėtų kelių buvo susiję su tam tikromis patogenų sukeliomomis ligomis, kita pusė – su ląstelių signaliniais keliais, tačiau neradome praturtintų kelių, susijusių su medžiagų apykaita. Tai iškėlė poreikį integruoti į analizę anksčiau gautus metabolomikos duomenis panaudojant GSMM duomenų interpretavimui. Iš 274 genų, pasižyminčių padidėjusia raiška abiejose navikinėse ląstelių linijose, 44 buvo metaboliniai genai, dalyvaujantys 131 metabolinėje reakcijoje. Iš 563 genų, pasižyminčių sumažėjusia raiška piktybinėse ląstelių linijose, 130 buvo metaboliniai, susiję su 832 metabolinėmis reakcijomis. Didelis pastarųjų reakcijų skaičius susijęs su šių genų dalyvavimu transmembraninėje pernašoje. Pavyzdžiui, genai SLC36A4 ir SLC6A15 susiję su aminorūgščių pernaša.

## Potencialių vaistų taikinių krūties piktybiniam navikams paieška derinant metabolinius ir genominius duomenis

Trys iš anksčiau minėtų pakitusios koncentracijos metabolitų (metioninas, taurinas ir hipotaurinas) turi bendrą pirmtaką – homocisteiną, kuris yra tarpinis metionino ciklo produktas. Kitas metabolitas, piroglutamato rūgštis, susidaranti glutatono skilimo metu, taip pat gali būti siejama su homocisteinu, nors jos skeletą sudarantys anglies atomai gaunami iš glutamino, kuris dalyvauja glutatono sintezėje. Mes nustatėme, kad genas AHCY, koduojantis fermentą adenozilhomocisteinazę, dalyvaujančią S-adenozilhomocisteinui skylant į adenoziną ir L-homocisteiną, pasižymi sumažėjusia raiška MCF-7 ir BCC ląstelėse, lyginant su MCF-10A. Jau anksčiau pastebėta, kad AHCY yra naviką slopinantis genas, susijęs su p53 sukeltu ląstelės ciklo sustabdymu [148]. Panašu, kad ši funkcija specifinė ląstelių tipui, nes kai kurios navikų rūšys, pavyzdžiui, neuroblastoma, turi padidėjusią AHCY raišką, kas reikštų, kad AHCY šiuo atveju yra onkogenas [149, 150]. Mūsų tyrimo atveju sumažėjusi AHCY raiška, kartu su sumažėjusia metionino koncentracija ląstelių ekstraktuose, leidžia daryti prielaidą, kad mūsų tiriamose piktybinėse ląstelių linijose metionino ciklo aktyvumas mažesnis. Du kiti pakitusios koncentracijos metabolitai, betainas ir cholinas, taip pat yra susiję su metionino ciklu. Cholinas yra vitaminas, gaunamas su maistu. Jis dalyvauja betaino sintezėje, o šis metionino ciklui tiekia metilo grupes. Šios grupės, kartu su S-adenozilmetioninu (SAM) kaip metilo donoru, naudojamos DNR ir baltymų metilimui [152]. Cholino telkinys abiejose navikinėse ląstelių linijose buvo mažesnis dėl sumažėjusios geno SLC44A5, atsakingo už cholino pernašą, raiškos. Ir atvirkščiai, piktybinėse ląstelėse betaino kiekis buvo didesnis greičiausiai dėl to, kad sumažėjus metionino ciklo aktyvumui, sumažėjo betaino suvartojimas.

Sumažėjęs metionino ciklo aktyvumas taip pat reiškia sumažėjusią SAM sintezę. SAM, kaip maisto papildas, potencialas onkologinių ligų terapijoje buvo įrodytas ne vienu tyrimu [154–156]. Tikslinėse vaistų taikinių paieškose naviką slopinantys genai dažnai pamirštami, kadangi atrodo paprasčiau mažomis molekulėmis slopinti onkogeno skatinamą funkciją, nei aktyvinti slopinančio geno slopinamą [160]. Tačiau, aminorūgščių kontekste, šią užduotį galima lengvai išspręsti papildant mitybą atitinkamomis aminorūgštimis. Keli tyrimai jau parodė, kad didesnė metionino koncentracija terpėje slopino MCF-7 ir kitų ląstelių proliferaciją per p53, nepaveikiant sveikų ląstelių [161–164]. Tačiau tokie gydymo būdai turėtų būti priimami kritiškai vertinant kiekvieną atvejį, kadangi, kaip minėta anksčiau, kai kurie navikai turi priklausomybę nuo metionino. Tai pabrėžia individualaus gydymo svarbą onkologijoje. Ateityje kiekvieno paciento gydymui įvertinti turėtų būti atliekamas nuodugnus metabolinis naviko ištyrimas, siekiant didžiausio efekto ir mažiausio nepageidaujamo poveikio.

Mūsų genų ekspresijos duomenys taip pat parodė, kad du genai, dalyvavę serino biosintezėje iš 3-fosfoglicerato (PHGDH ir PSPH), pasižymėjo padidėjusia raiška MCF-7 ir BCC, lyginant su MCF-10A. Genas PHGDH, koduojantis fosfoglicerato dehidrogenazę, padidėjusia raiška pasižymi ir kitų navikų tyrimuose [165], o padidėjusi jo raiška MCF-10A ląstelėse gali sukelti piktybinius pakitimus [166]. Padidėjusi krūties onkologinių pacientų PHGDH raiška susijusi su trumpesniu recidyvo laikotarpiu ir mažesniu bendru išgyvenamumu [167]. PSPH koduoja fosfoserino fosfatazę, kuri dalyvauja paskutiniame L-serino sintezės etape. Padidėjusi PSPH raiška taip pat perspektyvus kolorektalinių navikų biožymuo [168]. Šių dviejų genų vaidmuo navikuose vis dar nėra pilnai suprantamas. Kartu su susikaupusiu viduląstelinio serinu, mūsų rezultatai rodo didesnę serino biosintezės greitį. Serinas yra dar vienas svarbus vienos anglies metabolizmo dalyvis, nes yra pagrindinis metilo grupių šaltinis [169]. Dėl šios priežasties daugeliui navikų gali išsivystyti priklausomybė nuo viduląstelinio serino. Ksenografinių pelių modeliuose, navikai augo beveik dvigubai greičiau, kai pelės buvo šeriamos serinu ir glicinu papildytu pašaru [171]. Kiti tyrimai rodo, kad PSPH gali skatinti navikų metastazes ir nesusijusiais su L-serino sinteze keliais [172, 173], o tai rodo, kad farmakologinis fermento slopinimas šiuo atveju būtų geresnė alternatyva, nei dietinis serino ribojimas.

Padidėjęs mitochondrijų aktyvumas navikuose lemia padidėjusį reaktyviųjų deguonies rūšių, vaidinančių svarbų vaidmenį naviko signaliniuose keliuose, kiekį [174, 175]. Glutationas neutralizuoja laisvuosius radikalus ir detoksikuoja ląsteles [175]. Glutatioono skilimo metu susidaro piroglutamato rūgštis, kurios koncentracija mūsų tirtose piktybinėse ląstelių linijose yra padidėjusi. Integruota analizė atskleidė padidėjusią geno CHAC1 raišką tiek MCF-7, tiek BCC ląstelėse. Šio geno produktas, glutationui specifinė  $\gamma$ -glutamilciklotransferazė 1, skaido glutationą į cisteinil-gliciną ir piroglutamato rūgštį [176]. Slopinant CHAC1, sumažėja ląstelių migracija ir proliferacija, o padidėjusi šio geno raiška turi priešingą poveikį. Be to, didesnė CHAC1 raiška koreliuoja su prastesne krūties ir kiaušidžių navikų prognoze [177, 178]. Atsižvelgdami į savo ir kitų mokslininkų rezultatus, manome, kad piroglutamato rūgštis galėtų būti potencialus krūties navikų biožymuo, o CHAC1 – perspektyvus vaistų kūrimo taikinys.

Galiausiai, genų raiškos duomenys buvo panaudoti kuriant GSMM pasitelkiant prieš tai sukurtą Python biblioteką pyTARG [100]. Norėdami numatyti metabolinių srautų pasiskirstymą, pritaikėme srautų balanso analizę. Ji atskleidė sumažėjusį kvėpavimo grandinės aktyvumą navikinėse ląstelėse, o tai sutampa su Warburgo efektu ir buvo pastebėta didesnėje grupėje skirtingų navikų ląstelių [100]. Taip pat nustatėme, kad ATP-sintazės reakcijos greitis dviejose mūsų tirtose navikinėse ląstelėse buvo mažesnis bei susijusių genų

ATP1B3 ir ATP6V1H raiška sumažėjusi. Panašūs rezultatai gauti tyrimuose su 5-fluorouracilui atspariomis storosios žarnos navikinėmis ląstelėmis [182]. Kvėpavimo grandinės komplekso reakcijos greitis taip pat buvo mažesnis bei dviejų su juo susijusių genų (UQCRH ir UQCR1) raiška sumažėjusi. Pastebėtas mažesnis metabolitų srautas ir antrajame kvėpavimo grandinės komplekse dėl sumažėjusio geno NDUFB8 raiškos. Užląstelinio serino pasisavinimas abiejose navikinėse ląstelėse buvo blogesnis, dėl mažesnės serino/protonų simporterio, kurį koduoja SLC36A4, raiškos. Tai dar kartą įrodo serino sintezės svarbą navikinėse ląstelėse. Modelis taip pat numatė mažesnę  $\text{CO}_2$  virtimo bikarbonatu reakcijos greitį navikinėse ląstelėse dėl sumažėjusios karboninių anhidrazių CA6 ir CA2 raiškos. Karboninės anhidrazės svarbios navikų pH reguliavimui, IX ir XII izoformos pripažįstamos priešnavikinių vaistų taikiniams, tačiau kitos izoformos vis dar nėra pakankamai ištyrinėtos [184]. Tai galėtų būti tolimesnių tyrimų tąsa.

## IŠVADOS

1. BCAA skilimo įtaka ląstelinės energijos gamybai Krebso cikle buvo 34 proc. MCF-7 ląstelėse, 14 proc. BCC ląstelėse ir 10 proc. MCF-10A ląstelėse. Mevalonato sintezė iš leucino vyko išskirtinai krūties naviko ląstelėse; MCF-7 ląstelėse 67 proc. leuciną sudarančių anglies atomų galiausiai virto mevalonatu, BCC ląstelėse šis kiekis atitiko 22 proc. BCAA metabolizmo slopinimas taip pat žymiai sulėtino krūties naviko ląstelių invazyvumą.
2. Krūties navikais sergančių pacienčių kraujo plazmoje pastebėtas statistiškai reikšmingai didesnis 3-hidroksiizovalerato ir 3-hidroksiizobutirato kiekis bei mažesnis mevalonato kiekis, lyginant su sveikomis moterimis. Rezultatai rodo, kad krūties navikais sergančių pacienčių medžiagų apykaita pakitusi taip, kad patenkintų padidėjusį mevalonato ir acetil-KoA poreikį. Dėl šios priežasties, minėti metabolitai galėtų būti naudojami kaip biožymenys ankstyviems krūties navikams aptikti.
3. Buvo nustatyti 33 vidiniai metabolitai, kurie buvo bendri tarp BCC, MCF-7 ir MCF-10A ląstelių. Dešimt iš jų: tirozinas, manitolis, acetilkarnitinas, serinas, metioninas, taurinas, hipotaurinas, cholinas, betainas ir piroglutamato rūgštis buvo susiję su krūties piktybiniais navikais. Paskutinės šešios iš pirmiau minėtų medžiagų yra metaboliškai susijusios su metionino ciklu. Integruota metabolomo ir transkriptomo analizė atskleidė, kad su metionino ir serino metabolizmu susiję genai AHCY, PHGDH, PSPH bei CHAC1 gali būti tirtų krūties naviko ląstelių chemoterapinis taikynys.

## BIBLIOGRAPHY

1. World Health Organization (2023) Global breast cancer initiative implementation framework: assessing, strengthening and scaling-up of services for the early detection and management of breast cancer. Executive summary
2. DeSantis C, Ma J, Bryan L, Jemal A (2014) Breast cancer statistics, 2013. *CA Cancer J Clin* 64:52–62. <https://doi.org/10.3322/caac.21203>
3. Warburg O (1956) On the Origin of Cancer Cells. *Science* (1979) 123:309–314. <https://doi.org/10.1126/science.123.3191.309>
4. Hanahan D, Weinberg RA (2011) Hallmarks of Cancer: The Next Generation. *Cell* 144:646–674. <https://doi.org/10.1016/j.cell.2011.02.013>
5. Ling Z-N, Jiang Y-F, Ru J-N, Lu J-H, Ding B, Wu J (2023) Amino acid metabolism in health and disease. *Signal Transduct Target Ther* 8:345. <https://doi.org/10.1038/s41392-023-01569-3>
6. Tönjes M, Barbus S, Park YJ, Wang W, Schlotter M, Lindroth AM, Pleier S V, Bai AHC, Karra D, Piro RM, Felsberg J, Addington A, Lemke D, Weibrecht I, Hovestadt V, Rolli CG, Campos B, Turcan S, Sturm D, Witt H, Chan TA, Herold-Mende C, Kemkemer R, König R, Schmidt K, Hull W-E, Pfister SM, Jugold M, Hutson SM, Plass C, Okun JG, Reifenberger G, Lichter P, Radlwimmer B (2013) BCAT1 promotes cell proliferation through amino acid catabolism in gliomas carrying wild-type IDH1. *Nat Med* 19:901–908. <https://doi.org/10.1038/nm.3217>
7. Antanavičiūtė I, Mikalayeva V, Ceslevičienė I, Milašiūtė G, Skeberdis VA, Bordel S (2017) Transcriptional hallmarks of cancer cell lines reveal an emerging role of branched chain amino acid catabolism. *Sci Rep* 7:7820. <https://doi.org/10.1038/s41598-017-08329-8>
8. Nong X, Zhang C, Wang J, Ding P, Ji G, Wu T (2022) The mechanism of branched-chain amino acid transferases in different diseases: Research progress and future prospects. *Front Oncol* 12:. <https://doi.org/10.3389/fonc.2022.988290>
9. Polyak K (2007) Breast cancer: origins and evolution. *Journal of Clinical Investigation* 117:3155–3163. <https://doi.org/10.1172/JCI33295>
10. Zubair M, Wang S, Ali N (2021) Advanced Approaches to Breast Cancer Classification and Diagnosis. *Front Pharmacol* 11:. <https://doi.org/10.3389/fphar.2020.632079>
11. Feng Y, Spezia M, Huang S, Yuan C, Zeng Z, Zhang L, Ji X, Liu W, Huang B, Luo W, Liu B, Lei Y, Du S, Vuppalapati A, Luu HH, Haydon RC, He T-C, Ren G (2018) Breast cancer development and progression: Risk factors, cancer stem cells, signaling pathways, genomics, and molecular pathogenesis. *Genes Dis* 5:77–106. <https://doi.org/10.1016/j.gendis.2018.05.001>
12. Sprague BL, Trentham-Dietz A (2010) In situ Breast Cancer. In: *Breast Cancer Epidemiology*. Springer New York, New York, NY, pp 47–72
13. Yoder BJ, Wilkinson EJ, Massoll NA (2007) Molecular and Morphologic Distinctions between Infiltrating Ductal and Lobular Carcinoma of the Breast. *Breast J* 13:172–179. <https://doi.org/10.1111/j.1524-4741.2007.00393.x>
14. Tsang JYS, Tse GM (2020) Molecular Classification of Breast Cancer. *Adv Anat Pathol* 27:27–35. <https://doi.org/10.1097/PAP.0000000000000232>
15. Orrantia-Borunda E, Anchondo-Nuñez P, Acuña-Aguilar LE, Gómez-Valles FO, Ramírez-Valdespino CA (2022) Subtypes of Breast Cancer. In: *Breast Cancer*. Exon Publications, pp 31–42
16. Uxa S, Castillo-Binder P, Kohler R, Stangner K, Müller GA, Engeland K (2021) Ki-67 gene expression. *Cell Death Differ* 28:3357–3370. <https://doi.org/10.1038/s41418-021-00823-x>



17. Allison KH (2012) Molecular Pathology of Breast Cancer. *Am J Clin Pathol* 138:770–780. <https://doi.org/10.1309/AJCPIV9IQ1MRQMOO>
18. Waks AG, Winer EP (2019) Breast Cancer Treatment. *JAMA* 321:288. <https://doi.org/10.1001/jama.2018.19323>
19. Morrow M, White J, Moughan J, Owen J, Pajack T, Sylvester J, Frank Wilson J, Winchester D (2001) Factors Predicting the Use of Breast-Conserving Therapy in Stage I and II Breast Carcinoma. *Journal of Clinical Oncology* 19:2254–2262. <https://doi.org/10.1200/JCO.2001.19.8.2254>
20. Łukasiewicz S, Czeczelewski M, Forma A, Baj J, Sitarz R, Stanisławek A (2021) Breast Cancer—Epidemiology, Risk Factors, Classification, Prognostic Markers, and Current Treatment Strategies—An Updated Review. *Cancers (Basel)* 13:4287. <https://doi.org/10.3390/cancers13174287>
21. Rouzier R, Perou CM, Symmans WF, Ibrahim N, Cristofanilli M, Anderson K, Hess KR, Stec J, Ayers M, Wagner P, Morandi P, Fan C, Rabiul I, Ross JS, Hortobagyi GN, Pusztai L (2005) Breast Cancer Molecular Subtypes Respond Differently to Preoperative Chemotherapy. *Clinical Cancer Research* 11:5678–5685. <https://doi.org/10.1158/1078-0432.CCR-04-2421>
22. Yang TJ, Ho AY (2013) Radiation Therapy in the Management of Breast Cancer. *Surgical Clinics of North America* 93:455–471. <https://doi.org/10.1016/j.suc.2013.01.002>
23. Lumachi F, Luisetto G, M.M. Basso S, Basso U, Brunello A, Camozzi V (2011) Endocrine Therapy of Breast Cancer. *Curr Med Chem* 18:513–522. <https://doi.org/10.2174/092986711794480177>
24. Tinoco G, Warsch S, Glück S, Avancha K, Montero AJ (2013) Treating Breast Cancer in the 21st Century: Emerging Biological Therapies. *J Cancer* 4:117–132. <https://doi.org/10.7150/jca.4925>
25. Pavlova NN, Thompson CB (2016) The Emerging Hallmarks of Cancer Metabolism. *Cell Metab* 23:27–47. <https://doi.org/10.1016/j.cmet.2015.12.006>
26. DeBerardinis RJ, Chandel NS (2020) We need to talk about the Warburg effect. *Nat Metab* 2:127–129. <https://doi.org/10.1038/s42255-020-0172-2>
27. Patra KC, Wang Q, Bhaskar PT, Miller L, Wang Z, Wheaton W, Chandel N, Laakso M, Muller WJ, Allen EL, Jha AK, Smolen GA, Clasquin MF, Robey RB, Hay N (2013) Hexokinase 2 Is Required for Tumor Initiation and Maintenance and Its Systemic Deletion Is Therapeutic in Mouse Models of Cancer. *Cancer Cell* 24:213–228. <https://doi.org/10.1016/j.ccr.2013.06.014>
28. Fantin VR, St-Pierre J, Leder P (2006) Attenuation of LDH-A expression uncovers a link between glycolysis, mitochondrial physiology, and tumor maintenance. *Cancer Cell* 9:425–434. <https://doi.org/10.1016/j.ccr.2006.04.023>
29. Newsholme EA, Crabtree B, Ardawi MSM (1985) The role of high rates of glycolysis and glutamine utilization in rapidly dividing cells. *Biosci Rep* 5:393–400. <https://doi.org/10.1007/BF01116556>
30. DeBerardinis RJ, Cheng T (2010) Q's next: the diverse functions of glutamine in metabolism, cell biology and cancer. *Oncogene* 29:313–324. <https://doi.org/10.1038/onc.2009.358>
31. Michalak KP, Maćkowska-Kędziora A, Sobolewski B, Woźniak P (2015) Key Roles of Glutamine Pathways in Reprogramming the Cancer Metabolism. *Oxid Med Cell Longev* 2015:1–14. <https://doi.org/10.1155/2015/964321>
32. Kennedy L, Sandhu JK, Harper M-E, Cuperlovic-Culf M (2020) Role of Glutathione in Cancer: From Mechanisms to Therapies. *Biomolecules* 10:1429. <https://doi.org/10.3390/biom10101429>

33. Endicott M, Jones M, Hull J (2021) Amino acid metabolism as a therapeutic target in cancer: a review. *Amino Acids* 53:1169–1179. <https://doi.org/10.1007/s00726-021-03052-1>
34. Al-Koussa H, El Mais N, Maalouf H, Abi-Habib R, El-Sibai M (2020) Arginine deprivation: a potential therapeutic for cancer cell metastasis? A review. *Cancer Cell Int* 20:150. <https://doi.org/10.1186/s12935-020-01232-9>
35. Dillon BJ, Prieto VG, Curley SA, Ensor CM, Holtsberg FW, Bomalaski JS, Clark MA (2004) Incidence and distribution of argininosuccinate synthetase deficiency in human cancers. *Cancer* 100:826–833. <https://doi.org/10.1002/cncr.20057>
36. Kobayashi E, Masuda M, Nakayama R, Ichikawa H, Satow R, Shitashige M, Honda K, Yamaguchi U, Shoji A, Tochigi N, Morioka H, Toyama Y, Hirohashi S, Kawai A, Yamada T (2010) Reduced Argininosuccinate Synthetase Is a Predictive Biomarker for the Development of Pulmonary Metastasis in Patients with Osteosarcoma. *Mol Cancer Ther* 9:535–544. <https://doi.org/10.1158/1535-7163.MCT-09-0774>
37. Shan Y-S, Hsu H-P, Lai M-D, Yen M-C, Chen W-C, Fang J-H, Weng T-Y, Chen Y-L (2015) Argininosuccinate synthetase 1 suppression and arginine restriction inhibit cell migration in gastric cancer cell lines. *Sci Rep* 5:9783. <https://doi.org/10.1038/srep09783>
38. Sciacovelli M, Dugourd A, Jimenez LV, Yang M, Nikitopoulou E, Costa ASH, Tronci L, Caraffini V, Rodrigues P, Schmidt C, Ryan DG, Young T, Zecchini VR, Rossi SH, Massie C, Lohoff C, Masid M, Hatzimanikatis V, Kuppe C, Von Kriegsheim A, Kramann R, Gnanapragasam V, Warren AY, Stewart GD, Erez A, Vanharanta S, Saez-Rodriguez J, Frezza C (2022) Dynamic partitioning of branched-chain amino acids-derived nitrogen supports renal cancer progression. *Nat Commun* 13:7830. <https://doi.org/10.1038/s41467-022-35036-4>
39. Qiu F, Huang J, Sui M (2015) Targeting arginine metabolism pathway to treat arginine-dependent cancers. *Cancer Lett* 364:1–7. <https://doi.org/10.1016/j.canlet.2015.04.020>
40. Zhang Y, Chung S-F, Tam S-Y, Leung Y-C, Guan X (2021) Arginine deprivation as a strategy for cancer therapy: An insight into drug design and drug combination. *Cancer Lett* 502:58–70. <https://doi.org/10.1016/j.canlet.2020.12.041>
41. Yu K-M, Pang TP, Cutler M, Tian M, Huang L, Lau JY-N, Chung S-F, Lo TW, Leung TY (2021) Rational design, engineer, and characterization of a novel pegylated single isomer human arginase for arginine depriving anti-cancer treatment. *Life Sci* 264:118674. <https://doi.org/10.1016/j.lfs.2020.118674>
42. Sugimura T, Birnbaum SM, Winitz M, Greenstein JP (1959) Quantitative nutritional studies with water-soluble, chemically defined diets. VIII. The forced feeding of diets each lacking in one essential amino acid. *Arch Biochem Biophys* 81:448–455. [https://doi.org/10.1016/0003-9861\(59\)90225-5](https://doi.org/10.1016/0003-9861(59)90225-5)
43. Hoffman RM, Erbe RW (1976) High in vivo rates of methionine biosynthesis in transformed human and malignant rat cells auxotrophic for methionine. *Proceedings of the National Academy of Sciences* 73:1523–1527. <https://doi.org/10.1073/pnas.73.5.1523>
44. Cavuoto P, Fenech MF (2012) A review of methionine dependency and the role of methionine restriction in cancer growth control and life-span extension. *Cancer Treat Rev* 38:726–736. <https://doi.org/10.1016/j.ctrv.2012.01.004>
45. Ascierto PA, Scala S, Castello G, Daponte A, Simeone E, Ottaiano A, Beneduce G, De Rosa V, Izzo F, Melucci MT, Ensor CM, Prestayko AW, Holtsberg FW, Bomalaski JS, Clark MA, Savaraj N, Feun LG, Logan TF (2005) Pegylated Arginine Deiminase Treatment of Patients With Metastatic Melanoma: Results From Phase I and II Studies. *Journal of Clinical Oncology* 23:7660–7668. <https://doi.org/10.1200/JCO.2005.02.0933>

46. Glazer ES, Piccirillo M, Albino V, Di Giacomo R, Palaia R, Mastro AA, Beneduce G, Castello G, De Rosa V, Petrillo A, Ascierto PA, Curley SA, Izzo F (2010) Phase II Study of Pegylated Arginine Deiminase for Nonresectable and Metastatic Hepatocellular Carcinoma. *Journal of Clinical Oncology* 28:2220–2226. <https://doi.org/10.1200/JCO.2009.26.7765>
47. Miraki-Moud F, Ghazaly E, Ariza-McNaughton L, Hodby KA, Clear A, Anjos-Afonso F, Liapis K, Grantham M, Sohrabi F, Cavenagh J, Bomalaski JS, Gribben JG, Szlosarek PW, Bonnet D, Taussig DC (2015) Arginine deprivation using pegylated arginine deiminase has activity against primary acute myeloid leukemia cells in vivo. *Blood* 125:4060–4068. <https://doi.org/10.1182/blood-2014-10-608133>
48. Kawaguchi K, Han Q, Li S, Tan Y, Igarashi K, Miyake K, Kiyuna T, Miyake M, Chemielwski B, Nelson SD, Russell TA, Dry SM, Li Y, Singh AS, Eckardt MA, Unno M, Eilber FC, Hoffman RM (2018) Intra-tumor L-methionine level highly correlates with tumor size in both pancreatic cancer and melanoma patient-derived orthotopic xenograft (PDOX) nude-mouse models. *Oncotarget* 9:11119–11125. <https://doi.org/10.18632/oncotarget.24264>
49. Han Q, Tan Y, Hoffman RM (2020) Oral dosing of Recombinant Methioninase Is Associated With a 70 % Drop in PSA in a Patient With Bone-metastatic Prostate Cancer and 50 % Reduction in Circulating Methionine in a High-stage Ovarian Cancer Patient. *Anticancer Res* 40:2813–2819. <https://doi.org/10.21873/anticancer.14254>
50. Arany Z, Neinst M (2018) Branched Chain Amino Acids in Metabolic Disease. *Curr Diab Rep* 18:76. <https://doi.org/10.1007/s11892-018-1048-7>
51. Cole JT (2015) Metabolism of BCAAs. In: *Branched Chain Amino Acids in Clinical Nutrition*. Springer New York, New York, NY, pp 13–24
52. Peng H, Wang Y, Luo W (2020) Multifaceted role of branched-chain amino acid metabolism in cancer. *Oncogene* 39:6747–6756. <https://doi.org/10.1038/s41388-020-01480-z>
53. Shennan DB, Thomson J, Gow IF, Travers MT, Barber MC (2004) l-Leucine transport in human breast cancer cells (MCF-7 and MDA-MB-231): kinetics, regulation by estrogen and molecular identity of the transporter. *Biochimica et Biophysica Acta (BBA) - Biomembranes* 1664:206–216. <https://doi.org/10.1016/j.bbamem.2004.05.008>
54. Yoneshiro T, Wang Q, Tajima K, Matsushita M, Maki H, Igarashi K, Dai Z, White PJ, McGarrah RW, Ilkayeva OR, Deleze Y, Oguri Y, Kuroda M, Ikeda K, Li H, Ueno A, Ohishi M, Ishikawa T, Kim K, Chen Y, Sponton CH, Pradhan RN, Majd H, Greiner VJ, Yoneshiro M, Brown Z, Chondronikola M, Takahashi H, Goto T, Kawada T, Sidossis L, Szoka FC, McManus MT, Saito M, Soga T, Kajimura S (2019) BCAA catabolism in brown fat controls energy homeostasis through SLC25A44. *Nature* 572:614–619. <https://doi.org/10.1038/s41586-019-1503-x>
55. Mayers JR, Torrence ME, Danai L V., Papagiannakopoulos T, Davidson SM, Bauer MR, Lau AN, Ji BW, Dixit PD, Hosios AM, Muir A, Chin CR, Freinkman E, Jacks T, Wolpin BM, Vitkup D, Vander Heiden MG (2016) Tissue of origin dictates branched-chain amino acid metabolism in mutant Kras-driven cancers. *Science* (1979) 353:1161–1165. <https://doi.org/10.1126/science.aaf5171>
56. Dimou A, Tsimihodimos V, Bairaktari E (2022) The Critical Role of the Branched Chain Amino Acids (BCAAs) Catabolism-Regulating Enzymes, Branched-Chain Aminotransferase (BCAT) and Branched-Chain  $\alpha$ -Keto Acid Dehydrogenase (BCKD), in Human Pathophysiology. *Int J Mol Sci* 23:4022. <https://doi.org/10.3390/ijms23074022>
57. Shafei MA, Flemban A, Daly C, Kendrick P, White P, Dean S, Qualtrough D, Conway ME (2021) Differential expression of the BCAT isoforms between breast cancer subtypes. *Breast Cancer* 28:592–607. <https://doi.org/10.1007/s12282-020-01197-7>

58. Kingsbury JM, Sen ND, Cardenas ME (2015) Branched-Chain Aminotransferases Control TORC1 Signaling in *Saccharomyces cerevisiae*. *PLoS Genet* 11:e1005714. <https://doi.org/10.1371/journal.pgen.1005714>
59. Zhang B, Chen Y, Shi X, Zhou M, Bao L, Hatanpaa KJ, Patel T, DeBerardinis RJ, Wang Y, Luo W (2021) Regulation of branched-chain amino acid metabolism by hypoxia-inducible factor in glioblastoma. *Cellular and Molecular Life Sciences* 78:195–206. <https://doi.org/10.1007/s00018-020-03483-1>
60. Hattori A, Tsunoda M, Konuma T, Kobayashi M, Nagy T, Glushka J, Tayyari F, McSkimming D, Kannan N, Tojo A, Edison AS, Ito T (2017) Cancer progression by reprogrammed BCAA metabolism in myeloid leukaemia. *Nature* 545:500–504. <https://doi.org/10.1038/nature22314>
61. Qu Y-Y, Zhao R, Zhang H-L, Zhou Q, Xu F-J, Zhang X, Xu W-H, Shao N, Zhou S-X, Dai B, Zhu Y, Shi G-H, Shen Y-J, Zhu Y-P, Han C-T, Chang K, Lin Y, Zang W-D, Xu W, Ye D-W, Zhao S-M, Zhao J-Y (2020) Inactivation of the AMPK–GATA3–ECHS1 Pathway Induces Fatty Acid Synthesis That Promotes Clear Cell Renal Cell Carcinoma Growth. *Cancer Res* 80:319–333. <https://doi.org/10.1158/0008-5472.CAN-19-1023>
62. Gu Z, Liu Y, Cai F, Patrick M, Zmajkovic J, Cao H, Zhang Y, Tasdogan A, Chen M, Qi L, Liu X, Li K, Lyu J, Dickerson KE, Chen W, Ni M, Merritt ME, Morrison SJ, Skoda RC, DeBerardinis RJ, Xu J (2019) Loss of EZH2 Reprograms BCAA Metabolism to Drive Leukemic Transformation. *Cancer Discov* 9:1228–1247. <https://doi.org/10.1158/2159-8290.CD-19-0152>
63. Raffel S, Falcone M, Kneisel N, Hansson J, Wang W, Lutz C, Bullinger L, Poschet G, Nonnenmacher Y, Barnert A, Bahr C, Zeisberger P, Przybylla A, Sohn M, Tönjes M, Erez A, Adler L, Jensen P, Scholl C, Fröhling S, Cocciardi S, Wuchter P, Thiede C, Flörcken A, Westermann J, Ehninger G, Lichter P, Hiller K, Hell R, Herrmann C, Ho AD, Krijgsveld J, Radlwimmer B, Trumpp A (2017) BCAT1 restricts  $\alpha$ KG levels in AML stem cells leading to IDHmut-like DNA hypermethylation. *Nature* 551:384–388. <https://doi.org/10.1038/nature24294>
64. Wang Z-Q, Faddaoui A, Bachvarova M, Plante M, Gregoire J, Renaud M-C, Sebastianelli A, Guillemette C, Gobeil S, Macdonald E, Vanderhyden B, Bachvarov D (2015) BCAT1 expression associates with ovarian cancer progression: possible implications in altered disease metabolism. *Oncotarget* 6:31522–31543. <https://doi.org/10.18632/oncotarget.5159>
65. Wang P, Wu S, Zeng X, Zhang Y, Zhou Y, Su L, Lin W (2018) BCAT1 promotes proliferation of endometrial cancer cells through reprogrammed BCAA metabolism. *Int J Clin Exp Pathol* 11:5536–5546
66. Li J-T, Yin M, Wang D, Wang J, Lei M-Z, Zhang Y, Liu Y, Zhang L, Zou S-W, Hu L-P, Zhang Z-G, Wang Y-P, Wen W-Y, Lu H-J, Chen Z-J, Su D, Lei Q-Y (2020) BCAT2-mediated BCAA catabolism is critical for development of pancreatic ductal adenocarcinoma. *Nat Cell Biol* 22:167–174. <https://doi.org/10.1038/s41556-019-0455-6>
67. Lee JH, Cho Y, Kim JH, Kim J, Nam HY, Kim SW, Son J (2019) Branched-chain amino acids sustain pancreatic cancer growth by regulating lipid metabolism. *Exp Mol Med* 51:1–11. <https://doi.org/10.1038/s12276-019-0350-z>
68. Martin SB, Reiche WS, Fifelski NA, Schultz AJ, Stanford SJ, Martin AA, Nack DL, Radlwimmer B, Boyer MP, Ananieva EA (2020) Leucine and branched-chain amino acid metabolism contribute to the growth of bone sarcomas by regulating AMPK and mTORC1 signaling. *Biochemical Journal* 477:1579–1599. <https://doi.org/10.1042/BCJ20190754>
69. Zhang L, Han J (2017) Branched-chain amino acid transaminase 1 (BCAT1) promotes the growth of breast cancer cells through improving mTOR-mediated mitochondrial

- biogenesis and function. *Biochem Biophys Res Commun* 486:224–231. <https://doi.org/10.1016/j.bbrc.2017.02.101>
70. Yang D, Liu H, Cai Y, Lu K, Zhong X, Xing S, Song W, Zhang Y, Ye L, Zhu X, Wang T, Zhang P, Li S-T, Feng J, Jia W, Zhang H, Gao P (2022) Branched-chain amino acid catabolism breaks glutamine addiction to sustain hepatocellular carcinoma progression. *Cell Rep* 41:111691. <https://doi.org/10.1016/j.celrep.2022.111691>
  71. Lynch CJ, Halle B, Fujii H, Vary TC, Wallin R, Damuni Z, Hutson SM (2003) Potential role of leucine metabolism in the leucine-signaling pathway involving mTOR. *American Journal of Physiology-Endocrinology and Metabolism* 285:E854–E863. <https://doi.org/10.1152/ajpendo.00153.2003>
  72. Oliver DJ, Nikolau BJ, Wurtele ES (2009) Acetyl-CoA—Life at the metabolic nexus. *Plant Science* 176:597–601. <https://doi.org/10.1016/j.plantsci.2009.02.005>
  73. Chen M, Knifley T, Subramanian T, Spielmann HP, O'Connor KL (2014) Use of Synthetic Isoprenoids to Target Protein Prenylation and Rho GTPases in Breast Cancer Invasion. *PLoS One* 9:e89892. <https://doi.org/10.1371/journal.pone.0089892>
  74. Holstein SA, Hohl RJ (2004) Isoprenoids: Remarkable diversity of form and function. *Lipids* 39:293–309. <https://doi.org/10.1007/s11745-004-1233-3>
  75. Rikitake Y, Liao JK (2005) Rho GTPases, Statins, and Nitric Oxide. *Circ Res* 97:1232–1235. <https://doi.org/10.1161/01.RES.0000196564.18314.23>
  76. Göbel A, Rauner M, Hofbauer LC, Rachner TD (2020) Cholesterol and beyond - The role of the mevalonate pathway in cancer biology. *Biochimica et Biophysica Acta (BBA) - Reviews on Cancer* 1873:188351. <https://doi.org/10.1016/j.bbcan.2020.188351>
  77. Kuzu OF, Noory MA, Robertson GP (2016) The Role of Cholesterol in Cancer. *Cancer Res* 76:2063–2070. <https://doi.org/10.1158/0008-5472.CAN-15-2613>
  78. Wang X, Huang Z, Wu Q, Prager BC, Mack SC, Yang K, Kim LJY, Gimple RC, Shi Y, Lai S, Xie Q, Miller TE, Hubert CG, Song A, Dong Z, Zhou W, Fang X, Zhu Z, Mahadev V, Bao S, Rich JN (2017) MYC-Regulated Mevalonate Metabolism Maintains Brain Tumor-Initiating Cells. *Cancer Res* 77:4947–4960. <https://doi.org/10.1158/0008-5472.CAN-17-0114>
  79. Abate M, Laezza C, Pisanti S, Torelli G, Seneca V, Catapano G, Montella F, Ranieri R, Notarnicola M, Gaggero P, Bifulco M, Ciaglia E (2017) Deregulated expression and activity of Farnesyl Diphosphate Synthase (FDPS) in Glioblastoma. *Sci Rep* 7:14123. <https://doi.org/10.1038/s41598-017-14495-6>
  80. Brown DN, Caffa I, Cirmena G, Piras D, Garuti A, Gallo M, Alberti S, Nencioni A, Ballestrero A, Zoppoli G (2016) Squalene epoxidase is a bona fide oncogene by amplification with clinical relevance in breast cancer. *Sci Rep* 6:19435. <https://doi.org/10.1038/srep19435>
  81. Yang Y-F, Jan Y-H, Liu Y-P, Yang C-J, Su C-Y, Chang Y-C, Lai T-C, Chiou J, Tsai H-Y, Lu J, Shen C-N, Shew J-Y, Lu P-J, Lin Y-F, Huang M-S, Hsiao M (2014) Squalene Synthase Induces Tumor Necrosis Factor Receptor 1 Enrichment in Lipid Rafts to Promote Lung Cancer Metastasis. *Am J Respir Crit Care Med* 190:675–687. <https://doi.org/10.1164/rccm.201404-0714OC>
  82. Wang X, Xu W, Zhan P, Xu T, Jin J, Miu Y, Zhou Z, Zhu Q, Wan B, Xi G, Ye L, Liu Y, Gao J, Li H, Lv T, Song Y (2018) Overexpression of geranylgeranyl diphosphate synthase contributes to tumour metastasis and correlates with poor prognosis of lung adenocarcinoma. *J Cell Mol Med* 22:2177–2189. <https://doi.org/10.1111/jcmm.13493>
  83. Caruso MG, Notarnicola M (2005) Biochemical changes of mevalonate pathway in human colorectal cancer. *Anticancer Res* 25:3393–7
  84. Todenhöfer T, Hennenlotter J, Kühs U, Gerber V, Gakis G, Vogel U, Aufderklamm S, Merseburger A, Knapp J, Stenzl A, Schwentner C (2013) Altered expression of farnesyl pyrophosphate synthase in prostate cancer: evidence for a role of the mevalonate

- pathway in disease progression? *World J Urol* 31:345–350. <https://doi.org/10.1007/s00345-012-0844-y>
85. de Wolf E, Abdullah MI, Jones SM, Menezes K, Moss DM, Drijfhout FP, Hart SR, Hoskins C, Stronach EA, Richardson A (2017) Dietary geranylgeraniol can limit the activity of pitavastatin as a potential treatment for drug-resistant ovarian cancer. *Sci Rep* 7:5410. <https://doi.org/10.1038/s41598-017-05595-4>
  86. BA Djamgoz M (2014) Biophysics of Cancer: Cellular Excitability (“CELEX”) Hypothesis of Metastasis. *J Clin Exp Oncol* s1:. <https://doi.org/10.4172/2324-9110.S1-005>
  87. Bayat A (2002) Science, medicine, and the future: Bioinformatics. *BMJ* 324:1018–1022. <https://doi.org/10.1136/bmj.324.7344.1018>
  88. Wegner A (2020) Computational analysis of metabolic data. In: *Metabolomics for Biomedical Research*. Elsevier, pp 83–103
  89. Mateo J, Seed G, Bertan C, Rescigno P, Dolling D, Figueiredo I, Miranda S, Nava Rodrigues D, Gurel B, Clarke M, Atkin M, Chandler R, Messina C, Sumanasuriya S, Bianchini D, Barrero M, Petermolo A, Zafeiriou Z, Fontes M, Perez-Lopez R, Tunariu N, Fulton B, Jones R, McGovern U, Ralph C, Varughese M, Parikh O, Jain S, Elliott T, Sandhu S, Porta N, Hall E, Yuan W, Carreira S, de Bono JS (2020) Genomics of lethal prostate cancer at diagnosis and castration resistance. *Journal of Clinical Investigation* 130:1743–1751. <https://doi.org/10.1172/JCI132031>
  90. Agren R, Bordel S, Mardinoglu A, Pornputtapong N, Nookaew I, Nielsen J (2012) Reconstruction of Genome-Scale Active Metabolic Networks for 69 Human Cell Types and 16 Cancer Types Using INIT. *PLoS Comput Biol* 8:e1002518. <https://doi.org/10.1371/journal.pcbi.1002518>
  91. Wang L, Dash S, Ng CY, Maranas CD (2017) A review of computational tools for design and reconstruction of metabolic pathways. *Synth Syst Biotechnol* 2:243–252. <https://doi.org/10.1016/j.synbio.2017.11.002>
  92. Langmead B, Salzberg SL (2012) Fast gapped-read alignment with Bowtie 2. *Nat Methods* 9:357–359. <https://doi.org/10.1038/nmeth.1923>
  93. Ebrahim A, Lerman JA, Palsson BO, Hyduke DR (2013) COBRApy: CONstraints-Based Reconstruction and Analysis for Python. *BMC Syst Biol* 7:74. <https://doi.org/10.1186/1752-0509-7-74>
  94. Putri GH, Anders S, Pyl PT, Pimanda JE, Zanini F (2022) Analysing high-throughput sequencing data in Python with HTSeq 2.0. *Bioinformatics* 38:2943–2945. <https://doi.org/10.1093/bioinformatics/btac166>
  95. Pang Z, Chong J, Zhou G, de Lima Morais DA, Chang L, Barrette M, Gauthier C, Jacques P-É, Li S, Xia J (2021) MetaboAnalyst 5.0: narrowing the gap between raw spectra and functional insights. *Nucleic Acids Res* 49:W388–W396. <https://doi.org/10.1093/nar/gkab382>
  96. Liao Y, Wang J, Jaehnig EJ, Shi Z, Zhang B (2019) WebGestalt 2019: gene set analysis toolkit with revamped UIs and APIs. *Nucleic Acids Res* 47:W199–W205. <https://doi.org/10.1093/nar/gkz401>
  97. Sellick CA, Hansen R, Stephens GM, Goodacre R, Dickson AJ (2011) Metabolite extraction from suspension-cultured mammalian cells for global metabolite profiling. *Nat Protoc* 6:1241–1249. <https://doi.org/10.1038/nprot.2011.366>
  98. Virgiliou C, Gika HG, Theodoridis GA (2018) HILIC-MS/MS Multi-Targeted Method for Metabolomics Applications. pp 65–81
  99. Antoniewicz MR, Kelleher JK, Stephanopoulos G (2007) Elementary metabolite units (EMU): A novel framework for modeling isotopic distributions. *Metab Eng* 9:68–86. <https://doi.org/10.1016/j.ymben.2006.09.001>

100. Bordel S (2018) Constraint based modeling of metabolism allows finding metabolic cancer hallmarks and identifying personalized therapeutic windows. *Oncotarget* 9:19716–19729. <https://doi.org/10.18632/oncotarget.24805>
101. Ewald JD, Zhou G, Lu Y, Kolic J, Ellis C, Johnson JD, Macdonald PE, Xia J (2024) Web-based multi-omics integration using the Analyst software suite. *Nat Protoc.* <https://doi.org/10.1038/s41596-023-00950-4>
102. Emwas A-H, Szczepski K, Al-Younis I, Lachowicz JI, Jaremko M (2022) Fluxomics - New Metabolomics Approaches to Monitor Metabolic Pathways. *Front Pharmacol* 13:. <https://doi.org/10.3389/fphar.2022.805782>
103. Tian B, Chen M, Liu L, Rui B, Deng Z, Zhang Z, Shen T (2022) <sup>13</sup>C metabolic flux analysis: Classification and characterization from the perspective of mathematical modeling and application in physiological research of neural cell. *Front Mol Neurosci* 15:. <https://doi.org/10.3389/fnmol.2022.883466>
104. Dey P, Baddour J, Muller F, Wu CC, Wang H, Liao W-T, Lan Z, Chen A, Gutschner T, Kang Y, Fleming J, Satani N, Zhao D, Achreja A, Yang L, Lee J, Chang E, Genovese G, Viale A, Ying H, Draetta G, Maitra A, Wang YA, Nagrath D, DePinho RA (2017) Genomic deletion of malic enzyme 2 confers collateral lethality in pancreatic cancer. *Nature* 542:119–123. <https://doi.org/10.1038/nature21052>
105. Altman BJ, Stine ZE, Dang C V. (2016) From Krebs to clinic: glutamine metabolism to cancer therapy. *Nat Rev Cancer* 16:619–634. <https://doi.org/10.1038/nrc.2016.71>
106. Jain M, Nilsson R, Sharma S, Madhusudhan N, Kitami T, Souza AL, Kafri R, Kirschner MW, Clish CB, Mootha VK (2012) Metabolite Profiling Identifies a Key Role for Glycine in Rapid Cancer Cell Proliferation. *Science* (1979) 336:1040–1044. <https://doi.org/10.1126/science.1218595>
107. Krycer JR, Brown AJ (2013) Cholesterol accumulation in prostate cancer: A classic observation from a modern perspective. *Biochimica et Biophysica Acta (BBA) - Reviews on Cancer* 1835:219–229. <https://doi.org/10.1016/j.bbcan.2013.01.002>
108. Smith B, Land H (2012) Anticancer Activity of the Cholesterol Exporter ABCA1 Gene. *Cell Rep* 2:580–590. <https://doi.org/10.1016/j.celrep.2012.08.011>
109. Raškevičius V, Mikalayeva V, Antanavičiūtė I, Ceslevičienė I, Skeberdis VA, Kairys V, Bordel S (2018) Genome scale metabolic models as tools for drug design and personalized medicine. *PLoS One* 13:e0190636. <https://doi.org/10.1371/journal.pone.0190636>
110. Centonze G, Natalini D, Piccolantonio A, Salemme V, Morellato A, Arina P, Riganti C, Defilippi P (2022) Cholesterol and Its Derivatives: Multifaceted Players in Breast Cancer Progression. *Front Oncol* 12:. <https://doi.org/10.3389/fonc.2022.906670>
111. Xiao F, Wang C, Yin H, Yu J, Chen S, Fang J, Guo F (2016) Leucine deprivation inhibits proliferation and induces apoptosis of human breast cancer cells via fatty acid synthase. *Oncotarget* 7:63679–63689. <https://doi.org/10.18632/oncotarget.11626>
112. Kim MS, Wu KY, Auyeung V, Chen Q, Gruppuso PA, Phornphutkul C (2009) Leucine restriction inhibits chondrocyte proliferation and differentiation through mechanisms both dependent and independent of mTOR signaling. *American Journal of Physiology-Endocrinology and Metabolism* 296:E1374–E1382. <https://doi.org/10.1152/ajpendo.91018.2008>
113. Danilo C, Frank PG (2012) Cholesterol and breast cancer development. *Curr Opin Pharmacol* 12:677–682. <https://doi.org/10.1016/j.coph.2012.07.009>
114. Bjarnadottir O, Romero Q, Bendahl P-O, Jirstrom K, Rydén L, Loman N, Uhlén M, Johannesson H, Rose C, Grabau D, Borgquist S (2013) Targeting HMG-CoA reductase with statins in a window-of-opportunity breast cancer trial. *Breast Cancer Res Treat* 138:499–508. <https://doi.org/10.1007/s10549-013-2473-6>

115. O'Grady S, Crown J, Duffy MJ (2022) Statins inhibit proliferation and induce apoptosis in triple-negative breast cancer cells. *Medical Oncology* 39:142. <https://doi.org/10.1007/s12032-022-01733-9>
116. Feldt M, Bjarnadottir O, Kimbung S, Jirström K, Bendahl P-O, Veerla S, Grabau D, Hedenfalk I, Borgquist S (2015) Statin-induced anti-proliferative effects via cyclin D1 and p27 in a window-of-opportunity breast cancer trial. *J Transl Med* 13:133. <https://doi.org/10.1186/s12967-015-0486-0>
117. Ahern TP, Pedersen L, Tarp M, Cronin-Fenton DP, Garne JP, Silliman RA, Sorensen HT, Lash TL (2011) Statin Prescriptions and Breast Cancer Recurrence Risk: A Danish Nationwide Prospective Cohort Study. *JNCI Journal of the National Cancer Institute* 103:1461–1468. <https://doi.org/10.1093/jnci/djr291>
118. Boudreau DM, Yu O, Chubak J, Wirtz HS, Bowles EJA, Fujii M, Buist DSM (2014) Comparative safety of cardiovascular medication use and breast cancer outcomes among women with early stage breast cancer. *Breast Cancer Res Treat* 144:405–416. <https://doi.org/10.1007/s10549-014-2870-5>
119. Nickels S, Vrieling A, Seibold P, Heinz J, Obi N, Flesch-Janys D, Chang-Claude J (2013) Mortality and Recurrence Risk in Relation to the Use of Lipid-Lowering Drugs in a Prospective Breast Cancer Patient Cohort. *PLoS One* 8:e75088. <https://doi.org/10.1371/journal.pone.0075088>
120. Chae YK, Valsecchi ME, Kim J, Bianchi AL, Khemasuwan D, Desai A, Tester W (2011) Reduced Risk of Breast Cancer Recurrence in Patients Using ACE Inhibitors, ARBs, and/or Statins. *Cancer Invest* 29:585–593. <https://doi.org/10.3109/07357907.2011.616252>
121. Kwan ML, Habel LA, Flick ED, Quesenberry CP, Caan B (2008) Post-diagnosis statin use and breast cancer recurrence in a prospective cohort study of early stage breast cancer survivors. *Breast Cancer Res Treat* 109:573–579. <https://doi.org/10.1007/s10549-007-9683-8>
122. Nielsen SF, Nordestgaard BG, Bojesen SE (2012) Statin Use and Reduced Cancer-Related Mortality. *New England Journal of Medicine* 367:1792–1802. <https://doi.org/10.1056/NEJMoa1201735>
123. Pedersen TR, Wilhelmsen L, Færgeman O, Strandberg TE, Thorgeirsson G, Troedsson L, Kristianson J, Berg K, Cook TJ, Haghfelt T, Kjerkshus J, Miettinen T, Olsson AG, Pyörälä K, Wedel H (2000) Follow-up study of patients randomized in the scandinavian simvastatin survival study (4S) of cholesterol lowering. *Am J Cardiol* 86:257–262. [https://doi.org/10.1016/S0002-9149\(00\)00910-3](https://doi.org/10.1016/S0002-9149(00)00910-3)
124. Marelli C, Gunnarsson C, Ross S, Haas S, Stroup DF, Cload P, Clopton P, DeMaria AN (2011) Statins and Risk of Cancer. *J Am Coll Cardiol* 58:530–537. <https://doi.org/10.1016/j.jacc.2011.04.015>
125. Setoguchi S, Glynn RJ, Avorn J, Mogun H, Schneeweiss S (2007) Statins and the Risk of Lung, Breast, and Colorectal Cancer in the Elderly. *Circulation* 115:27–33. <https://doi.org/10.1161/CIRCULATIONAHA.106.650176>
126. Haukka J, Sankila R, Klaukka T, Lonnqvist J, Niskanen L, Tanskanen A, Wahlbeck K, Tiihonen J (2010) Incidence of cancer and statin usage—Record linkage study. *Int J Cancer* 126:279–284. <https://doi.org/10.1002/ijc.24536>
127. Ravnskov U, Rosch PJ, McCully KS (2015) Statins Do Not Protect Against Cancer: Quite the Opposite. *Journal of Clinical Oncology* 33:810–811. <https://doi.org/10.1200/JCO.2014.58.9564>
128. Antalis CJ, Uchida A, Buhman KK, Siddiqui RA (2011) Migration of MDA-MB-231 breast cancer cells depends on the availability of exogenous lipids and cholesterol esterification. *Clin Exp Metastasis* 28:733–741. <https://doi.org/10.1007/s10585-011-9405-9>



129. Guerra FS, Sampaio L da S, König S, Bonamino M, Rossi MID, Costa ML, Fernandes P, Mermelstein C (2016) Membrane cholesterol depletion reduces breast tumor cell migration by a mechanism that involves non-canonical Wnt signaling and IL-10 secretion. *Transl Med Commun* 1:3. <https://doi.org/10.1186/s41231-016-0002-4>
130. Kim HY, Bae SJ, Choi J-W, Han S, Bae S-H, Cheong J-H, Jang H (2022) Cholesterol Synthesis Is Important for Breast Cancer Cell Tumor Sphere Formation and Invasion. *Biomedicines* 10:1908. <https://doi.org/10.3390/biomedicines10081908>
131. Holroyd AK, Michie AM (2018) The role of mTOR-mediated signaling in the regulation of cellular migration. *Immunol Lett* 196:74–79. <https://doi.org/10.1016/j.imlet.2018.01.015>
132. Zhenyukh O, Civantos E, Ruiz-Ortega M, Sánchez MS, Vázquez C, Peiró C, Egado J, Mas S (2017) High concentration of branched-chain amino acids promotes oxidative stress, inflammation and migration of human peripheral blood mononuclear cells via mTORC1 activation. *Free Radic Biol Med* 104:165–177. <https://doi.org/10.1016/j.freeradbiomed.2017.01.009>
133. Chi R, Yao C, Chen S, Liu Y, He Y, Zhang J, Ellies LG, Wu X, Zhao Q, Zhou C, Wang Y, Sun H (2022) Elevated BCAA Suppresses the Development and Metastasis of Breast Cancer. *Front Oncol* 12:. <https://doi.org/10.3389/fonc.2022.887257>
134. Jové M, Collado R, Quiles JL, Ramírez-Tortosa M-C, Sol J, Ruiz-Sanjuan M, Fernandez M, de la Torre Cabrera C, Ramírez-Tortosa C, Granados-Principal S, Sánchez-Rovira P, Pamplona R (2017) A plasma metabolomic signature discloses human breast cancer. *Oncotarget* 8:19522–19533. <https://doi.org/10.18632/oncotarget.14521>
135. Baranovicova E, Racay P, Zubor P, Smolar M, Kudelova E, Halasova E, Dvorska D, Dankova Z (2022) Circulating metabolites in the early stage of breast cancer were not related to cancer stage or subtypes but associated with ki67 level. Promising statistical discrimination from controls. *Mol Cell Probes* 66:101862. <https://doi.org/10.1016/j.mcp.2022.101862>
136. Moore SC, Playdon MC, Sampson JN, Hoover RN, Trabert B, Matthews CE, Ziegler RG (2018) A Metabolomics Analysis of Body Mass Index and Postmenopausal Breast Cancer Risk. *NCI: Journal of the National Cancer Institute*. <https://doi.org/10.1093/jnci/djx244>
137. Nagata C, Wada K, Tsuji M, Hayashi M, Takeda N, Yasuda K (2014) Plasma amino acid profiles are associated with biomarkers of breast cancer risk in premenopausal Japanese women. *Cancer Causes & Control* 25:143–149. <https://doi.org/10.1007/s10552-013-0316-8>
138. Hankinson SE, Eliassen AH (2007) Endogenous estrogen, testosterone and progesterone levels in relation to breast cancer risk. *J Steroid Biochem Mol Biol* 106:24–30. <https://doi.org/10.1016/j.jsbmb.2007.05.012>
139. Kaaks R, Rinaldi S, Key TJ, Berrino F, Peeters PHM, Biessy C, Dossus L, Lukanova A, Bingham S, Khaw K-T, Allen NE, Bueno-de-Mesquita HB, van Gils CH, Grobbee D, Boeing H, Lahmann PH, Nagel G, Chang-Claude J, Clavel-Chapelon F, Fournier A, Thiébaud A, González CA, Quirós JR, Tormo M-J, Ardanaz E, Amiano P, Krogh V, Palli D, Panico S, Tumino R, Vineis P, Trichopoulou A, Kalapothaki V, Trichopoulos D, Ferrari P, Norat T, Saracci R, Riboli E (2005) Postmenopausal serum androgens, oestrogens and breast cancer risk: the European prospective investigation into cancer and nutrition. *Endocr Relat Cancer* 12:1071–1082. <https://doi.org/10.1677/erc.1.01038>
140. Batch BC, Shah SH, Newgard CB, Turer CB, Haynes C, Bain JR, Muehlbauer M, Patel MJ, Stevens RD, Appel LJ, Newby LK, Svetkey LP (2013) Branched chain amino acids are novel biomarkers for discrimination of metabolic wellness. *Metabolism* 62:961–969. <https://doi.org/10.1016/j.metabol.2013.01.007>

141. Hamaya R, Mora S, Lawler PR, Cook NR, Ridker PM, Buring JE, Lee I-M, Manson JE, Tobias DK (2021) Association of Plasma Branched-Chain Amino Acid With Biomarkers of Inflammation and Lipid Metabolism in Women. *Circ Genom Precis Med* 14:. <https://doi.org/10.1161/CIRCGEN.121.003330>
142. Newgard CB, An J, Bain JR, Muehlbauer MJ, Stevens RD, Lien LF, Haqq AM, Shah SH, Arlotto M, Slentz CA, Rochon J, Gallup D, Ilkayeva O, Wenner BR, Yancy WS, Eisensohn H, Musante G, Surwit RS, Millington DS, Butler MD, Svetkey LP (2009) A Branched-Chain Amino Acid-Related Metabolic Signature that Differentiates Obese and Lean Humans and Contributes to Insulin Resistance. *Cell Metab* 9:311–326. <https://doi.org/10.1016/j.cmet.2009.02.002>
143. Wang Z, Yip LY, Lee JHJ, Wu Z, Chew HY, Chong PKW, Teo CC, Ang HY-K, Peh KLE, Yuan J, Ma S, Choo LSK, Basri N, Jiang X, Yu Q, Hillmer AM, Lim WT, Lim TKH, Takano A, Tan EH, Tan DSW, Ho YS, Lim B, Tam WL (2019) Methionine is a metabolic dependency of tumor-initiating cells. *Nat Med* 25:825–837. <https://doi.org/10.1038/s41591-019-0423-5>
144. Kaiser P (2020) Methionine Dependence of Cancer. *Biomolecules* 10:568. <https://doi.org/10.3390/biom10040568>
145. Cavuoto P, Fenech MF (2012) A review of methionine dependency and the role of methionine restriction in cancer growth control and life-span extension. *Cancer Treat Rev* 38:726–736. <https://doi.org/10.1016/j.ctrv.2012.01.004>
146. Lien EC, Ghisolfi L, Geck RC, Asara JM, Toker A (2017) Oncogenic PI3K promotes methionine dependency in breast cancer cells through the cystine-glutamate antiporter xCT. *Sci Signal* 10:. <https://doi.org/10.1126/scisignal.aao6604>
147. Newman AC, Maddocks ODK (2017) One-carbon metabolism in cancer. *Br J Cancer* 116:1499–1504. <https://doi.org/10.1038/bjc.2017.118>
148. Leal JF, Ferrer I, Blanco-Aparicio C, Hernández-Losa J, Ramón y Cajal S, Carnero A, LLeonart ME (2008) S-adenosylhomocysteine hydrolase downregulation contributes to tumorigenesis. *Carcinogenesis* 29:2089–2095. <https://doi.org/10.1093/carcin/bgn198>
149. Chayka O, D'Acunto CW, Middleton O, Arab M, Sala A (2015) Identification and Pharmacological Inactivation of the MYCN Gene Network as a Therapeutic Strategy for Neuroblastic Tumor Cells. *Journal of Biological Chemistry* 290:2198–2212. <https://doi.org/10.1074/jbc.M114.624056>
150. Westermann F, Muth D, Benner A, Bauer T, Henrich K-O, Oberthuer A, Brors B, Beissbarth T, Vandesompele J, Pattyn F, Hero B, König R, Fischer M, Schwab M (2008) Distinct transcriptional MYCN/c-MYC activities are associated with spontaneous regression or malignant progression in neuroblastomas. *Genome Biol* 9:R150. <https://doi.org/10.1186/gb-2008-9-10-r150>
151. Zhao G, He F, Wu C, Li P, Li N, Deng J, Zhu G, Ren W, Peng Y (2018) Betaine in Inflammation: Mechanistic Aspects and Applications. *Front Immunol* 9:. <https://doi.org/10.3389/fimmu.2018.01070>
152. Zhao G, He F, Wu C, Li P, Li N, Deng J, Zhu G, Ren W, Peng Y (2018) Betaine in Inflammation: Mechanistic Aspects and Applications. *Front Immunol* 9:. <https://doi.org/10.3389/fimmu.2018.01070>
153. Pascale RM, Simile MM, Calvisi DF, Feo CF, Feo F (2022) S-Adenosylmethionine: From the Discovery of Its Inhibition of Tumorigenesis to Its Use as a Therapeutic Agent. *Cells* 11:409. <https://doi.org/10.3390/cells11030409>
154. Delle Cave D, Ilisso CP, Mosca L, Pagano M, Martino E, Porcelli M, Cacciapuoti G (2017) The anticancer effects of S-adenosylmethionine on breast cancer cells. *JSM Chem* 5:1049–1056
155. Chik F, Machnes Z, Szyf M (2014) Synergistic anti-breast cancer effect of a combined treatment with the methyl donor S-adenosyl methionine and the DNA methylation

- inhibitor 5-aza-2'-deoxycytidine. *Carcinogenesis* 35:138–144. <https://doi.org/10.1093/carcin/bgt284>
156. Wang Y, Sun Z, Szyf M (2017) S-adenosyl-methionine (SAM) alters the transcriptome and methylome and specifically blocks growth and invasiveness of liver cancer cells. *Oncotarget* 8:111866–111881. <https://doi.org/10.18632/oncotarget.22942>
  157. De Luca A, Sacchetta P, Di Ilio C, Favalaro B (2006) Identification and analysis of the promoter region of the human methionine sulphoxide reductase A gene. *Biochemical Journal* 393:321–329. <https://doi.org/10.1042/BJ20050973>
  158. De Luca A, Sanna F, Sallese M, Ruggiero C, Grossi M, Sacchetta P, Rossi C, De Laurenzi V, Di Ilio C, Favalaro B (2010) Methionine sulfoxide reductase A down-regulation in human breast cancer cells results in a more aggressive phenotype. *Proceedings of the National Academy of Sciences* 107:18628–18633. <https://doi.org/10.1073/pnas.1010171107>
  159. Diaz B, Shani G, Pass I, Anderson D, Quintavalle M, Courtneidge SA (2009) Tks5-Dependent, Nox-Mediated Generation of Reactive Oxygen Species Is Necessary for Invadopodia Formation. *Sci Signal* 2:. <https://doi.org/10.1126/scisignal.2000368>
  160. Wang H, Han H, Mousses S, Vonhoff D (2006) Targeting Loss-of-Function Mutations in Tumor-Suppressor Genes as a Strategy for Development of Cancer Therapeutic Agents. *Semin Oncol* 33:513–520. <https://doi.org/10.1053/j.seminoncol.2006.04.013>
  161. Kim HH, Park CS (2003) Methionine cytotoxicity in the human breast cancer cell line MCF-7. *In Vitro Cell Dev Biol Anim* 39:117–119. <https://doi.org/10.1007/s11626-003-0004-1>
  162. Benavides MA, Oelschlager DK, Zhang H-G, Stockard CR, Vital-Reyes VS, Katkooi VR, Manne U, Wang W, Bland KI, Grizzle WE (2007) Methionine inhibits cellular growth dependent on the p53 status of cells. *The American Journal of Surgery* 193:274–283. <https://doi.org/10.1016/j.amjsurg.2006.07.016>
  163. Benavides MA, Hagen KL, Fang W, Du P, Lin S, Moyer MP, Yang W, Bland KI, Grizzle WE, Bosland MC (2010) Suppression by L-Methionine of Cell Cycle Progression in LNCaP and MCF-7 Cells but not Benign Cells. *Anticancer Res* 30:1881
  164. Benavides MA, Bosland MC, da Silva CP, Gomes Sares CT, Cerqueira de Oliveira AM, Kemp R, dos Reis RB, Martins VR, Sampaio S V., Bland KI, Grizzle WE, dos Santos JS (2014) L-Methionine inhibits growth of human pancreatic cancer cells. *Anticancer Drugs* 25:200–203. <https://doi.org/10.1097/CAD.0000000000000038>
  165. Amelio I, Cutruzzolá F, Antonov A, Agostini M, Melino G (2014) Serine and glycine metabolism in cancer. *Trends Biochem Sci* 39:191–198. <https://doi.org/10.1016/j.tibs.2014.02.004>
  166. Locasale JW, Grassian AR, Melman T, Lyssiotis CA, Mattaini KR, Bass AJ, Heffron G, Metallo CM, Muranen T, Sharfi H, Sasaki AT, Anastasiou D, Mullarky E, Vokes NI, Sasaki M, Beroukhi R, Stephanopoulos G, Ligon AH, Meyerson M, Richardson AL, Chin L, Wagner G, Asara JM, Brugge JS, Cantley LC, Vander Heiden MG (2011) Phosphoglycerate dehydrogenase diverts glycolytic flux and contributes to oncogenesis. *Nat Genet* 43:869–874. <https://doi.org/10.1038/ng.890>
  167. Pollari S, Käkönen S-M, Edgren H, Wolf M, Kohonen P, Sara H, Guise T, Nees M, Kallioniemi O (2011) Enhanced serine production by bone metastatic breast cancer cells stimulates osteoclastogenesis. *Breast Cancer Res Treat* 125:421–430. <https://doi.org/10.1007/s10549-010-0848-5>
  168. Sato K, Masuda T, Hu Q, Tobo T, Kidogami S, Ogawa Y, Saito T, Nambara S, Komatsu H, Hirata H, Sakimura S, Uchi R, Hayashi N, Iguchi T, Eguchi H, Ito S, Nakagawa T, Mimori K (2017) Phosphoserine Phosphatase Is a Novel Prognostic Biomarker on Chromosome 7 in Colorectal Cancer. *Anticancer Res* 37:2365–2371. <https://doi.org/10.21873/anticancer.11574>

169. Kalhan SC, Hanson RW (2012) Resurgence of Serine: An Often Neglected but Indispensable Amino Acid. *Journal of Biological Chemistry* 287:19786–19791. <https://doi.org/10.1074/jbc.R112.357194>
170. Mattaini KR, Sullivan MR, Vander Heiden MG (2016) The importance of serine metabolism in cancer. *Journal of Cell Biology* 214:249–257. <https://doi.org/10.1083/jcb.201604085>
171. Maddocks ODK, Berkers CR, Mason SM, Zheng L, Blyth K, Gottlieb E, Vousden KH (2013) Serine starvation induces stress and p53-dependent metabolic remodelling in cancer cells. *Nature* 493:542–546. <https://doi.org/10.1038/nature11743>
172. Park S-M, Seo E-H, Bae D-H, Kim SS, Kim J, Lin W, Kim K-H, Park JB, Kim YS, Yin J, Kim S-Y (2019) Phosphoserine Phosphatase Promotes Lung Cancer Progression through the Dephosphorylation of IRS-1 and a Noncanonical L-Serine-Independent Pathway. *Mol Cells* 42:604–616. <https://doi.org/10.14348/molcells.2019.0160>
173. Bachelor MA, Lu Y, Owens DM (2011) l-3-Phosphoserine phosphatase (PSPH) regulates cutaneous squamous cell carcinoma proliferation independent of l-serine biosynthesis. *J Dermatol Sci* 63:164–172. <https://doi.org/10.1016/j.jdermsci.2011.06.001>
174. Liou G-Y, Storz P (2010) Reactive oxygen species in cancer. *Free Radic Res* 44:479–496. <https://doi.org/10.3109/10715761003667554>
175. Bansal A, Simon MC (2018) Glutathione metabolism in cancer progression and treatment resistance. *Journal of Cell Biology* 217:2291–2298. <https://doi.org/10.1083/jcb.201804161>
176. Kumar A, Tikoo S, Maity S, Sengupta S, Sengupta S, Kaur A, Kumar Bachhawat A (2012) Mammalian proapoptotic factor ChaC1 and its homologues function as  $\gamma$ -glutamyl cyclotransferases acting specifically on glutathione. *EMBO Rep* 13:1095–1101. <https://doi.org/10.1038/embor.2012.156>
177. Goebel G, Berger R, Strasak AM, Egle D, Müller-Holzner E, Schmidt S, Rainer J, Presul E, Parson W, Lang S, Jones A, Widschwendter M, Fiegl H (2012) Elevated mRNA expression of CHAC1 splicing variants is associated with poor outcome for breast and ovarian cancer patients. *Br J Cancer* 106:189–198. <https://doi.org/10.1038/bjc.2011.510>
178. Mehta V, Meena J, Kasana H, Munshi A, Chander H (2022) Prognostic significance of CHAC1 expression in breast cancer. *Mol Biol Rep* 49:8517–8526. <https://doi.org/10.1007/s11033-022-07673-x>
179. Console L, Scalise M, Mazza T, Pochini L, Galluccio M, Giangregorio N, Tonazzi A, Indiveri C (2020) Carnitine Traffic in Cells. *Link With Cancer*. *Front Cell Dev Biol* 8:. <https://doi.org/10.3389/fcell.2020.583850>
180. Lu Y, Li N, Gao L, Xu Y-J, Huang C, Yu K, Ling Q, Cheng Q, Chen S, Zhu M, Fang J, Chen M, Ong CN (2016) Acetylcarnitine Is a Candidate Diagnostic and Prognostic Biomarker of Hepatocellular Carcinoma. *Cancer Res* 76:2912–2920. <https://doi.org/10.1158/0008-5472.CAN-15-3199>
181. Pisano C, Vesci L, Milazzo FM, Guglielmi MB, Foderà R, Barbarino M, D’Incalci M, Zucchetti M, Petrangolini G, Tortoreto M, Perego P, Zuco V, Orlandi A, Passeri D, Carminati P, Cavazza C, Zunino F (2010) Metabolic Approach to the Enhancement of Antitumor Effect of Chemotherapy: a Key Role of Acetyl-l-Carnitine. *Clinical Cancer Research* 16:3944–3953. <https://doi.org/10.1158/1078-0432.CCR-10-0964>
182. Shin Y-K, Yoo BC, Chang HJ, Jeon E, Hong S-H, Jung M-S, Lim S-J, Park J-G (2005) Down-regulation of Mitochondrial F1F0-ATP Synthase in Human Colon Cancer Cells with Induced 5-Fluorouracil Resistance. *Cancer Res* 65:3162–3170. <https://doi.org/10.1158/0008-5472.CAN-04-3300>
183. Sánchez-Cenizo L, Formentini L, Aldea M, Ortega AD, García-Huerta P, Sánchez-Aragó M, Cuezva JM (2010) Up-regulation of the ATPase Inhibitory Factor 1 (IF1) of

- the Mitochondrial H<sup>+</sup>-ATP Synthase in Human Tumors Mediates the Metabolic Shift of Cancer Cells to a Warburg Phenotype. *Journal of Biological Chemistry* 285:25308–25313. <https://doi.org/10.1074/jbc.M110.146480>
184. Mboge M, Mahon B, McKenna R, Frost S (2018) Carbonic Anhydrases: Role in pH Control and Cancer. *Metabolites* 8:19. <https://doi.org/10.3390/metabo8010019>
  185. Järvinen P, Kivelä AJ, Nummela P, Lepistö A, Ristimäki A, Parkkila S (2017) Carbonic anhydrase II : a novel biomarker for pseudomyxoma peritonei. *APMIS* 125:207–212. <https://doi.org/10.1111/apm.12653>
  186. Parkkila S, Lasota J, Fletcher JA, Ou W, Kivelä AJ, Nuorva K, Parkkila A-K, Ollikainen J, Sly WS, Waheed A, Pastorekova S, Pastorek J, Isola J, Miettinen M (2010) Carbonic anhydrase II. A novel biomarker for gastrointestinal stromal tumors. *Modern Pathology* 23:743–750. <https://doi.org/10.1038/modpathol.2009.189>
  187. Zhou R, Huang W, Yao Y, Wang Y, Li Z, Shao B, Zhong J, Tang M, Liang S, Zhao X, Tong A, Yang J (2013) CA II, a potential biomarker by proteomic analysis, exerts significant inhibitory effect on the growth of colorectal cancer cells. *Int J Oncol* 43:611–621. <https://doi.org/10.3892/ijo.2013.1972>
  188. Nordfors K, Haapasalo J, Korja M, Niemelä A, Laine J, Parkkila A-K, Pastorekova S, Pastorek J, Waheed A, Sly WS, Parkkila S, Haapasalo H (2010) The tumour-associated carbonic anhydrases CA II, CA IX and CA XII in a group of medulloblastomas and supratentorial primitive neuroectodermal tumours: an association of CA IX with poor prognosis. *BMC Cancer* 10:148. <https://doi.org/10.1186/1471-2407-10-148>
  189. Liu C, Lin Y, Yeh K, Chen M, Chang J, Chen C, Chou M, Yang S, Chien M (2012) Expression of carbonic anhydrases I/II and the correlation to clinical aspects of oral squamous cell carcinoma analyzed using tissue microarray. *Journal of Oral Pathology & Medicine* 41:533–539. <https://doi.org/10.1111/j.1600-0714.2012.01135.x>
  190. Liu L-C, Xu W-T, Wu X, Zhao P, Lv Y-L, Chen L (2013) Overexpression of carbonic anhydrase II and Ki-67 proteins in prognosis of gastrointestinal stromal tumors. *World J Gastroenterol* 19:2473. <https://doi.org/10.3748/wjg.v19.i16.2473>
  191. Waterman EA, Cross NA, Lippitt JM, Cross SS, Rehman I, Holen I, Hamdy FC, Eaton CL (2007) The antibody MAB8051 directed against osteoprotegerin detects carbonic anhydrase II: Implications for association studies with human cancers. *Int J Cancer* 121:1958–1966. <https://doi.org/10.1002/ijc.22946>

## PUBLICATIONS

### Publications of dissertation results:

1. **Pankevičiūtė-Bukauskienė M**, Mikalayeva V, Žvikas V, Skeberdis VA, Bordel Velasco S. Multi-Omics Analysis Revealed Increased De Novo Synthesis of Serine and Lower Activity of the Methionine Cycle in Breast Cancer Cell Lines. *Molecules*. MDPI. 2023, vol. 28, no. 11, p. 1-13. <https://doi.org/10.3390/molecules28114535> [Impact Factor 4.6; CiteScore 6.7]
2. Mikalayeva V, **Pankevičiūtė M**, Žvikas V, Skeberdis VA, Bordel Velasco, S. Contribution of branched chain amino acids to energy production and mevalonate synthesis in cancer cells. *Biochemical and biophysical research communications*. Elsevier. 2021, vol. 585, p. 61-67. doi: 10.1016/j.bbrc.2021.11.034. [Impact Factor 3.1; CiteScore 6.1]

### Scientific conferences:

1. **Pankevičiūtė Bukauskienė, Monika**; Bordel Velasco, Sergio. Multi-omics unveils lower metabolic activity of the methionine cycle in breast cancer cells // FEBS Open Bio : FEBS 2023 - The 47th FEBS congress “Together in bioscience for a better future” : July 8-12, 2023, Tours, France / Federation of European Biochemical Societies (FEBS). Wiley. ISSN 2211-5463, 2023, vol.13, suppl. 2, p. 74-74. doi: <https://doi.org/10.1002/2211-5463.13646>.
2. **Pankevičiūtė Bukauskienė, Monika**; Bordel Velasco, Sergio. Multi-omic analysis shows increased de novo synthesis of serine in breast cancer cells // 18th WIMC - Warsaw International Medical Congress : abstract book : 21st-23rd April 2023, Warsaw, Poland / Students’ Scientific Association at Medical University of Warsaw. Warsaw : Students’ Scientific Association at Medical University of Warsaw, 2023, p. 276-276.
3. Mikalayeva, Valeryia; **Pankevičiūtė Bukauskienė, Monika**; Žvikas, Vaidotas; Skeberdis, Vytenis Arvydas; Bordel Velasco, Sergio. Branched chain amino acids are an important energy source in cancer cells // FEBS Open Bio : Supplement: The Biochemistry Global Summit, 25th IUBMB Congress, 46th FEBS Congress, 15th PABMB Congress : July 9-14, 2022, Lisbon, Portugal / Federation of European Biochemical Societies (FEBS). West Sussex : John Wiley & Sons Ltd. ISSN 2211-5463, 2022, vol. 12, suppl. 1, p. 293-293. doi:10.1002/2211-5463.134402022.

4. Mikalayeva, Valeryia; **Pankevičiūtė, Monika**; Žvikas, Vaidotas; Skeberdis, Vytenis Arvydas; Bordel Velasco, Sergio. Alternative energy: the role of branched-chained amino acids in breast cancer cells // FEBS3+ Conference of Estonian, Latvian and Lithuanian Biochemical Societies : abstract book : Tallinn, Estonia, 15-17 June 2022 / Editor Tiit Lukk. Tallinn : Tallinn University of Technology Press, 2022. ISBN 9789949838639, p. 46-47.
5. **Pankevičiūtė Bukauskienė, Monika**; Bordel Velasco, Sergio. RNA Sequencing of two Breast Cancer Cell Lines in Comparison to Healthy Epithelial Breast Cells // Lithuanian Biochemical Society 2022 Mini-Conference: Biochemistry in the Big Data Age = [Biochemistry in the big data age: Lietuvos biochemikų draugijos 2022 minikonferencija] : The Programme and Abstract Book : Vilnius, September 30, 2022 / Lithuanian Biochemical Society. Vilnius : Lithuanian Biochemical Society, 2022. ISBN 9786099603018.

# SUPPLEMENTS

## S1. Bioethics permit

Dokumentas pasirašytas el. parašu.  
Pasirašiusios šalys:

GINTAUTAS GUMBREVIČIUS  
Data: 2021-03-24 13:46:57 GMT+2



### KAUNO REGIONINIS BIOMEDICININIŲ TYRIMŲ ETIKOS KOMITETAS

Lietuvos sveikatos mokslų universitetas, A. Mickevičiaus g. 9, LT 44307 Kaunas, tel. (+370) 37 32 68 89; el. paštas: kaunorbtek@ismuni.lt

### LEIDIMAS ATLIKTI BIOMEDICININĮ TYRIMĄ

2021-03-23 Nr. BE-2-32

<b>Biomedicininio tyrimo pavadinimas: „Šakotos grandinės amino rūgščių degradavimo įtaka navikinių ląstelių metabolizmui ir proliferacijai“</b>	
Protokolo Nr.:	<b>01</b>
Data:	<b>2021-03-15</b>
Versija:	<b>04</b>
Asmens informavimo forma:	<b>Versija 04, data: 2021-03-15</b>
Pagrindinis tyrėjas:	<b>Dr. Sergio Bordel Velasco</b>
Biomedicininio tyrimo vieta:	Lietuvos sveikatos mokslų universiteto ligoninė Kauno
Įstaigos pavadinimas:	klinikos, Chirurgijos klinika, Krūties chirurgijos skyrius
Adresas:	Eivenių g. 2A, LT - 50009, Kaunas

#### Išvada:

Kauno regioninio biomedicininių tyrimų etikos komiteto posėdžio, įvykusio **2021 m. kovo mėn. 2 d.** (protokolo Nr. 2021-BE10-0003) sprendimu pritarta biomedicininio tyrimo vykdymui.

Mokslinio eksperimento vykdytojai įsipareigoja: (1) nedelsiant informuoti Kauno Regioninį biomedicininių Tyrimų Etikos komitetą apie visus nenumatytus atvejus, susijusius su studijos vykdymu, (2) iki sausio 15 dienos – pateikti metinį studijos vykdymo apibendrinimą bei, (3) per mėnesį po studijos užbaigimo, pateikti galutinį pranešimą apie eksperimentą.

Kauno regioninio biomedicininių tyrimų etikos komiteto nariai			
Nr.	Vardas, Pavardė	Veiklos sritis	Dalyvavo posėdyje
1.	Doc. dr. Gintautas Gumbrevičius	Klinikinė farmakologija	Taip
2.	Prof. dr. Kęstutis Petrikonis	Neurologija	Taip
3.	Dr. Saulius Raugėlė	Chirurgija	Taip
4.	Dr. Lina Jankauskaitė	Pediatrija	Ne
5.	Prof. dr. Džilda Veličkienė	Endokrinologija	Taip
6.	Doc. dr. Eimantas Peičius	Visuomenės sveikata	Taip
7.	Aušra Degutytė	Visuomenės sveikata	Taip
8.	Dr. Žydrūnė Luneckaitė	Visuomenės sveikata	Taip
9.	Viktorija Bučinskaitė	Teisė	Taip

Kauno regioninis biomedicininių tyrimų etikos komitetas dirba vadovaudamasis etikos principais nustatytais biomedicininių tyrimų Etikos įstatyme, Helsinkio deklaracijoje, vaistų tyrinėjimo Geros klinikinės praktikos taisyklėmis.

Kauno RBTEK pirmininkas



Doc. dr. Gintautas Gumbrevičius



## S2. Python script for flux distribution calculations

```
import numpy as np

def convolution(a, b):
    lo = len(a) + len(b) - 2
    con = []
    for k in range(lo + 1):
        v = 0
        for i in range(len(a)):
            if i < k + 1 and (k - i) < len(b):
                v = v + a[i] * b[k - i]
        con.append(v)
    return con

def labels(f, V4, V6, V1):
    V5 = V4 + V6
    V3 = V1 + V5 - 1

    #EMUs of 4 carbons
    #External variables

    unlabeledAcCoA = convolution([0.989, 0.011], [0.989, 0.011])
    AcCoA = [
        unlabeledAcCoA[0] * (1 - f),
        unlabeledAcCoA[1] * (1 - f),
        unlabeledAcCoA[2] * (1 - f) + f
    ]

    AcetCoAex = convolution(AcCoA, AcCoA)

    MG3456un = convolution(
        convolution([0.989, 0.011], [0.989, 0.011]),
        convolution([0.989, 0.011], [0.989, 0.011])
    )
    MGCoA3456 = [
        0.3 * MG3456un[0],
        0.3 * MG3456un[1],
        0.3 * MG3456un[2],
        0.3 * MG3456un[3] + 0.7,
        0.3 * MG3456un[4]
    ]
    print MGCoA3456

    #Matrix of balances

    HMGCoA3456 = [-V1 -V5, 0, V5]
    AcetCoA = [V3, -V3, 0]
    AcetCoAex = [0, V4, -V4 - V6]
    A = np.array([HMGCoA3456, AcetCoA, AcetCoAex])

    HMGCoA3456 = [V1, 0]
    AcetCoA = [0, 0]
    AcetCoAex = [0, V6]

    B = np.array([HMGCoA3456, AcetCoA, AcetCoAex])
    x = np.array([MGCoA3456, AcetCoAex])

    C = np.dot(B, x)

    y = np.linalg.solve(A, -C)

    print y
```

```

AcetoCoA = y[2]

#EMUs of 6 carbons
#External

MGun = convolution(MG3456un, unlabeledAcCoA)
MGlabs = [0, 0, 0, 0, 0, 1, 0]

MG=[]

for i in range(7):
    MG.append(0.3 * MGun[i] + 0.7 * MGlabs[i])

#Convolutions

AcCoAxAcetoCoA = convolution(AcetoCoA, AcCoA)

f1 = float(V1) / float(V1 + V5)
f2 = float(V5) / float(V1 + V5)

Mev=[]
for i in range(7):
    Mev.append(f1 * MG[i] + f2 * AcCoAxAcetoCoA[i])

return Mev

Mev = labels(0.1, 0, 2.5, 0.3)

print Mev

```

### *S3. Python script for processing sequence alignment files*

```
import HTSeq
import math
import pickle

#Get transcript lengths

transcripts = HTSeq.FastaReader('Transcripts.fasta')
lengths = {}
for t in transcripts:
    lengths[t.name.split('|')[1]] = len(t.seq)

#Make a dictionary of splicing variants

vardic = {}
for t in transcripts:
    sp = t.name.split('|')
    if sp[0] not in vardic:
        vardic[sp[0]] = [sp[1]]
    else:
        vardic[sp[0]].append(sp[1])

import os

#Process SAM files

for subdir, dirs, files in os.walk('.'):
    for f in files:
        s = f.find('1.sam')
        if s != -1:
            genexp = {}
            gencount = {}
            transabs = {}
            fragments = 0

            alms = HTSeq.SAM_Reader(f)
            for bundle in HTSeq.pair_SAM_alignments(alms, bundle=True):
                fragments += 1
                genes = []
                transcripts = []

                for m in bundle:
                    first_al, second_al = m
                    if first_al.aligned and second_al.aligned:
                        if first_al.iv.chrom == second_al.iv.chrom:
                            if first_al.inferred_insert_size < 600:
                                genes.append(first_al.iv.chrom.split('|')[0])
                                transcripts.append(
                                    first_al.iv.chrom.split('|')[1]
                                )

                if len(genes) > 0:
                    ambiguous = 0
                    for g in genes:
                        if g != genes[0]:
                            ambiguous = 1
                    if ambiguous == 0:
                        l = 0
                        n = len(transcripts)
                        for t in transcripts:
                            l += lengths[t]
                        avlen = float(l) / float(n)
```

```

fpk = 1000 / float(avlen)

if genes[0] not in genexp:
    genexp[genes[0]] = fpk
    gencount[genes[0]] = 1
else:
    genexp[genes[0]] += fpk
    gencount[genes[0]] += 1

for tr in vardic[genes[0]]:
    if tr not in transcripts:
        if tr not in transabs:
            transabs[tr] = 1
        else:
            transabs[tr] += 1

gen_fpkm = {}
for g in genexp:
    gen_fpkm[g] = genexp[g] * float(1000000) / float(fragments)
name = f[:s] + '.pk1'

with open(name, 'wb') as output:
    pickle.dump(gen_fpkm, output)

```

## *S4. Python script for differential gene analysis*

```
import pickle
import HTSeq
import math
import sys
import scipy
from scipy import stats
from scipy.stats import ttest_ind
from scipy.stats import pearsonr
import numpy as np
import matplotlib as mpl
mpl.use('agg')
import matplotlib.pyplot as plt
import os

#Read expression files

refe = {}
sal = {}

for subdir, dirs, files in os.walk('.'):
    for f in files:
        if f.find('.pkl') != -1:
            with open(f, 'rb') as input:
                expression = pickle.load(input)

                if f.find('MCF7') != -1:
                    refe[f[:-4]] = expression
                if f.find('BCC') != -1:
                    sal[f[:-4]] = expression

print(sal)
print(refe)

#Read all the sequenced genes

genes = []

for s in refe:
    for g in refe[s]:
        if g not in genes:
            genes.append(g)

for s in sal:
    for g in sal[s]:
        if g not in genes:
            genes.append(g)

#Differential expression

pvals = {}
mlogpvals = {}
lograts = {}
dif = {}

for ge in genes:
    x = []
    for s in refe:
        if ge in refe[s]:
            x.append(refe[s][ge])
        else:
            x.append(0)
    y = []
```

```

for s in sal:
    if ge in sal[s]:
        y.append(sal[s][ge])
    else:
        y.append(0)

t, pv = ttest_ind(x, y, equal_var=False)
if math.isnan(pv) == False:
    pvals[ge] = pv
    mlogpvals[ge] = -math.log10(pvals[ge])
    dif[ge] = np.mean(y)-np.mean(x)
if np.mean(x) > 0 and np.mean(y) > 0:
    lograts[ge] = math.log(float(np.mean(y)) / float(np.mean(x)), 2)

import operator

sorted_vals = sorted(pvals.items(), key = operator.itemgetter(1))

#Correct for multiple testing

n = len(sorted_vals)
print(n)
hvals = {}
for i in range(n):
    hvals[sorted_vals[i][0]] = float(n) * float(sorted_vals[i][1]) /
    float(i + 1)

for j in range(n - 1):
    for i in range(n - 1):
        if hvals[sorted_vals[i][0]] > hvals[sorted_vals[i + 1][0]]:
            hvals[sorted_vals[i][0]] = hvals[sorted_vals[i + 1][0]]

upre = []

#Differential expression results

with open("Upregulated.txt", "w") as text_file:
    for g in hvals:
        if hvals[g] < 0.01 and dif[g] > 0:
            upre.append(g)
            if g not in lograts:
                line = g + '\t' + str(pvals[g]) + '\t' + str(hvals[g]) +
                '\t' + str(dif[g]) + '\r'
                text_file.write(line)
            else:
                if lograts[g] > 1:
                    line = g + '\t' + g + '\t' + str(pvals[g]) + '\t' +
                    str(hvals[g]) + '\t' + str(dif[g]) + '\r'
                    text_file.write(line)

with open("Downregulated.txt", "w") as text_file:
    for g in hvals:
        if hvals[g] < 0.01 and dif[g] < 0:
            if g not in lograts:
                line = g + '\t' + str(pvals[g]) + '\t' + str(hvals[g]) +
                '\t' + str(dif[g]) + '\r'
                text_file.write(line)
            else:
                if lograts[g] < -1:
                    line = g + '\t' + g + '\t' + str(pvals[g]) + '\t' +
                    str(hvals[g]) + '\t' + str(dif[g]) + '\r'
                    text_file.write(line)

with open("AllTheGenes.txt", "w") as text_file:
    for g in hvals:
        if g not in lograts:

```

```

        line = g + '\t' + str(pvals[g]) + '\t' + str(hvals[g]) + '\t' +
        str(dif[g]) + '\r'
        text_file.write(line)
    else:
        line = g + '\t' + g + '\t' + str(pvals[g]) + '\t' +
        str(hvals[g]) + '\t' + str(dif[g]) + '\r'
        text_file.write(line)

x = []
y = []
for g in lograts:
    x.append(lograts[g])
    y.append(mlogpvals[g])

xu = []
yu = []
for g in lograts:
    if hvals[g] < 0.01 and lograts[g] > 1:
        xu.append(lograts[g])
        yu.append(mlogpvals[g])

xd = []
yd = []
for g in lograts:
    if hvals[g] < 0.01 and lograts[g] < -1:
        xd.append(lograts[g])
        yd.append(mlogpvals[g])

plt.scatter(x, y, s=3, c='black')
plt.scatter(xu, yu, s=5, c='red')
plt.scatter(xd, yd, s=5, c='blue')

plt.xlabel('log2(FC)')
plt.ylabel('-log10(p-val)')
plt.savefig('volcano.png')
plt.close()

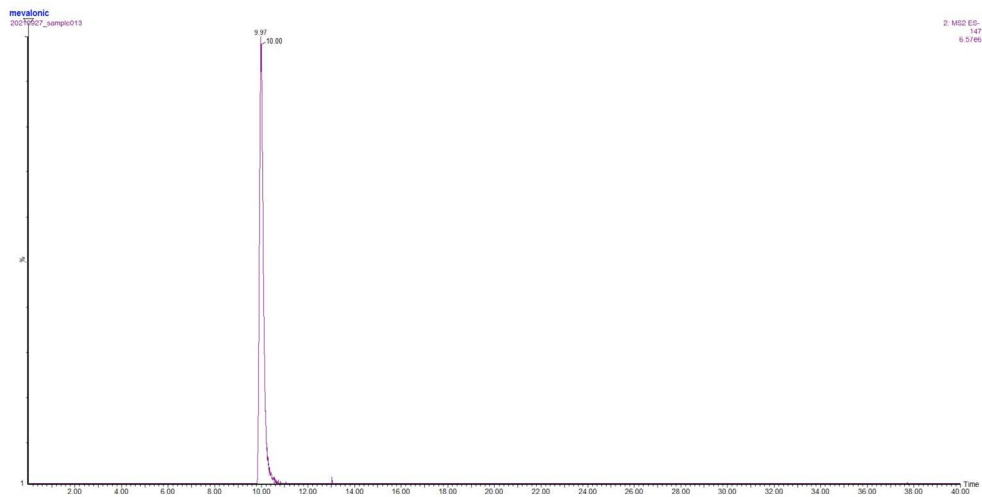
with open('pvals.pkl', 'wb') as output:
    pickle.dump(pvals, output)

with open('dif.pkl', 'wb') as output:
    pickle.dump(dif, output)

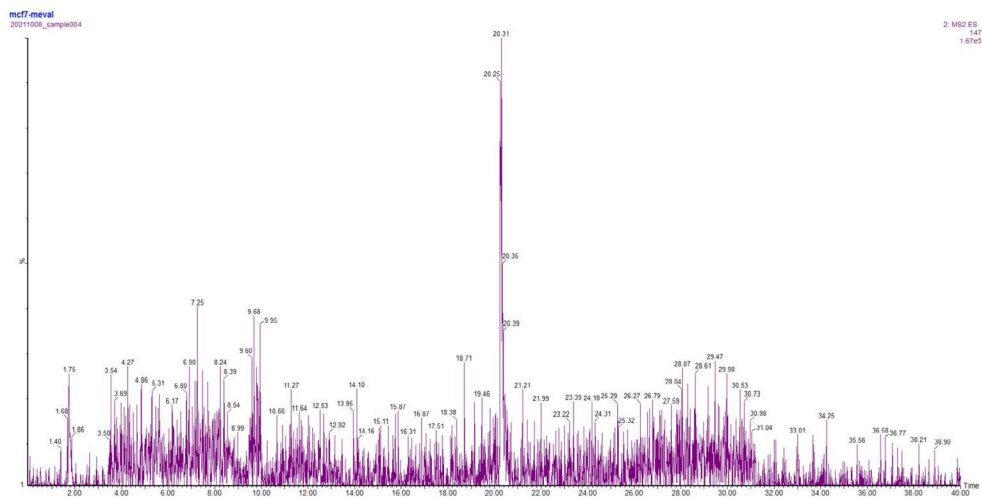
```

## S5. Chromatograms

Mevalonate standard (retention time 9.97)

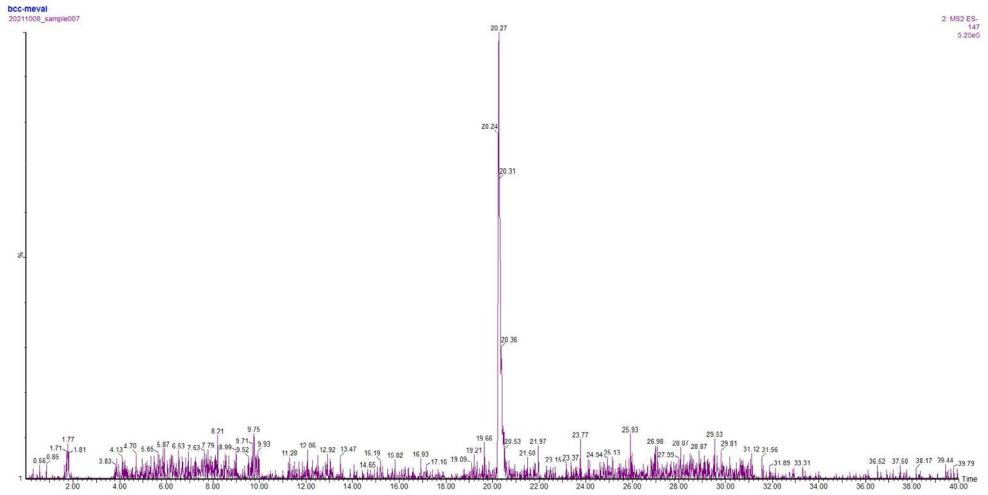


MCF-7

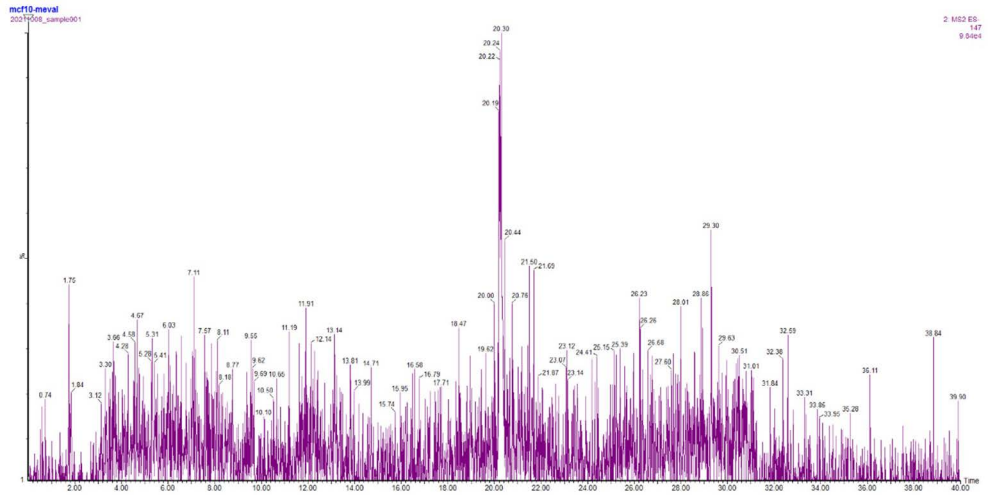




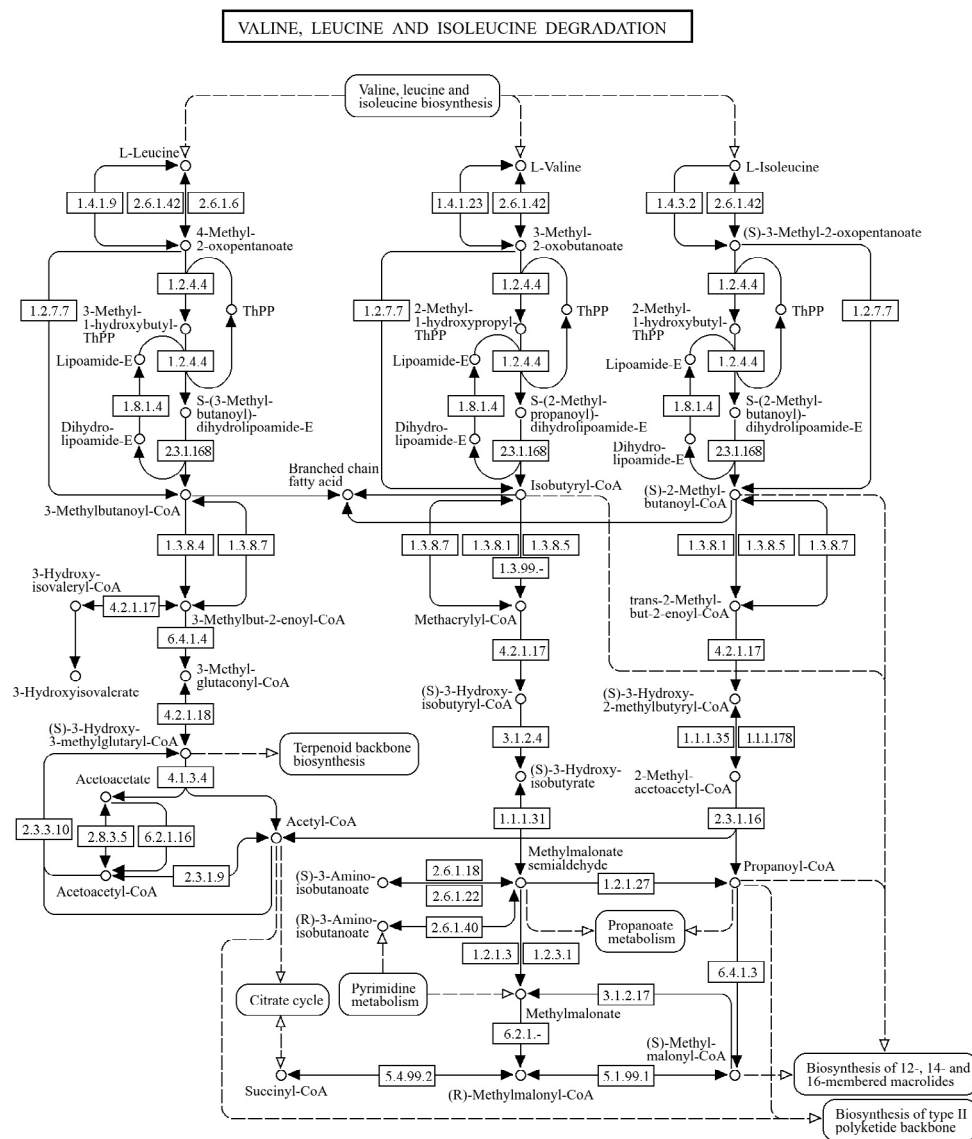
# BCC



# MCF-10A (no signal following the retention time 9.97)



## S6. BCAA degradation scheme from KEGG



## S7. Complete list of perturbed metabolic reactions

Reaction ID	Reaction	Flux difference mmol/h g-DW	Associated genes
HMR_4396	glucose-1-phosphate[c] <=> glucose-6-phosphate[c]	-0.009947666195208055	ENSG000000169299
HMR_3944	UTP[c] + glucose-1-phosphate[c] => PPI[c] + UDP-glucose[c]	-0.009947666195208055	ENSG000000169764
HMR_4354	ribose-1-phosphate[c] <=> ribose-5-phosphate[c]	-0.0013655170440140803	ENSG000000169299
HMR_6916	ADP[m] + Pi[m] => ATP[m] + 4 H+[m] + H2O[m]	-0.23762895693606872	ENSG000000069849
HMR_6918	2 H+[m] + 2 ferricytochrome C[m] + ubiquinol[m] => 2 ferrocytochrome C[m] + ubiquinone[m]	-0.13083295985996092	ENSG000000173660
HMR_6921	4 H+[m] + NADH[m] + ubiquinone[m] => NAD+[m] + ubiquinol[m]	-0.10871794202221118	ENSG000000166136
HMR_0217	AMP[c] + PPi[c] + palmitoyl-CoA[c] <=> ATP[c] + CoA[c] + palmitate[c]	-0.002784639620192083	ENSG000000068366
HMR_2152	acetyl-[ACP][c] + malonyl-[ACP][c] => CO2[c] + [ACP][c] + acetoacetyl-[ACP][c]	-0.001391965986773689	ENSG000000143797
HMR_2153	H+[c] + NADPH[c] + acetoacetyl-[ACP][c] => (R)-3-hydroxybutanoyl-[ACP][c] + NADP+[c]	-0.001391965986773689	ENSG000000137124
HMR_2156	butyryl-[ACP][c] + malonyl-[ACP][c] => 3-oxohexanoyl-[ACP][c] + CO2[c] + [ACP][c]	-0.001391965986773689	ENSG000000143797
HMR_2160	hexanoyl-[ACP][c] + malonyl-[ACP][c] => 3-oxooctanoyl-[ACP][c] + CO2[c] + [ACP][c]	-0.001391965986773689	ENSG000000143797
HMR_2164	malonyl-[ACP][c] + octanoyl-[ACP][c] => 3-oxodecanoyl-[ACP][c] + CO2[c] + [ACP][c]	-0.001391965986773689	ENSG000000143797
HMR_2168	decanoyl-[ACP][c] + malonyl-[ACP][c] => 3-oxododecanoyl-[ACP][c] + CO2[c] + [ACP][c]	-0.001391965986773689	ENSG000000143797
HMR_2173	dodecanoyl-[ACP][c] + malonyl-[ACP][c] => 3-oxotetradecanoyl-[ACP][c] + CO2[c] + [ACP][c]	-0.0013943768988846795	ENSG000000143797
HMR_2175	HMA[c] => (2E)-tetradecenoyl-[ACP][c] + H2O[c]	-0.0013943768988846795	ENSG000000138029
HMR_2178	malonyl-[ACP][c] + tetradecanoyl-[ACP][c] => 3-oxohexadecanoyl-[ACP][c] + CO2[c] + [ACP][c]	-0.0013652921085777411	ENSG000000143797
HMR_2181	(2E)-hexadecenoyl-[ACP][c] + H+[c] + NADPH[c] => NADP+[c] + hexadecanoyl-[ACP][c]	-0.0013652921085777411	ENSG000000138029
HMR_2190	malonyl-CoA[c] + palmitoyl-CoA[c] => 3-oxooctadecanoyl-CoA[c] + CO2[c] + CoA[c]	-0.0016980834512816487	ENSG000000143797
HMR_2191	3-oxooctadecanoyl-CoA[c] + H+[c] + NADPH[c] => 3-hydroxyoctadecanoyl-CoA[c] + NADP+[c]	-0.0016980834512816487	ENSG000000170786
HMR_1445	(R)-mevalonate[c] + ATP[c] => (R)-5-phosphomevalonate[c] + ADP[c]	-0.0018373949273137614	ENSG00000010921
HMR_4262	PPI[c] + nicotinamide D-ribonucleotide[c] <=> PRPP[c] + nicotinamide[c]	-0.001347062159561675	ENSG000000105835
HMR_5406	CO2[c] + H2O[c] <=> carbonate[c]	-0.06026252543535833	ENSG000000131686
HMR_6374	H+[s] + serine[s] => H+[c] + serine[c]	-0.04327475523810602	ENSG000000180773

# CURRICULUM VITAE

**Name, Surname:** Monika Pankevičiūtė-Bukauskienė  
**e-mail:** monika.pankeviciute-bukauskiene@lsmu.lt  
**Born:** April 27, 1996, Kaunas, Lithuania

## Education:

2020–2024 PhD in Biophysics, Lithuanian University of Health Sciences, Kaunas, Lithuania  
2015–2020 Master’s degree in Pharmacy, Lithuanian University of Health Sciences, Kaunas, Lithuania

## Work experience:

2022–2024 Junior researcher for a project funded by Lithuanian Research Council (The mechanisms regulating breast cancer cell migration and invasion; S-MIP-22-60) Institute of Cardiology, Lithuanian University of Health Sciences  
2020–2021 Junior researcher for a project funded by Lithuanian Research Council (The effect of branched-chain amino acid degradation on cancer cell metabolism and proliferation; S-SEN-20-6) Institute of Cardiology, Lithuanian University of Health Sciences  
2019–2020 Scientific laboratory technician, Institute of Cardiology, Lithuanian University of Health Sciences

## Internships:

2022.04–2022.06 Erasmus+ internship at University of Valladolid, Valladolid, Spain  
2024.03–2024.05 Erasmus+ internship at Utrecht University, Utrecht, The Netherlands

## ACKNOWLEDGEMENTS

If you have read this far, I would like to take the opportunity to thank the people in my life, without whom this dissertation would not have been possible.

First and foremost, I have to thank my supervisor, Sergio Bordel, for gently guiding me throughout the journey of becoming a scientist. The ideas and methodology of his work continue to amaze me to this day, and I am forever grateful for the opportunity to be a part of his team.

That being said, the ideas could not have been carried out without the competence of the staff and the infrastructure of the Laboratory of Cell Culture. My sincere gratitude goes to the head of our lab, Vytenis Arvydas Skeberdis and my daily supervisor, Valeryia Mikalayeva, for the immense help with planning and executing the experiments. I also appreciate the work of Ieva Sarapinienė, Ieva Ceslevičienė and Vytautas Raškevičius, who laid the groundwork for my research before I even knew anything about it. For my other colleagues – Rokas Mickus, Gintarė Jančiukė, Revathi Sampath, and Kamilė Eitkevičiūtė – thank you for keeping me somewhat sane throughout the years. You deserve a separate chapter in this book, and I can proudly call you my second family.

This work was also made possible thanks to the funding from the Research Council of Lithuania and the Open Fund of the Lithuanian University of Health Sciences. Kudos to all of the staff in our Research Affairs Department, especially Jūratė Janušaitienė, for the sincere help regarding my studies and all of the paperwork she assisted me with.

A big part of my self-development over the years is owed to the Erasmus+ mobility programme, which allowed me to gain experience in different science fields by travelling to universities abroad. The adventures, long-distance colleagues, and friends I made along the way will forever be engraved in my heart.

Last but not least, I want to thank my family: the one that birthed me and the one that found me. Thank you for always believing in me and checking up on my sleep-deprived self over the last couple of years.